

University of Calabria-Italy, Laboratory of Cardiovascular Pathophysiology, Dept. DiBEST

University of Rouen Normandy-France, DC2N- French National Institute of Health and Medical
Research (INSERM) U1239

XXX Cycle of Doctorate in **Life Sciences**

Co-tutorship with the Normandy's Doctoral School of **Integrative Biology, Health and Environment**
(EdN BISE 497)

*Disciplines: **Physiology and Biochemistry***

Selenoprotein T as a novel cardiac modulator: from production to expression measurement and pathophysiological implications

Director of Doctorate in Life Science

Prof. Maria Carmela Cerra




Director of Doctoral School of Integrative Biology, Health and Environment

Prof. François Dauphin

Ph.D. student

Dr. Carmine Rocca



Tutor

Prof. Tommaso Angelone



Co-tutor

Dr. Youssef Anouar



Index

Résumé français	6
1. Production du SelT recombinante (rSelT)	8
2. Enzyme-Linked Immunosorbent Assay (ELISA) pour la quantification de la SelT	10
3. Etudes cardiaques ex vivo	14
Summary	19
Introduction	23
1. Selenium and Selenocysteine in protein chemistry	24
1.1 Selenium: biochemistry and physiology	24
1.2 Selenocysteine (Sec): reactivity and selectivity	26
1.3 Sec biosynthesis	28
1.3.1 Sec tRNA ^{[Ser]Sec}	28
1.3.2 Selenophosphate Synthetase.....	31
1.3.3 Sec Lyase	31
1.4 Sec incorporation into proteins	31
2. Structure and activity of mammalian selenoproteins	34
2.1 Selenoproteins as ROS-detoxifying enzymes	37
2.1.1 Oxidants generation and oxidative stress	37
2.1.2 Antioxidant activity of selenoproteins	38
2.2 Pathophysiological implications of selenoproteins	39
2.2.1 Thioredoxin reductases (TrxRs).....	40
2.2.2 Glutathione Peroxidases (GPxs)	41
2.2.3 Iodothyronine Deiodinases (DIOs)	42
2.2.4 Rdx family of selenoproteins.....	43
3. The Rrx member Selenoprotein T (SelT or SELENOT)	44
3.1 Involvement of SelT in the regulation of Ca²⁺ homeostasis and neuroendocrine function	46
3.2 Involvement of SelT in the regulation of pancreatic β-cell function and glucose homeostasis	48
3.3 Role of SelT in neurodegeneration	49
4. Oxidative stress in cardiovascular disease (CVD)	51
Aims of the doctoral project	53
Materials and methods	56
1. Production of recombinant SelT	57

1.1 Cloning of rat SelT cDNA	57
1.2 Preparation of competent E. coli	57
1.3 Plasmid DNA purification and enzymatic digestion	57
1.4 Expression of rSelT in E. coli	58
1.5 Purification of 6His-rSelT protein under denaturing conditions and protein refolding	59
1.6 Post-refolding analysis: activity assessment of rSelT	60
1.7 Purity of rSelT	61
2. SelT Enzyme-Linked Immunosorbent Assay development for SelT detection	62
2.1 Production of sera against SelT	62
2.2 Western blot for determination of rabbit sera antibodies	62
2.3 Chequerboard titrations (CBTs)	63
2.4 I-ELISA for antibody measurement	63
2.5 IC-ELISA for antigen detection	64
2.5.1 Construction of a standard-inhibition curve	65
3. Ex vivo cardiac studies	65
3.1 Animals	65
3.2 Peptides and drugs	65
3.3 Isolated heart perfusion	66
3.4 Experimental protocols	67
3.4.1 PSELT-stimulated preparations	67
3.4.2 Ischemia/Reperfusion (I/R) studies	67
3.5 Assessment of myocardial injury	68
3.6 SDS-PAGE and Western blot	68
3.7 ELISA for ROS detection	69
3.8 Mitochondrial isolation	70
3.9 Immunofluorescence	70
4. Statistics	71
Results	72
1. Production of recombinant SelT	73
1.1 Enzymatic digestion of plasmid DNA	73
1.2 Expression of rSelT in E. coli	74
1.3 Determination of 6His-rSelT solubility	75
1.3.1 Solubilization of 6His-rSelT by the bacterial insoluble fraction	75
1.4 Purification of the expressed 6His-rSelT under denaturing conditions and protein refolding	77
1.5 Post-refolding analysis: activity assessment of rSelT	78
2. Enzyme-Linked Immunosorbent Assay for SelT detection	79

2.1 Assessment of sera ability to react with rSelT and C57Bl/6 mice tissue extracts	79
2.2 Determination of sera and rSelT working conditions by CBT	81
2.3 Measurement of SelT-specific antibodies by endpoint titer ELISA.....	84
2.3.1 Determination of the cutoff between negative and positive results for SelT-antibody	84
2.3.2 Determination of the antibody titers by I-ELISA	84
2.4 CBT for commercial SelT-antiserum	87
2.5 SelT detection by IC-ELISA	89
2.5.1 Standard antigen-inhibition curve	89
2.5.2 SelT detection in C57Bl/6 mice tissue extracts	90
3. Ex vivo cardiac studies	93
3.1 SelT expression during heart ontogenesis	93
3.2 SelT expression during cardiac ischemia	95
3.3 Full length rSelT and PSELT effects on post-ischemic cardiac function	97
3.4 PSELT affects cardioprotective pathways	100
3.5 PSELT influence on apoptotic indexes	102
3.6 PSELT influence on cellular redox balance control	104
Discussion	107
1. Production of recombinant SelT	108
2. Development of Enzyme-Linked Immunosorbent Assay for SelT detection	109
3. Ex vivo cardiac studies	110
3.1 Cardiac expression of SelT during ontogenesis and under ischemic conditions	110
3.2 Cardioprotective effect of rSelT and PSELT	111
3.3 PSELT triggers various intracellular signaling mechanisms to provide cardioprotection	113
3.4 PSELT inhibits oxidative and nitrosative stress	114
Conclusions	115
References	116
Abbreviations.....	126

Doctorat en cotutelle de thèse

Université de Calabre, Italie

INSERM U1239, Université de Rouen-Normandie, France

Titre de la thèse

***La sélénoprotéine T en tant que nouveau modulateur
cardiaque: de la production et la mesure de l'expression aux
implications physiopathologiques***

Auteur

Dr. Carmine Rocca

Tuteur

Prof. Tommaso Angelone

Co-tuteur

Dr. Youssef Anouar

Résumé français

Les sélénoprotéines représentent une classe particulière d'enzymes contenant du sélénium et caractérisée par une réactivité chimique spécifique. Ces systèmes protéiques agissent comme des capteurs redox intercellulaires et sont largement reconnus comme médiateurs essentiels pour la prévention de maladies, y compris les pathologies cardiovasculaires. Parmi ces protéines, la sélénoprotéine T (SelT ou SELENOT) est une nouvelle enzyme localisée au niveau du réticulum endoplasmique (ER) appartenant à la famille des rédoxines, dont la suppression de gène chez la souris est associée à une létalité embryonnaire précoce. A travers son domaine catalytique redox (Cys-X-X-Sec), la SelT exerce une action antioxydante et cytoprotective essentielle au niveau cérébral durant l'embryogenèse et suite à des lésions tissulaires. De nombreuses études ont démontré l'implication de la SelT via son activité redox, dans les processus de différenciation et protection des cellules nerveuses et endocrines dans des conditions physiopathologiques spécifiques. En revanche, rien n'est connu sur l'expression et la fonction de cette protéine dans d'autres organes vitaux comme le cœur, un tissu physiologiquement sujet à un stress oxydatif élevé, surtout après un dommage d'ischémie-réperfusion (I/R).

Les études actuelles montrent un grand intérêt pour les molécules capables de réduire le stress oxydatif qui représente un des facteurs majeurs impliqués dans la pathogenèse des dommages myocardiques de l'I/R.

Plusieurs études ont démontré les effets bénéfiques au niveau cardiaque des antioxydants endogènes spécifiques tels que les enzymes catalase, superoxyde dimutase et glutathion peroxydase sur les cœurs isolés soumis à l'I/R. Dans ce contexte, les antioxydants exogènes incluant les substances contenant des groupements thiols, exercent une action protectrice significative contre le déséquilibre redox typique des lésions myocardiques induites par l'I/R (*kalaycioglu et al., 1999; khaper et al., 1997*).

A la lumière de ces observations, mon projet de thèse de doctorat a eu pour but de développer un immunodosage spécifique de la SelT et d'évaluer les implications physiopathologiques au niveau cardiovasculaire d'une forme de SelT recombinante (rSelT) et de son peptide dérivé PSELT (SelT 43-52) synthétisé chimiquement dans sa forme réduite, qui comprend le domaine catalytique redox Cys-Val-Ser-Sec.

- La première partie du travail a eu pour but de:
 - optimiser la surexpression d'une forme recombinante de SelT de souris dans les cellules de *E. coli*,
 - calculer l'activité enzymatique exercée par la protéine pure.

- Le second but de cette thèse a été:
 - le développement de deux essais spécifiques ELISA. En utilisant la protéine recombinante rSelT et un antisérum polyclonal de lapin contre rSelT, respectivement comme antigène et anticorps primaire, des dosages ELISA compétitif indirect (I-ELISA) pour évaluer les titres d'anticorps et indirect (C-ELISA) pour quantifier les niveaux des SelT solubles ont été mis au point.

- La troisième partie de ce projet a eu pour objectif de:
 - déterminer l'expression de la SelT durant l'ontogenèse cardiaque et après un dommage ischémique *ex vivo* induit sur le cœur de souris adultes.
 - évaluer l'effet cardioprotecteur exercé par la rSelT et PSELT en tant qu'agents pharmacologiques en post-conditionnement contre les dommages de l'I/R dans un modèle de cœur isolé de souris perfusé selon la méthode de Langendorff.

1. Production du SelT recombinante (rSelT)

Durant la première partie du travail, nous avons optimisé la production hétérologue d'une forme recombinante de SelT (rSelT) dans les cellules de *E. coli*. Dans ce but, le cDNA correspondant à la SelT a été amplifié à partir de cellules PC12 et ensuite cloné dans le vecteur pGEM-T; la protéine a été exprimée comme protéine de fusion His-tag dans *E. coli*. La rSelT a été purifiée par chromatographie d'affinité dans des conditions dénaturantes et immédiatement renaturée sur colonne en appliquant un protocole de renaturation en présence d'urée. La protéine purifiée a été identifiée comme une bande protéique correspondant au poids moléculaire de 23KDa (**Fig. 1**).

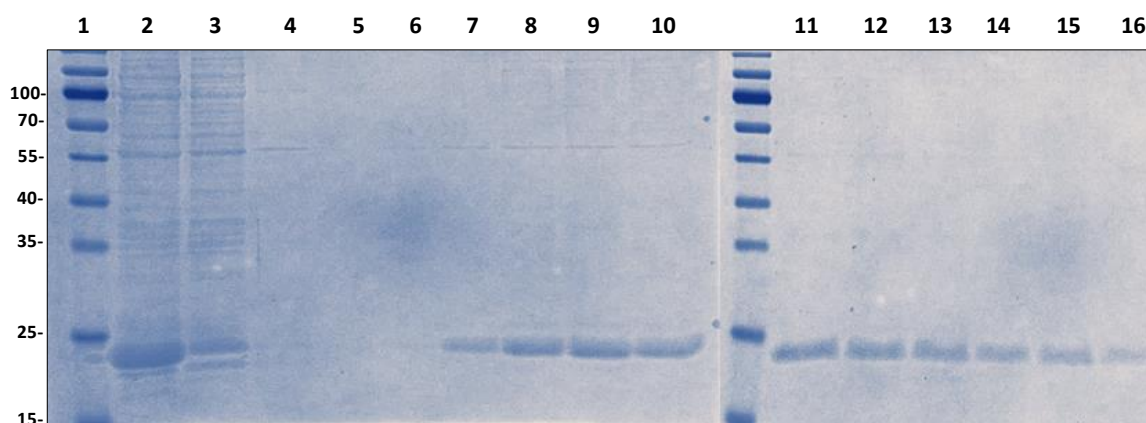


Fig. 1. Purification de 6His-rSelT dans les conditions dénaturantes et analysée sur gel SDS-PAGE à 12% suivi de coloration au bleu de Coomassie. **Ligne 1.** Marqueur, **Ligne 2.** Surnageant après lyse bactérienne avec DNPI-10 ("cleared lysate"), **Ligne 3.** Lysat bactérien après la colonne ("flow-through"), **Ligne 4** Fraction après tampon de lavage DNPI-20, **Ligne 5.** Fraction après tampon de lavage 7:1 (v/v) NPI-20/DNPI-20, **Ligne 6.** Dernières fractions (10 CV) après tampon de lavage NPI-20, **Lignes 7-16.** Fractions d'élution (0.5 ml) après tampon d'élution NPI-250.

Après le protocole de renaturation, rSelT a montré une activité enzymatique identique à celle de la tiorédoxine réductase (TrxR) de foie de souris utilisée comme contrôle. Nous avons utilisé un kit spécifique de TrxR puisque cette enzyme représente une des sélénoprotéines più importante avec ce type d'activité enzymatique (*Dikiy et al, 2007*).

Cette activité enzymatique est dépendante des résidus Cys/Sec du motif catalytique et est similaire à celle de la TrxR dont l'activité est inhibée par l'aurotiomalate (ATM), un inhibiteur sélectif (**Fig. 2**).

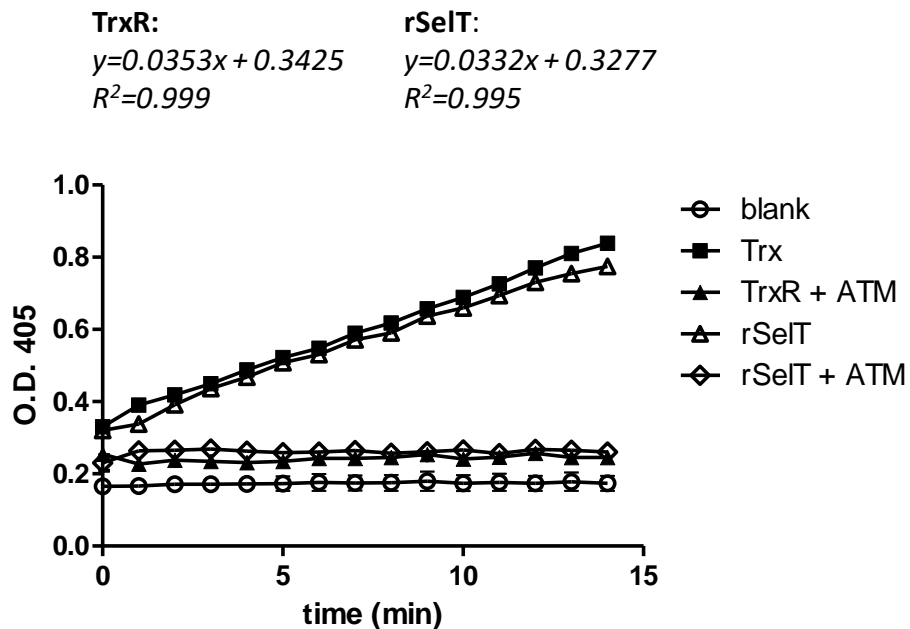


Fig. 2. *Activité enzymatique exercée par rSelT (10 µg) avec un résidu Cys substituant un résidu de Sec dans le domaine catalitique redox (SelT CVSU/C) testé en utilisant un kit spécifique de la TrxR en comparaison avec une TrxR hépatique de souris (20 µl d'échantillon fourni de producteur), en présence et en absence d'aurotiomalate (ATM) 20 µM. L'absorption de substrat réduit a été mesurée à 405 nm. Le graphique montre un essai représentatif de 3 autres expériences qui ont montré des résultats similaires.*

L'étude a permis d'obtenir, pour la première fois une forme de rSelT pure et active.

2. Enzyme-Linked Immunosorbent Assay (ELISA) pour la quantification de la SelT

Le développement de dosages immunologiques sélectifs pour certains antigènes et protéines pourrait être d'une grande aide pour des études aussi bien biologiques spécifiques que pour des applications cliniques. Actuellement un test immunologique spécifique pour évaluer les niveaux des SelT dans les échantillons biologiques n'est pas encore disponible.

La deuxième partie de ce travail a eu comme but celui de développer un ELISA indirect compétitif spécifique (IC-ELISA), utilisant la protéine recombinante et un antisérum polyclonal de lapin contre la rSelT, respectivement comme antigènes et anticorps primaires.

L'antisérum de lapin immunisé avec des fractions purifiées de SelT a réagi sélectivement avec l'immunogène homologue (rSelT); une réactivité élevée a été observée aussi avec les extraits protéiques de tissus murins (cœur, cerveau, testicule, foie, pancréas et rein) analysés par Western blotting, indiquant l'efficacité du protocole d'immunisation.

Afin de contrôler la qualité de la réaction des anticorps produits, les échantillons de sérum de lapin ont été prélevés dans divers intervalles du temps à partir de la première immunisation (au 27^{ème}, 42^{ème} et 91^{ème} jour, indiqués respectivement comme D27, D42 et D91) et ont été analysés par ELISA indirect (I-ELISA). Ainsi, il a été possible d'évaluer comment rSelT a généré durant toute la période d'immunisation une réponse immunogénique sélective chez les lapins, confirmant la génération d'un antisérum hyper-immun. L'absence de signal observée dans le sérum non-immun a été un indice d'une réactivité immunologique spécifique des anticorps produits. Ces données ont indiqué que le test L-ELISA développé était à même de discerner les antisera SelT-négatifs des anti-sera SelT-positifs (**Fig. 3**).

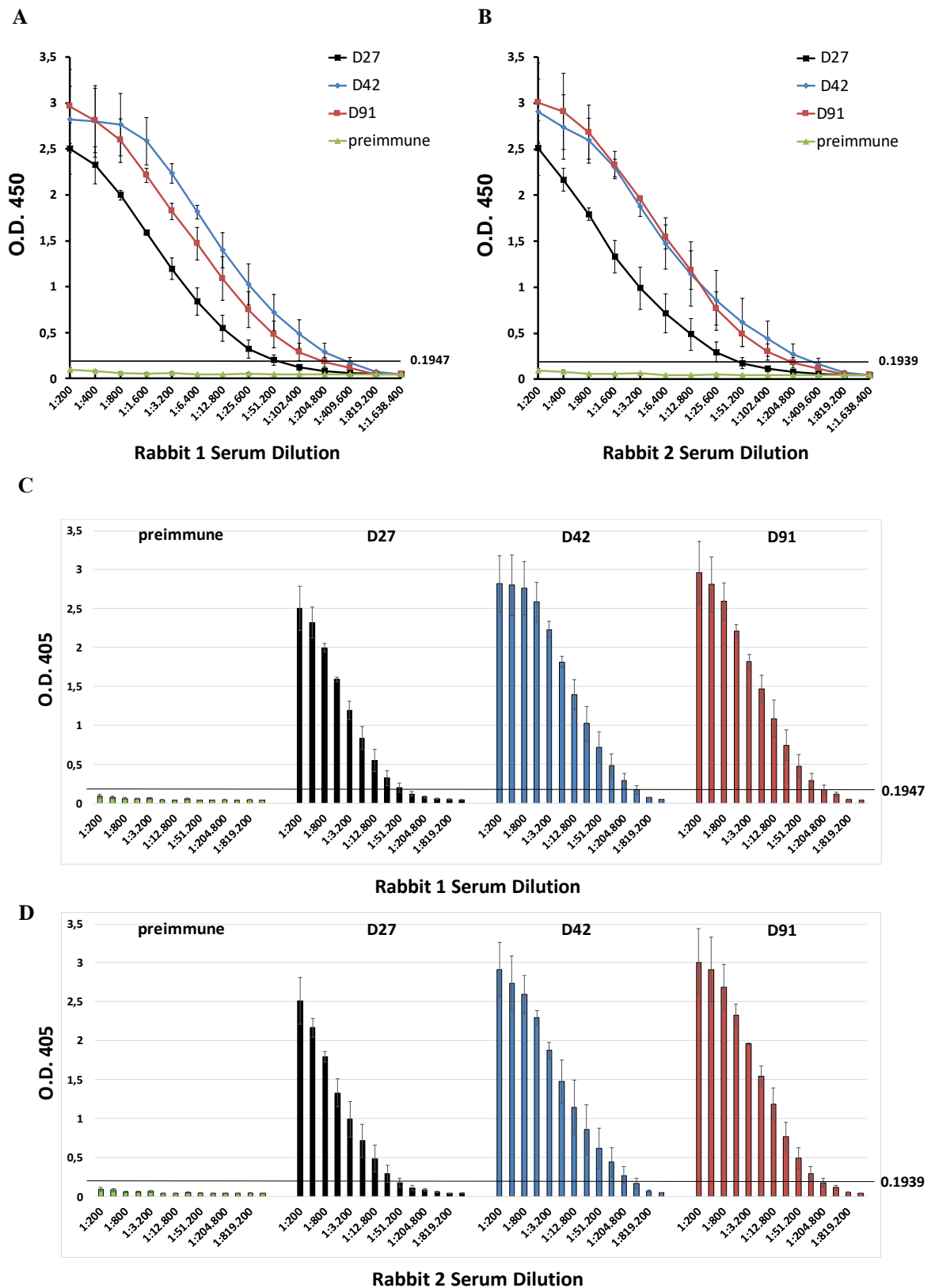


Fig. 3. A., B. Cinétique de réponse des anticorps (titres d'anticorps) de lapin n.1 et du lapin n.2. C., D. valeurs O.D. par rapport au cutoff O.D. de 0.1947 et O.D. de 0.1939 pour le lapin n.1 et lapin n.2, respectivement, mesurés par I-ELISA, aux divers intervalles après le protocole d'immunisation (D27, D42, D91). Chaque courbe

IC-ELISA exprimé comme régression non linéaire de pourcentage de compétition. Les trois graphiques ont été obtenus en utilisant le modèle sigmoïdal (logistique) à quatre paramètres de GraphPad.

Dans le but d'évaluer si l'antisérum est capable de reconnaître la SelT dans les tissus biologiques, l'IC-ELISA a été appliqué aussi à des extraits protéiques de tissus de souris C57Bl/6 (Fig. 5).

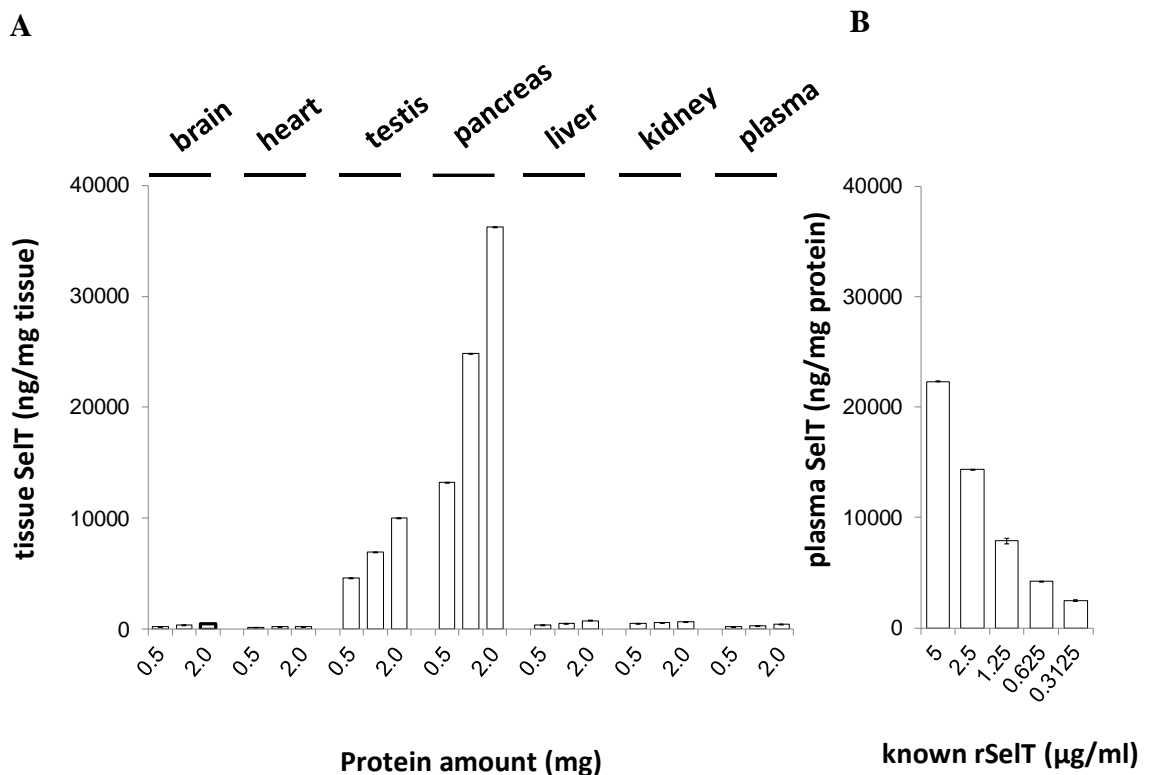


Fig. 5.A. Détection de la SelT par IC-ELISA dans les extraits protéiques de tissus de souris C57Bl/6 (cerveau, cœur, testicule, pancréas, foie, rein, plasma). **B.** Détection de SelT par IC-ELISA dans le plasma de souris C57Bl/6 pré-incubé avec différentes concentrations de rSelT (5-0.3125 µg/ml).

Les concentrations de SelT relevés au moyen d'IC-ELISA sont confirmées par le profil d'expression de la protéine dans les mêmes organes d'après les résultats rapportés précédemment par Tanguy et al., 2011 et Prevost et al., 2013. Ces résultats indiquent que l'essai ELISA développé pourrait représenter un outil à améliorer pour le développement d'un kit ELISA standardisé pour la quantification de la SelT dans le plasma et autres tissus.

D'autres études en cours visent à augmenter la sensibilité, la spécificité, et la précision du test dans le but d'obtenir une validation définitive du dosage.

3. Etudes cardiaques *ex vivo*

La troisième partie du travail a été réalisée pour étudier l'expression et la régulation de la SelT dans le cœur de souris durant l'ontogenèse et suite à un stress pathologique. En particulier, l'effet cardioprotecteur de la rSelT et par PSELT en tant qu'agent pharmacologique en post-conditionnement contre les dommages du myocarde induits par I/R, a été évalué dans un modèle de cœur de souris. Il est largement admis que chez les patients présentant un infarctus aigu du myocarde, l'extension de la zone infarctée pourrait être limitée par des interventions précoces de réperfusion du myocarde à travers l'intervention coronarienne percutanée (PCI). Toutefois, la restauration du flux sanguin après un épisode ischémique prolongé, peut aussi causer un dommage irréversible au myocarde dans un phénomène nommé "*dommage létal induit par réperfusion*" (Murphy and Steenbergen, 2008; Hausenloy and Yellon, 2004). Les interventions réalisées au début de la réperfusion pour préserver le tissu myocardique vital, sont décrits comme des traitements en post-conditionnement (Bice and Baxter, 2015). Pour les études cardiaques destinées à évaluer l'action pharmacologique post-conditionnement exercée par la rSelT et PSELT, nous avons utilisé le modèle du cœur de souris isolé et perfusé selon la méthode de Langendorff, et nous avons effectué des analyses d'immunohistochimie, western blot et ELISA.

Les premiers résultats intéressants montrent que la SelT est très abondante durant l'ontogenèse en phase embryonnaire dans le cœur de souris, alors qu'elle est réduite de manière significative chez les nouveau-nés et n'est pas détectée dans le cœur de l'adulte (**Fig. 6**). Par conséquent, la SelT pourrait avoir un rôle très important durant la croissance hyperplastique précoce des cardiomyocytes.

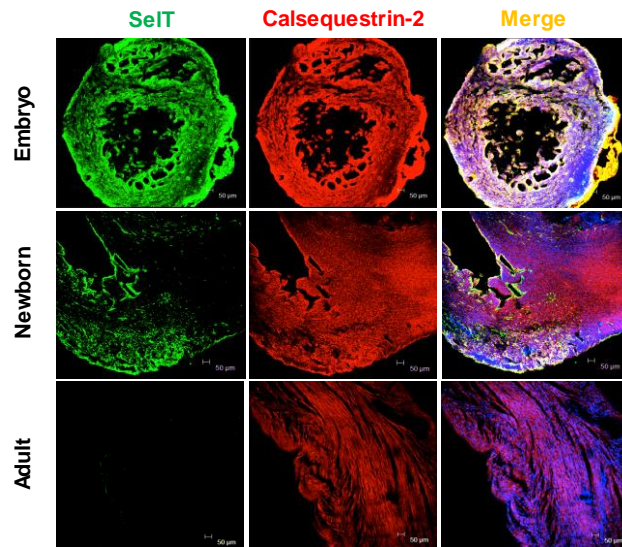


Fig. 6. Immunofluorescence de la SeIT et de la calsequestrine-2 sur des tissus embryonnaires (E7), nouveau-né (P14) et adulte (3 mois de vie) de cœur de souris. La calsequestrine-2 a été utilisée comme marqueur du réticulum sarcoplasmique cardiaque. Les noyaux ont été marqués en bleu avec une solution DAPI.

Dans le cœur adulte de souris arrivé en phase terminale de maturation, l'expression de la SeIT n'est pas essentielle sauf si le tissu est soumis à des conditions nocives comme un dommage par I/R, capable de déclencher une ré-expression de la protéine dans les cardiomyocytes (**Fig. 7**)

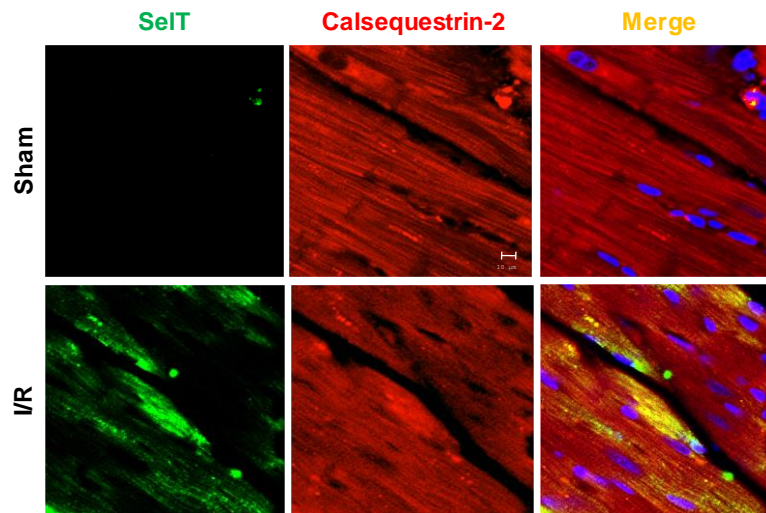


Fig. 7. Immunofluorescence de la SelT et de la calsequestrine-2 sur des tissus cardiaques soumis à un protocole Sham et I/R en ex vivo. La calsequestrine-2 a été utilisée comme marqueur de réticulum sarcoplasmique cardiaque. Les noyaux ont été marqués en bleu avec solution DAPI.

Ce résultat est en accord avec l'expression élevée des autres sélénoprotéines rencontrées au niveau du système nerveux (comme SelW, SelT et GPx) dans des conditions de stress particulières, comme celles associées à la protection contre le stress oxydatif (*Petit et al., 2003; Baek et al., 2005; Lee et al., 2008; Chung et al., 2009*).

Les études de cardioprotection ont démontré que PSELT à une dose de 5nM, correspondant à la valeur de l'EC₅₀ calculée en fonction des courbes concentration-réponse, et rSelT à la même dose, induisent une cardioprotection comme agents pharmacologiques en post-conditionnement, comme révélé par une récupération post-ischémique de la contractilité (développement significatif de la pression ventriculaire gauche, dLVP) (**Fig. 8A**) et de la réduction de la zone d'infarctus (IS) (**Fig. 8C**), sans variation de l'indice de contracture cardiaque (pression endo-diastolique ventriculaire gauche, LVEDP) (**Fig. 8B**). Par contre, un peptide contrôle sans le site catalytique redox contenant la Sec qui a été remplacé par un résidu Ser, n'a conféré aucun effet cardioprotecteur (**Fig. 8**), mettant en évidence le rôle essentiel de la Sec dans la cardioprotection conférée par la SelT.

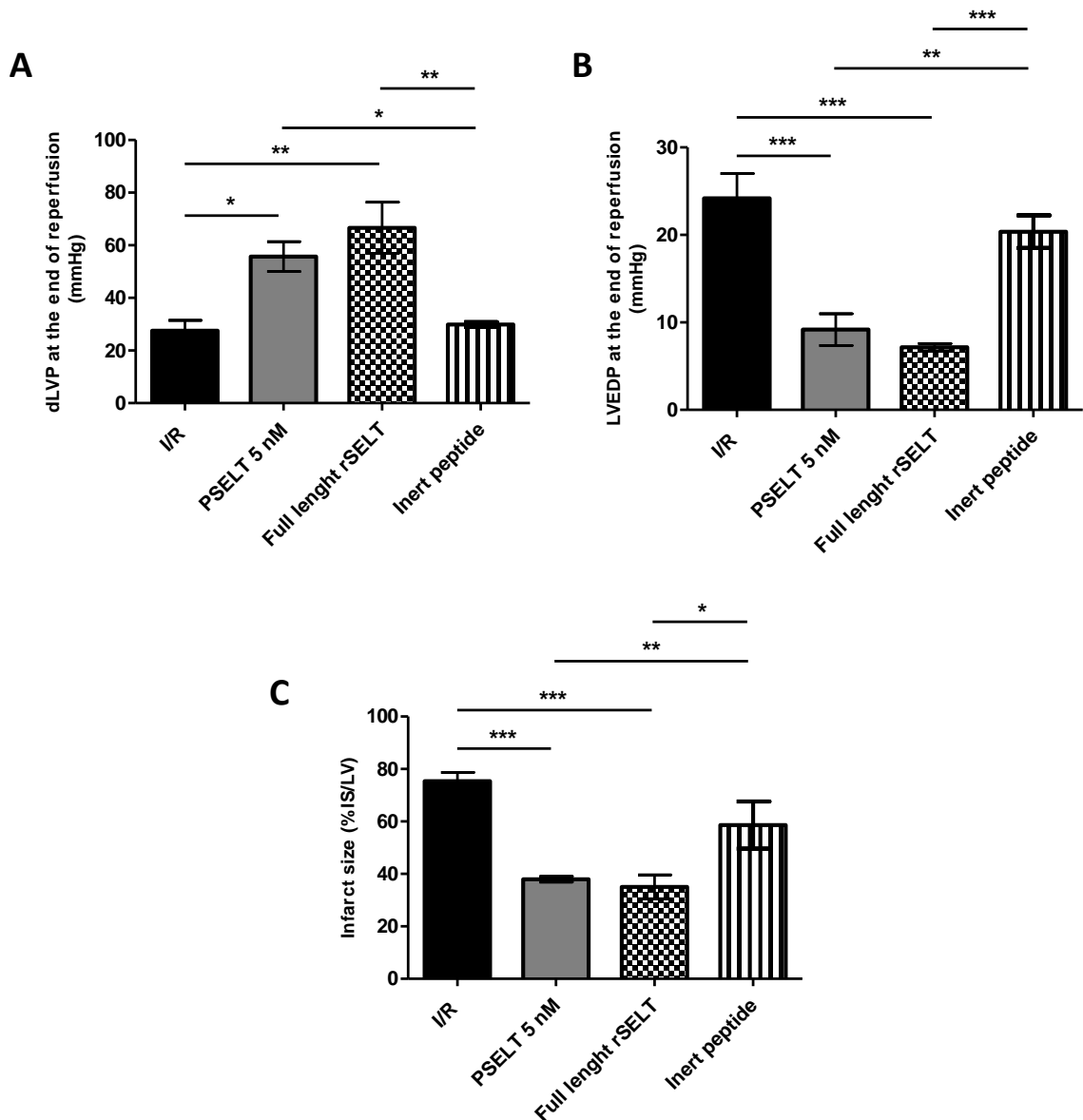


Fig. 8. A. Variation de dLVP e **B.** LVEDP. Les données sont exprimées comme la variation des valeurs dLVP et LVEDP (en mm Hg) à la fin de 120 min de réperfusion pour les cœurs soumis aux protocoles I/R et d' I/R en présence de PSELT 5 nM, PSELT inerte et rSelt. **C.** Zone d'infarctus de cœurs soumis aux protocoles d'I/R e de I/R in presence di PSELT 5 nM, PSELT inerte et rSelt. La quantité de tissu nécrotique après 30 min d'ischémie globale et 120 min de réperfusion est exprimée en pourcentage par rapport à la masse de ventriculaire gauche (LV) (% IS/LV). $p < 0,05$ (*), $p < 0,01$ (**), $p < 0,001$ (***), par One-Way ANOVA/Newman-Keuls Multiple Comparison Test.

Puisque PSELT et la rSelt à la même dose induisent une cardioprotection comparable, nous avons étudié le mécanisme d'action induit par le peptide. Les études de western blot ont

révélé que la cardioprotection s'accompagne d'une augmentation significative des niveaux de phosphorylation des kinases Akt, Erk1/2 et GSK3 α - β et une diminution du niveau de phosphorylation de la protéine p38MAPK. PSELT exerce son effet cardioprotecteur en inhibant des facteurs pro-apoptotiques comme Bax, la caspase 3 et le cytochrome c, et en stimulant en même temps le facteur anti-apoptotique Bcl-2. En outre, PSELT réduit significativement divers marqueurs du stress oxydatif et nitrosatif induits par l'I/R, qui contribuent aux dommages cardiaques provoqués par les radicaux libres comme les enzymes xanthines oxydases et aldéhydes oxydases et le produit de nitration 3-nitrotyrosine. Ces résultats ont permis de déterminer le rôle de la SelT comme modulateur cardiaque, et d'identifier rSelT et PSELT comme des agents pharmacologiques efficaces capables de protéger en post-conditionnement le myocarde suite à un dommage ischémique.

Summary

Selenoproteins represent a particular class of selenium-containing enzymes with specific chemical reactivity, functioning as intracellular redox sensors; these proteins are increasingly recognized as essential mediators for disease prevention, including cardiovascular pathologies. Among these proteins, Selenoprotein T (SelT or SELENOT) is a novel thioredoxin-like endoplasmic-reticulum (ER) enzyme whose genetic ablation in mice results in early embryonic lethality. SelT exerts an essential antioxidant and cytoprotective action in the brain during development and after injury, through its redox active catalytic site (Cys-X-X-Sec). Although a large body of evidence has now been accumulated showing that SelT affects, via its redox activity, the differentiation, function, the protection of nervous and endocrine cells in pathophysiological conditions, nothing is known about the expression and function of SelT in other vital organs such as the heart, which is normally severely exposed to oxidative stress, particularly as in the case of ischemia/reperfusion (I/R) damage. Therefore, the present doctoral project aimed to investigate, in a rat heart model, the pathophysiological cardiovascular implications of a recombinant form of SelT (rSelT) and its derived-peptide PSEL (SelT₄₃₋₅₂), chemically synthesized in its reduced form, which encompasses the key redox Cys-Val-Ser-Sec motif, and to evaluate the possible application of rSelT for the development of a specific immunoassay.

In the first part of the work, the production of a recombinant form of full-length rat SelT (rSelT) was optimized in *E. coli* cells; for this purpose, the cDNA corresponding to rat SelT was amplified from PC12 cells and cloned into the pGEM-T vector, and the protein was expressed as a His-tag fusion protein in *E. coli*. rSelT was purified under denaturing conditions and simultaneously renatured on-column by affinity chromatography.

Purified rSelT was detected as a protein band corresponding to the molecular weight of about 23 kDa. Re-folded rSelT exhibited a thioredoxin reductase (TrxR)-like enzymatic activity comparable to that of a control rat liver TrxR, dependent on the Cys/Ser residues of the thioredoxin-like fold, as demonstrated by the ability of a selective inhibitor (aurothiomalate) to abrogate the enzymatic activity of both rSelT and TrxR.

Selective immunoassays for some antigens and proteins are instrumental for biological studies and clinical applications. So far, a specific immunoassay to evaluate SelT amounts in biological samples is not available. The second part of the work aimed to develop a specific indirect competitive enzyme-linked immunosorbent assay (IC-ELISA), using the recombinant protein and a rabbit polyclonal antiserum against rSelT, as antigen and primary antibody, respectively. Immunization of two rabbits against the refolded rSelT allowed the production of a polyclonal antiserum, whose immunoreactivity was tested by western blot and its titer was determined by an indirect ELISA (I-ELISA) and by using rSelT-coated plates. Optimal working conditions for rSelT concentration and primary antiserum dilution were determined by checkerboard titration, using the hyperimmune rabbit antiserum collected at different times after immunization. The developed I-ELISA and IC-ELISA may constitute a valuable tool to discern SelT-negative and positive sera and to quantify SelT in plasma or tissues, respectively.

The third part of the project aimed to determine the expression and the regulation of SelT in the rat heart during ontogenesis and after a pathological stress. In particular, the cardioprotective effect of rSelT and of PSELT against I/R injury in a rat heart model, as postconditioning agents, has been evaluated. It is widely known that the patients presenting acute myocardial infarction, the infarct size can be limited by early myocardial reperfusion *via* percutaneous coronary intervention (PCI), in order to preserve the left ventricular systolic function and to improve clinical outcome. However, restoring blood flow after a prolonged ischemic episode, may also paradoxically cause irreversible damage to the myocardium in a phenomenon known as “lethal reperfusion-induced injury” (Murphy and Steenbergen, 2008; Hausenloy and Yellon, 2004). Interventions applied at the onset of reperfusion to salvage the viable myocardium, are described as *postconditioning* treatments (Bice and Baxter, 2015). With the purpose to identify an optimal application for a myocardial reperfusion recovery strategy, several animal and human models were used to demonstrate that the administration of pharmacologically active agents at the onset of the reperfusion induces cardioprotection, named *pharmacological postconditioning*. This represents an approach able to recruit or mimic the well-established pathways associated with *ischemic postconditioning*, a maneuver, whose cardioprotective effects are largely described (Hausenloy, 2009). For the cardiac study aimed to describe the pharmacological postconditioning action of rSelT and PSELT, the isolated Langendorff rat heart model was

used and immunohistochemical, western blot, and ELISA analyses were carried out. First, it was found that SelT expression is very abundant in rat embryo, but is undetectable in the adult rat heart; however, protein expression tremendously increased after I/R stress. Both exogenous PSELT at 5 nM, corresponding to the EC₅₀ concentration calculated on the basis of concentration-response curves, and rSelT were able to induce pharmacological post-conditioning, as evidenced by a significant post-ischemic recovery of contractility (developed Left Ventricular Pressure, dLVP) and a reduction of infarct size (IS), without changes in cardiac contracture (Left Ventricular EndoDiastolic Pressure, LVEDP). In contrast, exogenous PSELT at a higher dose (100 nM) showed a reduced ability to protect the heart after an I/R insult compared to the 5-nM dose, while a control peptide lacking the redox site (Inert PSELT), in which the Sec residue was replaced with a Serine (Ser), did not confer cardioprotection. Since both PSELT 5 nM and rSelT induced comparable cardioprotection, the detailed mechanism of action for PSELT was investigated. Immunoblot analysis showed that cardioprotection is accompanied by a significant increase of phosphorylated Akt, Erk1/2 and Gsk3 α - β , and a decrement of p38MAPK. PSELT inhibited the pro-apoptotic factors Bax, caspase 3 and cytochrome c, and stimulated the anti-apoptotic factor Bcl-2. Furthermore, PSELT significantly reduced several markers of I/R-induced oxidative and nitrosative stress, which contribute to free radical-mediated cardiac damage (i.e. xanthine oxidase, (XO), aldehyde oxidase-1, (AOX-1) and 3-nitrotyrosine, 3-NT). These results unraveled the role of SelT as a cardiac modulator and identified rSelT and PSELT as effective post-conditioning agents able to protect the heart after ischemic injury.

Overall:

- 1) The SelT immunoassays developed and related preliminary data indicate that this tool could be used for the immunodetection of SelT in physiological and pathological conditions.
- 2) The results obtained in the present doctoral project regarding the cardioprotective effects of rSelT and PSELT, provide new information on the implication of this protein and its derived peptide (redox site) in cardiac development, function and protection. These observations pave the way for future studies aimed to investigate the possible clinical relevance of rSelT and/or PSELT, which might represent a new class of drugs to be tested for reducing cardiac I/R injury. This is important in a medical context since it could allow

the development of new adjunctive therapies to be coupled with the reperfusion to reduce morbidity and mortality.

Introduction

1. Selenium and Selenocysteine in protein chemistry

1.1 Selenium: biochemistry and physiology

Selenium (Se) is an essential micronutrient incorporated into selenoproteins. It has pleiotropic effects, ranging from antioxidant and anti-inflammatory effects to the synthesis of thyroid hormones (*Rayman, 2012*). The beneficial actions of selenium for the human health are clinically relevant and widely recognized with growing interest in understanding its biologic role for the prevention of diseases, and its potential use as a therapeutic agent (*Rayman, 2012*).

Compared with many other micronutrients, selenium intake varies in the world, ranging from deficit associated with selenium-deficiency diseases to harmful concentrations that may cause several disorders, such as alteration of the nervous system and paralysis (*Johnson et al., 2010*).

The effects of selenium are concentration-dependent, resulting in an essential antioxidant impact in the nanomolar-micromolar range to potentially pro-oxidant effects at concentrations above that required for maximal selenoprotein synthesis. At even higher levels, selenium compounds may accumulate and generate reactive oxygen species (ROS) in redox cycles with intracellular thiols, leading to oxidative stress and cellular damage, with consequent toxic effects (*Vinceti et al., 2001*). Recommendations for selenium intake average 60 µg per day for men and 53 µg per day for women (*Rayman, 2004*). Foods represent the major natural source of selenium and the reasons for the variable intake regard the soil selenium content and factors that determine its availability to the food chain including selenium speciation, soil pH and organic-matter content, and the presence of ions that can complex with selenium (*Johnson et al., 2010*). An additional very important aspect is that foods provide selenium in distinct combinations of chemical forms which in turn entail a different bioavailability (*Rayman et al., 2008*). The most important selenium species in vegetables are represented by selenomethionine (SeMet) and selenate/selenite (SeO_4^{2-} , SeO_3^{2-}); minor species are selenocysteine (Sec), Se-methyl-selenocysteine (SeMCys) and gamma-glutamyl-Se-methylselenocysteine (GGSeMCys) (*Rayman et al., 2008*). Selenate/ite, SeMet and SeCys are the most important species in animal products, with

widely variable proportions depending on the animal's diet (Rayman *et al.*, 2008). A simplified overview of selenium metabolism in mammals is represented in **Fig.1**.

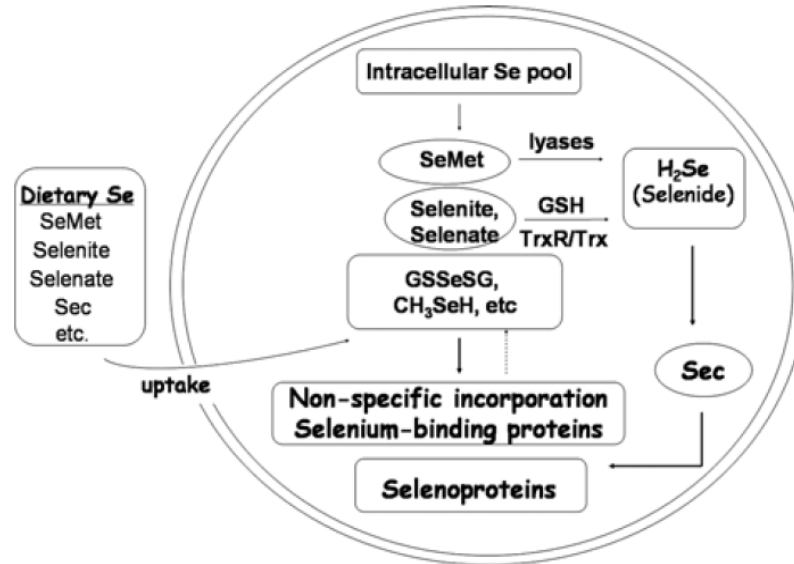


Fig. 1. Selenium metabolism in mammalian. Dietary selenium metabolites are internalized into the cell, where, together with the existing intracellular pool, they become metabolized by different pathways, to yield selenide, which serves as the selenium source for Sec biosynthesis. (Se, selenium; GSSeSG, selenodiglutathione; CH₃SeH methylselenol; H₂Se selenide; SeMet, selenomethionine; Sec, selenocysteine; GSH, glutathione; TrxR, thioredoxin reductase; Trx, thioredoxin).

Until few years ago, most of the studies focusing on selenium status assessment evaluated only the total level of the element in tissues or body fluids. Plasma or serum selenium concentration was generally considered a biomarker of both selenium status and dietary intake in the short-term, while erythrocyte selenium better reflects the long-term status (Thomson, 2004). However, recently, it has been established that the total selenium concentration is not a complete representative index of the real functional activity of this micronutrient, because the element is incorporated in a large variety of proteins with different biological functions (Thomson, 2004); in addition, the distribution of selenium among selenoproteins is strongly dependent on a hierarchy in its incorporation, the average dietary intake, the speciation of selenium in food, health condition, age, other environmental factors and genetic polymorphism of selenoproteins (Kryukov *et al.*, 2003).

In this regard, the two plasma/serum selenoproteins, namely selenoprotein P (SeP) and the isoform 3 of glutathione peroxidase (GPx3) are the most commonly used markers for the assessment of selenium status also because they can be determined with a not invasive procedure compared to tissue selenoproteins, which requires a biopsy (*Roman et al., 2014*). Plasma SeP has been proposed as a biomarker (*Hurst et al., 2010*); however, the concentration of SeP mostly reflects the short-term status of selenium in the organism because it has a plasma half-life of about 3-4 hours in the rat (*Burk and Hill, 2005*). The activity of GPx3, as well as the erythrocyte isoform 1 of glutathione peroxidase (GPx1), are well correlated with the total level of selenium in the blood (*Thomson, 2004*). Notably, the choice of a selenoprotein as biomarker must consider its specific biological function, which therefore provides partial information in terms of selenium bioactivity. In fact, the most effective biomarker should not be a single protein, but a set of combined parameters, applied to a specific problem associated with optimal selenium status, including an analysis of health parameters, endocrine and immunological status, selenoprotein polymorphism and other genetic and environmental variables; so far, this is considered as the most important and promising approach for this purpose (*Reszka et al., 2012*).

1.2 Selenocysteine (Sec): reactivity and selectivity

Selenium represents a component of selenocysteine (Sec, U), the 21st amino acid in the genetic code (*Atkins and Gesteland, 2000, Böck et al., 1991*) and 5-methylamino-2-selenouridine, a modified base found in transfer RNAs (tRNAs) of some prokaryote species (*Wittwer et al., 1984*). Among the trace elements used as cofactors for enzymes, selenium has unique properties. Unlike metal cofactors such as zinc and copper, it is actually part of the polypeptide chain as part of an amino acid. Sulfur and selenium are members of the chalcogen group of elements, in which selenium occupies the position immediately below sulfur on the periodic chart. Thus, the two elements have very similar chemical-physical properties, and can be involved in similar chemical reactions such as thiol/disulfide (and thiol-disulfide-like, that is selenol/disulfide or thiol/selenosulfide when selenium replaces sulfur) exchange reactions (*Wessjohann et al., 2007*). Unlike methionine, in which sulfur is in a relatively less reactive thioether form, the thiol group of cysteine is ionizable, with a negatively charged thiolate group generated after deprotonation, and this improves its

reactivity (**Fig. 2A,B**) (Poole, 2015). In addition, this thiol/thiolate group undergoes alkylation by electrophiles and oxidation by ROS and reactive nitrogen species (RNS), with consequent post-translational modifications that significantly alter its functions (Poole, 2015). The most important characteristic of Sec is its unique localization in catalytic sites of enzymes. In selenoproteins, Sec function is partially preserved only when cysteine (Cys) replaces Sec; however, in most cases, the substitution of Sec with Cys leads to a marked reduction in catalytic efficiency (Hondal *et al.*, 2013). Considering the functional predominance of Sec in proteins, many studies have been carried out to investigate its role and the exact nature of its chemical properties. A common view is that, since Sec and Cys differ for a single atom, the presence of selenium provides some superior chemical or physical properties, improving the functions of macromolecules (Hondal *et al.*, 2013).

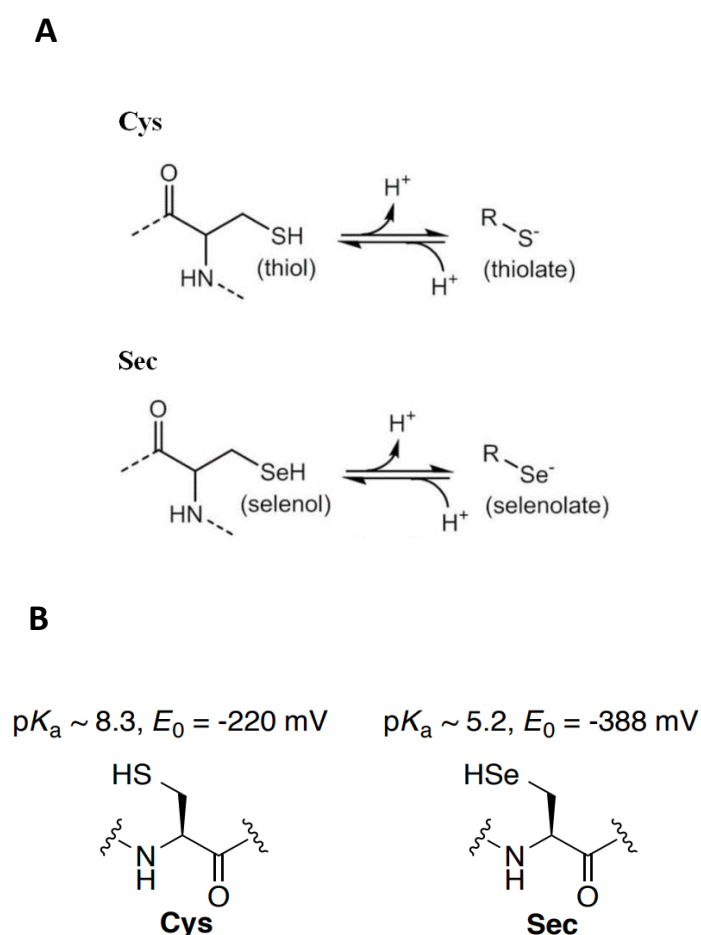


Fig. 2. A. Protonated (left) and deprotonated (right) forms of Cys and Sec **B.** Comparison of Cys and Sec structures, pK_a values, and redox potentials.

The unique chemical-physical characteristics of Sec are related to its relatively low pKa value (5.2), with respect to the pKa of cysteine (Cys) (8.3) (*Huber, 1967*); this implies that most of the side chain selenols are deprotonated at physiological pH; another fact regards the lower redox potential of Sec, ($E_0 = -388$ mV), (*Nauser et al., 2006*) compared to that of Cys ($E_0 = -220$ mV) (*Jocelyn., 1967*) (**Fig. 2**). Consequently, Sec is readily oxidized under physiological conditions to form the diselenide dimer, Sec. In addition, the largest atomic ray of selenium makes it highly polarizable, allowing it to act both as an electrophile and a nucleophile (*Steinmann et al., 2010*). These chemical properties confer to Sec its higher reactivity with respect to Cys, as also indicated by the higher catalytic activity exerted by the Sec-containing enzymes, which are typically 100- to 1000-fold more active than their cysteine (Cys) mutants (*Kim and Gladyshev, 2005*). This has been considered the reason for the presence of Sec in biological systems. However, some selenoproteins have orthologs in which Cys is used in place of Sec, and are catalytically competent as selenoproteins (*Kim and Gladyshev, 2005*).

1.3 Sec biosynthesis

1.3.1 Sec tRNA^{[Ser]Sec}

The majority of selenium biological effects are elicited by selenoproteins (*Atkins and Gesteland, 2000*). Sec-containing proteins are present in all evolutionary lines: eukarya, archaea, and eubacteria, as well as in certain types of viruses (*Labunskyy et al., 2014*). The pathway for Sec biosynthesis was revealed only in the last years by using different approaches based on a combination of comparative genomic, molecular, and structural analyses. The genetic code is redundant; thus, the translational termination is encoded by UGA, UAA, and UAG (*Voet et al., 1999*). However, in mitochondria, UGA encodes for tryptophan (*Osawa et al., 1992*), and in the nuclear genome, UGA also encodes for Sec. Thus, Sec is considered the 21st genetically encoded amino acid translated into proteins by reading of the UGA codon (*Lee et al., 1989*). Sec is incorporated into protein by a tRNA molecule with an anti-codon complementary to UGA. Unlike the other 20 amino acids, an important property of Sec is that it is universally synthesized on its own tRNA designated as Sec tRNA^{[Ser]Sec} (*Leinfelder et al., 1989; Lee et al., 1989*). Sec tRNA^{[Ser]Sec} controls the expression of all the selenoprotein family, a process that is not reported for any other tRNA

species. For Sec biosynthesis, tRNA^{[Ser]^{Sec}} is firstly aminoacylated with serine in a reaction catalyzed by seryl-tRNA synthetase (SerRS) to form seryl-tRNA^{[Ser]^{Sec}}, and this provides the backbone for Sec biosynthesis (Lee et al., 1989; Leinfelder et al., 1989).

The biological characteristics of tRNA^{[Ser]^{Sec}} make this tRNA different from all other tRNAs (Hatfield et al., 1994). The structures of tRNA^{[Ser]^{Sec}} from *E. coli*, *M. jannaschii*, and *H. sapiens* are represented in clover leaf models in **Fig. 3**.

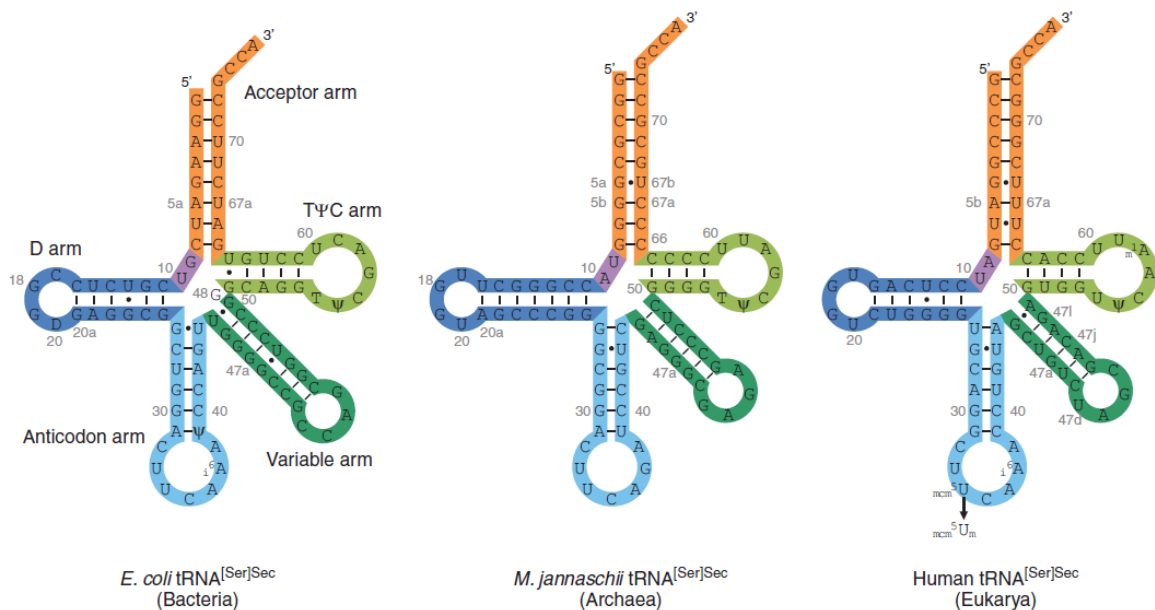


Fig. 3. Clover leaf models of eukaryotic, archaeal, and bacterial tRNAs^{[Ser]^{Sec}}

The gene for tRNA^{[Ser]^{Sec}} is designated as *Trsp*; it is a single copy gene involved in selenoprotein synthesis machinery. Human *Trsp* is localized on chromosome 19q13.2 → q13.3 (Mitchell et al., 1992). Aminoacylation of tRNA^{[Ser]^{Sec}} with serine (Ser) represents the first reaction which leads to Sec biosynthesis in eubacteria and eukaryotes (Labunskyy et al., 2014).

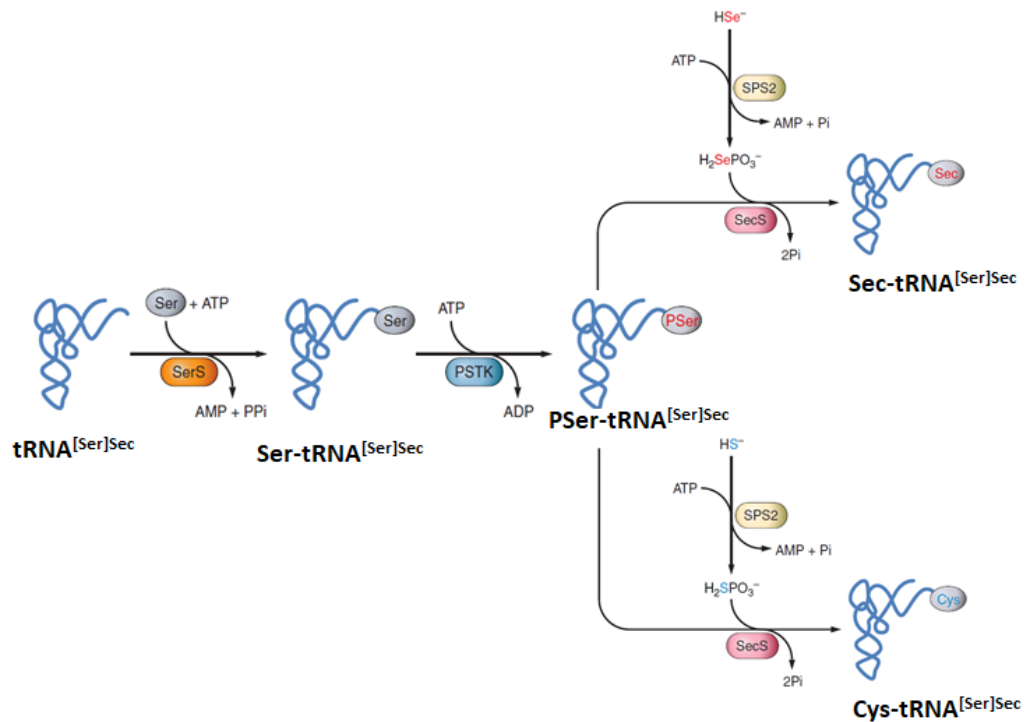


Fig. 4. Mechanism of Sec biosynthesis in eukaryotes and the Sec machinery-based pathway for synthesis of Cys. Phosphoserine-tRNA kinase (PSTK) provides the phosphorylated intermediate P-Ser-tRNA^[Ser]Sec used as a substrate for Sec synthase (SecS). Selenophosphate ($H_2SePO_3^-$) generated by Selenophosphate Synthetase-2 (SPS2) from selenite and ATP is used as a donor of active selenium for SecS. The de novo synthesis of Cys using the Sec biosynthetic machinery is shown on the bottom right.

The conversion of Ser on tRNA^[Ser]Sec to selenocysteyl-tRNA^[Ser]Sec is catalyzed by the enzyme Sec synthase (SecS), which incorporates selenophosphate into the amino acid backbone forming Sec-tRNA. For details, see **Fig. 4**. The essential functional role of SecS in Sec biosynthesis on its tRNA is corroborated by a recent finding of two different homozygous mutations in the *SecS* gene in humans (Agamy *et al.*, 2010), which were associated with progressive cerebello-cerebral atrophy in these patients. Despite the lack of tRNA^[Ser]Sec as a result of the whole-body *Trsp* gene *knockout* in mice results in embryonic lethality, patient mutations in *SecS* have been associated with a less dramatic phenotype (Wirth *et al.*, 2010). Based on the SecS structure, these mutations should be involved into the disruption of protein folding and catalytic activity of SecS (Wirth *et al.*, 2010).

1.3.2 Selenophosphate Synthetase

Selenophosphate synthetase (SPS) is involved in the *de novo* synthesis of selenophosphate and in Sec recycling through a selenium salvage system (Xu *et al.*, 2007). In addition to its role in Sec biosynthesis, SPS has been implicated in Cys biosynthesis (Xu *et al.*, 2010). In this context, it is important to note that Cys mutants of selenoproteins partially preserve their activities whereas other mutations disrupt their functions. Moreover, Cys was observed in place of Sec in several selenoproteins (i.e. TrxR1) in rodents subjected to selenium deprivation (Lu *et al.*, 2009). During selenium deficiency, SPS is able to use sulfide instead of selenide and generate thiophosphate (H_2SPO_3^-) as an active donor for the reaction catalyzed by SecS (**Fig.4**). SecS then makes Cys tRNA^{[Ser]Sec} from H_2SPO_3^- and O-phosphoseryl-tRNA^{[Ser]Sec} intermediates, and Cys is further inserted into selenoproteins at the UGA-encoded sites instead of Sec. Since Cys is an essential amino acid in mammals, the synthesis of Cys on tRNA^{[Ser]Sec} is a novel *de novo* pathway for the synthesis of this amino acid (Xu *et al.*, 2010).

1.3.3 Sec Lyase

Sec degradation is mediated by the enzyme Sec lyase (SCL), in a PLP-dependent reaction, where Sec is converted to L-alanine and elemental selenium (Mihara *et al.*, 2000). SCL is highly conserved across species and is expressed in several tissues with the highest activity observed in liver and kidney; during its catalysis, SCL is able to discern Sec from Cys and Ser residues (Omi *et al.*, 2010). Despite the role of SCL in selenium recycling from Sec, this enzyme seems to be involved in other processes, but its physiological function remains not completely understood.

1.4 Sec incorporation into proteins

Unlike the common process of tRNA aminoacylation, Sec is co-translationally incorporated into proteins due to the in-frame UGA codons present in selenoprotein mRNAs and this requires the formation of a quaternary complex (Leibundgut *et al.*, 2005). In particular, Sec is introduced into selenoproteins by a complex mechanism that requires the Sec-tRNA^{[Ser]Sec}

and several factors, including special *trans*-acting proteins and a *cis*-acting Sec insertion sequence (SECIS) element (Leibundgut et al., 2005) (Fig.5).

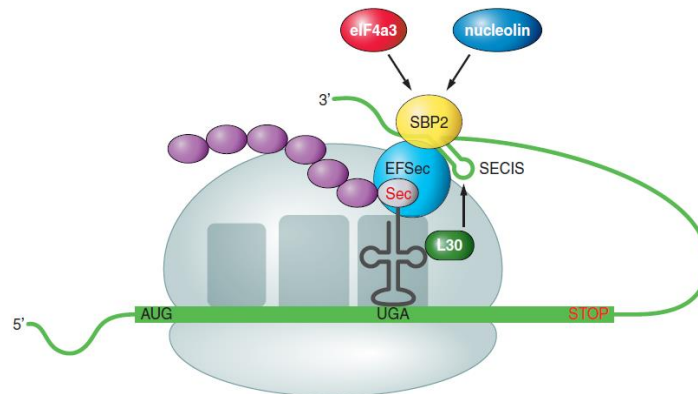


Fig. 5. Mechanism of Sec insertion in eukaryotes, showing the factors required for Sec incorporation into proteins in response to the UGA codon.

SECIS elements are *cis*-acting stem-loop RNA structures found in the 3'-untranslated regions of the mRNAs (Low et al., 1996); these elements are located immediately downstream of the UGA triplet nucleotide encoding Sec, within the coding region of selenoprotein genes (Böck et al., 2006). SECIS elements are factors that dictate recoding of UGA as Sec (Böck et al., 2000). In response to the SECIS element in selenoprotein mRNA, Sec-tRNA^{[Ser]Sec}, which has an anticodon complementary to UGA, translates UGA as Sec. In this complex process, at least two *trans*-acting factors are required for efficient recoding of UGA as Sec in eukaryotes: the SECIS binding protein-2 (SBP2) and the Sec-specific translation elongation factor (eEFSec). SBP2 is strongly associated with ribosomes and, via a specific RNA-binding domain in the central part of the protein, binds SECIS elements with high affinity and specificity (Copeland et al., 2000). SBP2 also interacts with eEFSec, which is involved in the recruitment of Sec-tRNA^{[Ser]Sec} and allows the incorporation of Sec into the nascent, growing polypeptide (Tujebajeva et al., 2000). Instead of SBP2 and eEFSec, bacteria use a Sec-specific translation elongation factor (named selenoprotein B, SelB in *E. coli*) which directly recognizes SECIS and is required for the binding and the delivery of the SECIS elements to the ribosome (Fagegaltier et al., 2000). SBP2 may be considered a

limiting factor for selenoprotein synthesis; in fact, it has been demonstrated that the *knockdown* of SBP2 in mammalian cells, by using siRNA, is associated with a significantly decreased expression of selenoproteins (*Papp et al., 2006*), while overexpression of SBP2 has been shown to enhance Sec incorporation (*Low et al., 1996*). These findings are supported by recent data regarding homozygous missense mutations in the *SBP2* gene in patients with hypothyroidism caused by defects in the synthesis of type 2 deiodinase (DIO2), a selenoprotein involved in thyroid hormone activation (see later) (*Dumitrescu et al., 2005*). This mutation impaired the SBP2-SECIS elements binding, which is necessary for the Sec insertion into selenoproteins with a consequent defective synthesis of some selenoproteins, including DIO2, GPx1, and SelP (*Bubenik et al., 2007*). Other SECIS-binding proteins include ribosomal protein L30, eukaryotic initiation factor 4a3 (eIF4a3) and nucleolin (*Labunskyy et al., 2014*). It is important to emphasize that the requirement of several specialized factors that take part to the incorporation of Sec into proteins, suggests the evolutionary importance of selenoproteins, as well as the complexity of this biological process. An overview of selenoprotein synthesis is shown in **Fig.6**.

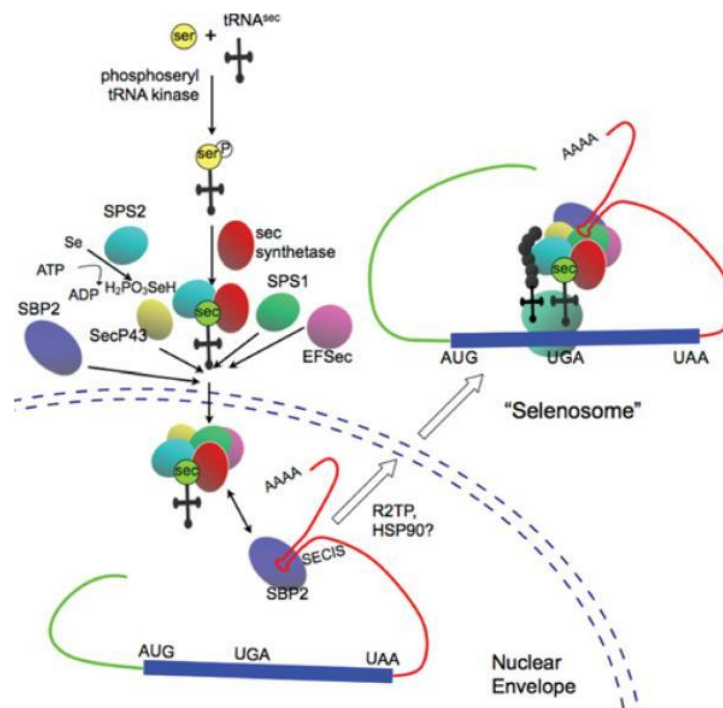


Fig. 6. Machinery involved in synthesis of selenoproteins. Selenium phosphorylated by SPS1 is used to synthesize Sec from serine directly on the tRNA^{Sec} by the enzyme Sec synthetase (SecS). tRNA^{Sec} is transported

to the nucleus with many cofactors bound. The protein SBP2 binds to the SECIS element in the 3-UTR of selenoprotein mRNAs, and recruits the tRNA^{Sec} complex along with bound cofactors. The assembled complex is transported from the nucleus for translation to protein (HSP90, heat-shock protein 90).

2. Structure and activity of mammalian selenoproteins

The early periods of selenoprotein research, were characterized by different experimental approaches aimed to analyze the presence of selenium by mass spectrometry and detection of radioactive ⁷⁵Se, metabolically incorporated into proteins in the form of Sec (Ballihaut et al., 2007). The first selenoprotein identified was the mammalian glutathione peroxidase 1 (GPx1) (Flohe et al., 1973), followed by the discovery of bacterial glycine reductase (Turner and Stadtman, 1973) and formate dehydrogenase (Andreesen et al., 1973). Subsequently, thanks to a combination of bioinformatic and experimental approaches, a number of selenoproteins have been identified in all life kingdoms and the full human selenoproteome encoded by 25 selenoprotein genes was characterized (Kryukov et al., 2003) (Fig. 7).

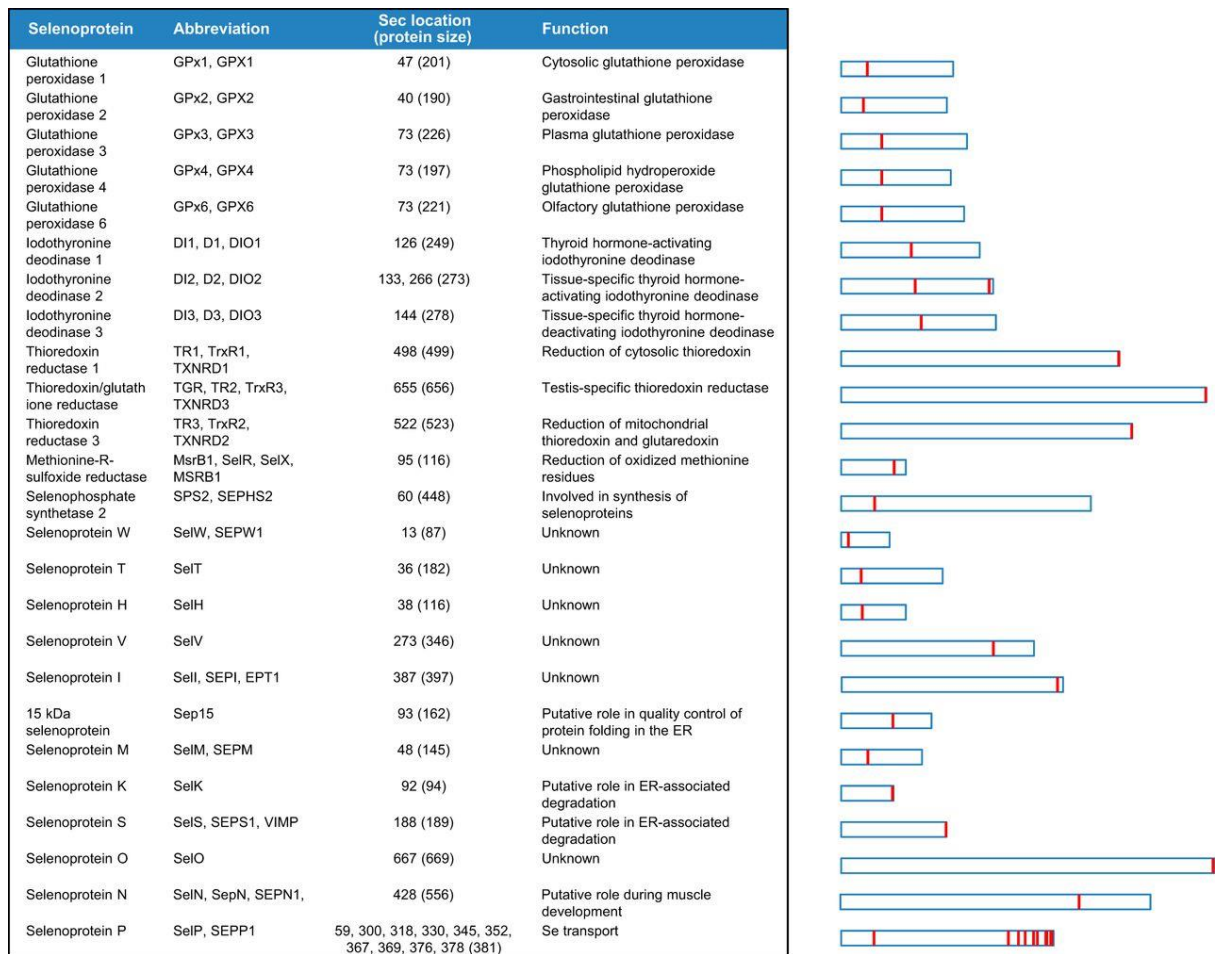


Fig. 7. Human selenoproteome. The relative length of selenoproteins and location of Sec within different proteins are shown on the right.

Since the selenoprotein genes contain UGA codons, these proteins are often misannotated in sequence databases (*Kryukov et al., 2003*). An experimental approach was based on the two characteristic genomic features typical of selenoproteins, the in-frame UGA codon encoding Sec residue and the SECIS element (*Labunskyy et al., 2014*). By searching candidate SECIS elements in completely sequenced genomes, and by analyzing the genomes of strongly related species for evolutionarily conserved SECIS elements belonging to orthologous selenoproteins, it was possible to identify selenoprotein genes through analyses of upstream coding sequences containing UGA (*Labunskyy et al., 2014 and references therein*). In a second approach, selenoproteins were identified by searching the in-frame UGA codons through analyses of sequences near to UGA in genomes which were completely sequenced (*Labunskyy et al., 2014 and references therein*). Considering that

almost all selenoproteins contain homologs in which Sec is replaced with Cys, this approach allowed the identification of selenoproteins independent from searching for SECIS elements (Labunskyy *et al.*, 2014).

Selenoproteins are found in bacteria, archaea and eukaryota. However, some organisms do not use Sec, such as yeast and some plants, which lost the Sec insertion machinery during evolution (Lobanov *et al.*, 2009). Based on the Sec location, mammalian selenoproteins can be classified into two groups (Fig. 8).

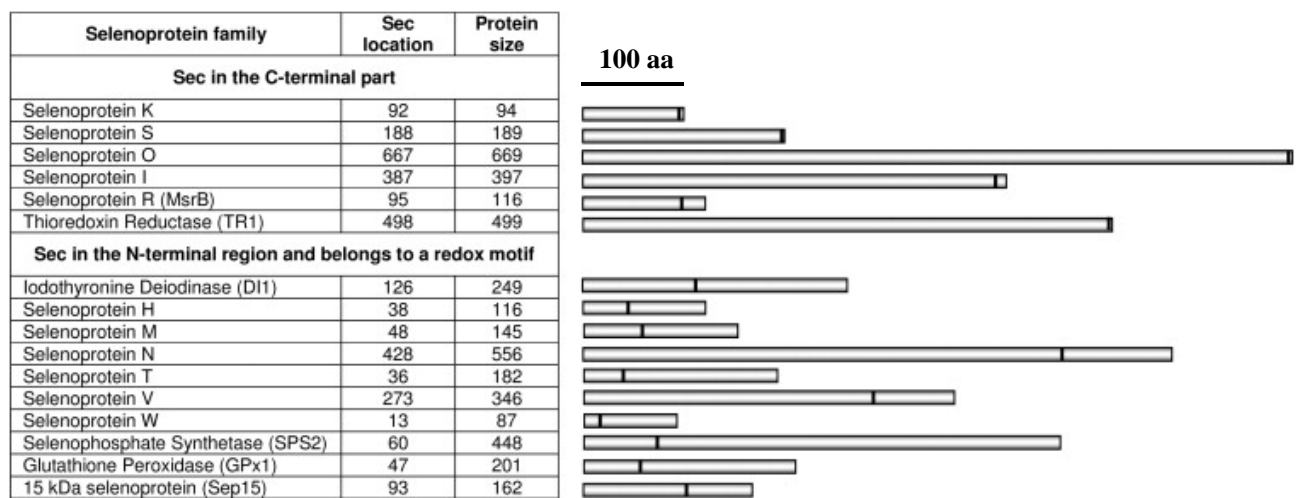


Fig. 8. Mammalian selenoproteins divided on the basis of Sec location. In one group Sec is located very close to the C-terminus, often in the C-terminal penultimate position. In the second group Sec is located in the N-terminal or middle regions of selenoproteins, often in a redox motif within a thioredoxin fold and have an α -helix downstream of Sec. Selenoprotein P, which has both an N-terminal redox Sec and multiple Sec residues in the C-terminal region (see fig.7), is not shown in this figure. Sec positions and selenoprotein lengths refer to human proteins. Close homologs of GPx1 (four selenoproteins), DI1 and TR1 (two each) are not shown.

One group of selenoproteins such as TrxRs and selenoproteins S, R, O, I, and K contains Sec in a site very close to the C-terminus of the protein. The other group [(including Glutathione Peroxidases (GPxs); Iodothyronine Deiodinases (DIOs); selenoproteins H, M, N, T, V, and W, SPS2, and selenoprotein Sep15)] has Sec in the N-terminus, often it has a thioredoxin fold structure, and some selenoproteins contain a C-X-X-U motif, corresponding to the thioredoxin catalytic active-site (Lu and Holmgren, 2009 and references therein).

Considering their structure, a key characteristic of all selenoproteins is the presence of Sec residues; except some cases, this amino acid is located in the enzyme active sites, whose function is to perform catalytic redox reactions (*Arnér, 2010*).

2.1 Selenoproteins as ROS-detoxifying enzymes

2.1.1 Oxidants generation and oxidative stress

On the basis of its electrochemical properties, molecular oxygen (O_2) is a potent oxidizing agent. When, at physiological temperature conditions an electron is added to form the superoxide radical ($O_2^{\bullet-}$), oxygen becomes much more reactive (*Fallab, 1967*). Under aerobic condition, cells continuously react with ROS, such as $O_2^{\bullet-}$, H_2O_2 , lipid and hydroxyl radical (OH^{\bullet}), which derived from several metabolic reactions and counteract their effects through a wide range of antioxidant enzymes (*Fallab, 1967*). ROS can damage all cellular macromolecules; thus, harmful effect of these species occurs thanks to their ability to react with the Cys and Met residues present in proteins structure, thus inactivating their function, and to react with DNA and chromatin to cause mutations or double-stranded breaks in a phenomena overall known as “oxidative damage” (*Hoshi and Heinemann, 2001*). The current concept of “oxidative damage or oxidative stress” include pathways related to the “nitrosative stress” and, considering their implication in cellular and extracellular metabolic processes, to the “metabolic stress” (*Rahman et al., 2012*). So far, the definition of oxidative stress confined to ROS has been also extended to RNS, such as nitric oxide (NO), peroxynitrite ($ONOO^-$) and S-nitrosothiols (RSNO) (*Rahman et al., 2012*).

Cells have potent antioxidative systems for ROS detoxification and for repair of deleterious oxidative modifications on cellular structures (*Sies, 1986*). High and persistent ROS levels and/or inadequate antioxidant protection results in oxidative stress, cytotoxicity and apoptosis. However, little changes of oxidation–reduction (redox) cellular homeostasis are normally sufficient to activate a redox response-stress related pathway based on the upregulation and activation of protective enzymes (*Winterbourn and Hampton, 2008*). The redox signaling is an important part of the physiological cellular metabolism and it is an essential step in many signaling processes in not-stressed cells (*Stone and Yang, 2006*); in fact, several hormones, growth factors and cytokines induce ROS production in their

receptor-dependent mechanism of action. Based on the involvement of low ROS levels as part of intracellular signaling, the definition of oxidative damage has been recently refined as a “disruption of redox signaling and control” (*Sies and Jones, 2007*).

Therefore, it is widely accepted that an increase of the ROS and RNS-mediated oxidative damage to DNA and other biomolecules may impair the physiological functions of cells and tissues, leading to metabolic damage as the base for human aging and disease (*Beckman and Ames, 1999*). Accordingly, oxidative stress has been associated with diverse pathophysiological events, including cancer, renal disease, immunological pathologies, neurodegeneration and cardiovascular disease (*Griendling and FitzGerald, 2003*). Short-term oxidative stress may occur in tissues after exposition to specific stimuli, such as acute injury, infection and toxins. These injured tissues increase their expression of radical generating enzymes (i.e. xanthine oxidase and cyclooxygenase) activation of phagocytes, release of free iron, alteration in the electron transport chains of oxidative phosphorylation, leading to an excess of ROS production (*Nathan and Cunningham-Bussel, 2013*). The promotion and progression of complex and multifactorial pathologies, as well as the side-effects of specific therapeutic regimes, are linked with a dramatic imbalance between ROS and the antioxidant defence system (*Nathan and Cunningham-Bussel, 2013*).

2.1.2 Antioxidant activity of selenoproteins

The precise functions of many selenoproteins are still unknown. In general, all selenoproteins with a known enzymatic activity, catalyse redox reactions by involving the oxidation of sulfhydryl groups and/or reduction of disulfides (**Fig. 9**); as ROS-detoxifying enzymes, selenoproteins belong to an array of antioxidants with different specific subcellular localization and chemical reactivities (*Steinbrenner and Sies, 2009*). In this context, all these antioxidant systems might exist in some hierarchical network or redox circuit, whose function is to maintain the overall cysteine proteome and the intracellular redox homeostasis (*Jones and Go, 2011*). In the mechanism of action mediated by selenoproteins in the H₂O₂ neutralization, these enzyme act through their unique ability to trap and reduce H₂O₂ in a reaction mediated by selenols (R-Se-H) to give selenenic acid (R-Se-OH, where R ≠ H), which is then used to form specific disulfide bonds in the presence of

GSH; selenols are re-reduced by thiol-containing enzymes (*Winterbourn and Hampton, 2008*). Therefore, selenoproteins are well suited for controlling the formation of disulfide bonds with specific Cys residues. In this process, due to the rapid oxidation kinetics of selenols, H₂O₂ in the cytosol completely reacts with Sec-containing proteins to produce Sec selenenic acid before it can react with other potential targets (*Winterbourn and Hampton, 2008*). Consequently, the ability of selenoproteins to rapidly consume and neutralize H₂O₂, result in a significant decrease of H₂O₂ levels and in a limitation of the space for its signal transmission by diffusion in the cell (*Winterbourn and Hampton, 2008*).

2.2 Pathophysiological implications of selenoproteins

Selenoproteins are involved in many biological processes that are essential for life; therefore, this class of enzymes is considered critical for disease prevention, as in the case of cardiovascular disease, neurodegeneration, liver disease, cancer, immune and endocrine disorders (*Papp et al., 2007*). However, considering that the function of many mammalian selenoproteins is not completely known, their therapeutic potential so far has only limited applications (*Papp et al., 2007*). Many developed organoselenium compounds were tested as antioxidants, immunomodulators, anticancer and antihypertension agents. In this context, the organoselenium drug *ebsele*n received particular attention, since it mimics the action of GPx (*Muller et al., 1984*). It is considered a peroxiredoxin-like agent, whose target is the thioredoxin system (*Zhao and Holmgren, 2002*); in fact *ebsele*n is reduced to selenol by TrxR or Trx and reoxidized by peroxides, including H₂O₂. *Ebsele*n revealed a significant action against H₂O₂ and smaller organic hydroperoxides with neuroprotective, antioxidant and anti-inflammatory actions in a rat model of transient cerebral artery occlusion (*Dawson et al., 1995*). These properties allowed an application of *ebsele*n in the treatment of patients with acute ischemic stroke (*Papp et al., 2007 and references therein*). Another important selenoenzyme of clinical interest is TrxR, another suitable target for anticancer therapies. It is required for cancer cell proliferation, it is highly expressed in cancer cells, and shows an active site that is accessible for reaction with reactive compounds (*Papp et al., 2007*). Moreover, it has been demonstrated that many of the clinical anticancer drugs, such as cisplatin (*Arnér et al., 2001*), diaziquone and doxorubicin are excellent inhibitors of

TrxR. This may pave the way for TrxR potential applications in cancer treatment (*Mau and Powis, 1992*).

Overall, TrxRs, GPxs and DIOs are the three-best characterized selenoprotein families. They have different enzymatic activities, but all require reductants to provide the electrons for their catalytic redox cycle (**Fig. 9**).

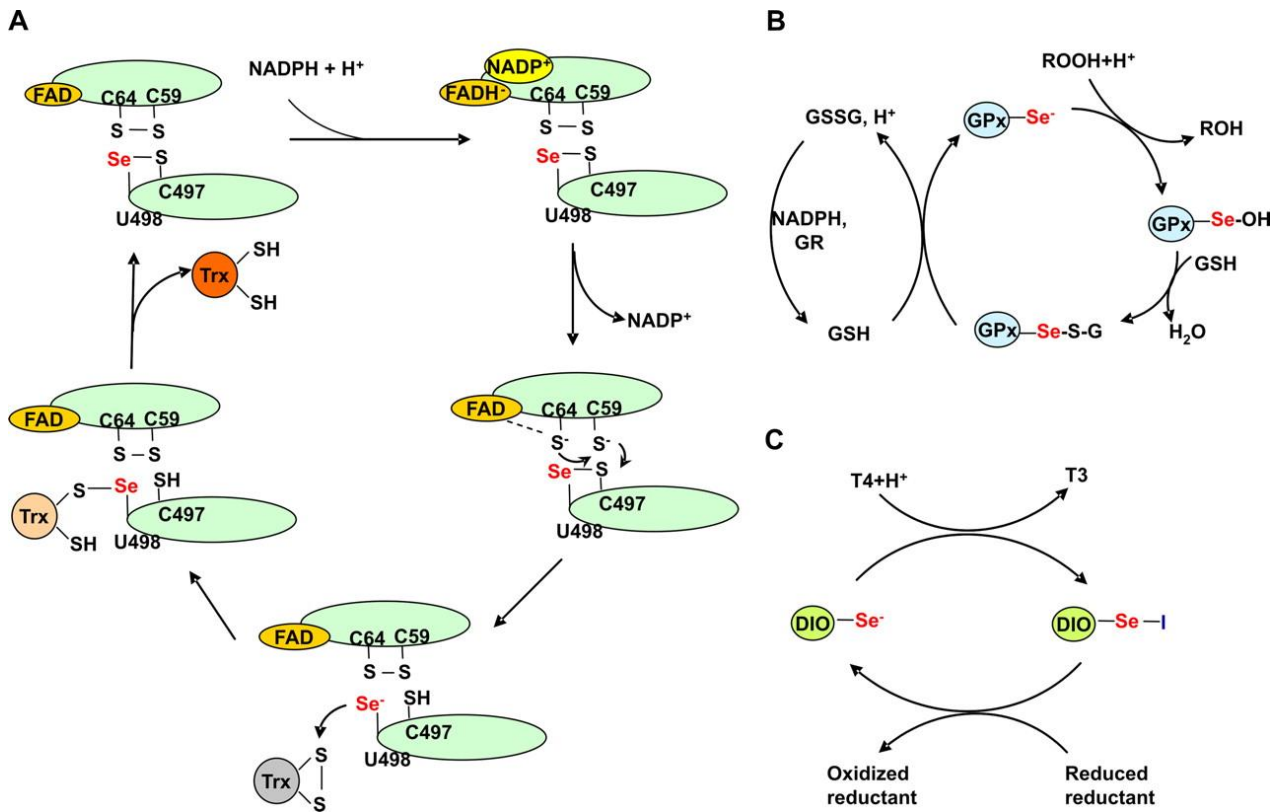


Fig. 9. Putative catalytic mechanism of the three best characterized mammalian selenoproteins, TrxRs, GPxs and DIOs. GR, glutathione reductase.

2.2.1 Thioredoxin reductases (TrxRs)

TrxRs are members of the pyridine nucleotide-disulfide oxidoreductases that, together with thioredoxin (Trx), represent the major disulphide reduction system of the cell (*Labunskyy et al., 2014*). Three TrxRs have been identified in mammals: TrxR1 in the cytosol/nucleus (*Gladyshev et al., 1996*), TrxR2 in mitochondria (*Lee et al., 1999*), and thioredoxin glutathione reductase in the testes with the latter also possessing glutathione and

glutaredoxin reductase activity (Sun *et al.*, 2001). In addition to the N-terminal redox-active dithiol/disulfide in one subunit (sequence: -Cys-Val-Asn-Val-Gly-Cys-), mammalian TrxRs contain a 16-residue C-terminal elongation with the conserved selenothiol active-site in the adjacent subunit (sequence: -Gly-Cys-Sec-Gly-OH) (Zhong and Holmgren, 2000). This structure forms the redox-active center of the enzyme (Sandalova *et al.*, 2001). The proposed mechanism of action mediated by the mammalian TrxR involves the N-terminal active-site disulfide reduction by NADPH via FAD and then the electron transfer from the N-terminal active thiol to the C-terminal selenenylsulfide bond in the opposite subunit of TrxR, and finally from the C-terminal active site to the substrates (**Fig. 9A**) (Zhong and Holmgren, 2000). The accessibility and high reactivity of the C-terminal active-site selenolate confer to the TrxRs a wide range of substrates ranging from small molecules (i.e. selenite, lipid hydroperoxides, synthetic organoselenium drug *eb-selen*) to proteins [i.e. Trx, protein-disulfide isomerases (PDIs), and GPx] (Papp *et al.*, 2007). The TrxR/Trx system is essential for life; TrxR is the only enzyme able to reduce the oxidized Trx, which transfers electrons to ribonucleotide reductase, and thus is crucial for DNA synthesis for converting ribonucleotide to deoxyribonucleotides (Arnér and Holmgren, 2000). Trx can also reduce methionine-sulfoxide reductase and thioredoxin peroxidase (peroxiredoxin), confirming its involvement in the repair of methionine sulfoxide-oxidized proteins or redox signaling via H₂O₂ (Arnér and Holmgren, 2000). Furthermore, the TrxR/Trx system takes part in several biological actions by controlling the activity of transcription factors containing critical Cys residues in their DNA-binding domains such as NFκβ, AP-1 and p53 (Lillig and Holmgren, 2007). The central role played by the Trx is highlighted by the embryonic lethal phenotype of the Trx and TrxR gene *knockout* mouse models (Matsui *et al.*, 1996).

2.2.2 Glutathione Peroxidases (GPxs)

GPxs are involved in a wide range of physiological functions particularly in H₂O₂ signaling, detoxification of hydroperoxides and for maintaining cellular redox homeostasis. Accordingly, GPxs are major components of the antioxidant defence (Lu and Holmgren, 2009). In humans, there are five Sec-containing GPxs: the ubiquitous cytosolic GPx (GPx1), the gastrointestinal-specific GPx (GPx2), the plasma GPx (GPx3), the ubiquitous phospholipid hydroperoxide GPx (GPx4), and the olfactory epithelium- and embryonic

tissue-specific GPx (GPx6) (Kryukov *et al.*, 2003). In particular, GPx1 is the most abundant selenoprotein in mammals and is considered as one of the major antioxidant enzymes, that together with catalases and peroxiredoxins, protects cells from oxidative damage by degrading toxic H₂O₂ (Lubos *et al.*, 2011). H₂O₂ has been implicated as an important signaling molecule that regulates a variety of biological processes and pathways, including cell proliferation, apoptosis, stress response, and mitochondria-related functions and many of the physiological roles of H₂O₂ are modulated by GPx1 (D'Autreaux and Toledano, 2007). In fact, this cytosolic enzyme catalyzes GSH-dependent reduction of H₂O₂ to H₂O (Lubos *et al.*, 2011). As show in **Fig. 9B**, the catalytic redox cycle of GPxs involves the oxidation of Sec to selenenic acid by H₂O₂ and organic hydroperoxides and reduction to the selenolate anion form by the GSH system.

2.2.3 Iodothyronine Deiodinases (DIOs)

DIOs family of selenoproteins are integral membrane proteins characterized by a thioredoxin fold (Labunskyy *et al.*, 2014); these enzymes consist of three paralogous proteins in mammals (DIO1, DIO2 and DIO3), which are involved in the regulation of thyroid hormone activity by reductive deiodination. These proteins have diverse subcellular localizations and tissue expression. DIO1 is mostly expressed in the liver, kidney, and thyroid, while DIO2 is present in the brain, pituitary, thyroid, skeletal muscle, and brown adipose tissue. DIO3 was found in the cerebral cortex and skin and is expressed at a very high level in the placenta and pregnant uterus (Kuiper *et al.*, 2005). DIO1 and DIO2 catalyse the deiodination of the inactive form of the major thyroxine (T4) or tetraiodothyronine, thyroid hormone secreted by the thyroid gland, into the active hormone 3,3',5-triiodothyronine (T3); DIO3 converts T4 into reverse T3 and also T3 into 3,3'-diiodothyronine. DIO1 and DIO2 can also convert reverse T3 into 3,3'-diiodothyronine (Kuiper *et al.*, 2005). The proposed deiodination mechanism is the generation of an oxidized DIO-Sel intermediate, and thus, the intermediate is reduced by thiol-containing reductants and releases iodide (Lu and Holmgren, 2009) (**Fig. 9C**).

2.2.4 Rdx family of selenoproteins

As mentioned above, the major functionally characterized selenoproteins (TrxRs, GPxs and DIOs), take part to an essential oxidoreductase activity for maintaining the redox balance; however, the role of many selenoproteins and their mechanisms of action are still elusive (*Labunskyy et al., 2014*). In this context, the role of other selenoproteins is emerging; most of them are implicated in several biological functions through redox mechanisms, as it is the case of a subfamily of selenoproteins designated as Rdx, which include a family of thioredoxin-like proteins (*Dikiy et al., 2007*). Selenoproteins T (SelT), W (SelW), H (SelH), and V (SelV) are members of this subfamily. They contain a thioredoxin-like fold and are characterized by the presence of a conserved Cys-X-X-Cys or Cys-X-X-Sec motif near the N-terminus region. Rdx proteins can use catalytic Cys (or Sec) to form transient mixed disulphides with substrate proteins (*Dikiy et al., 2007*). Considering the presence of the thioredoxin fold and the Cys-X-X-Sec motif in their active site, it has been proposed that the Rdx subfamily proteins are thiol-based oxidoreductase enzymes (*Dikiy et al., 2007*); however, the detailed mechanism of function of any of these proteins remains unknown.

SelW is a 9-kDa cytosolic selenoprotein and one of the most abundant in mammals; it is highly expressed in muscles and brain (*Gu et al., 2000*) and it belongs to the stress-related group of selenoproteins, since its expression is regulated by the nutritional selenium contribution (*Howard et al., 2013*). It has been found that, when purified from rat muscle, the native SelW form a complex with glutathione (*Beilstein et al., 1996*).

SelH is a 14-kDa selenoprotein with unique subcellular (nuclear) localization (*Novoselov et al., 2007*). Its expression was found to be relatively low in adult mouse tissues, but is elevated during embryonic development. By an *in vitro* chromatin immunoprecipitation assay, it has been observed that SelH specifically binds to sequences containing heat shock and stress response elements, and it has been correlated with the transcriptional regulation of specific genes involved in *de novo* glutathione synthesis, suggesting a nuclear oxidoreductase activity (*Panee et al., 2007*).

SelV is one of the selenoproteins less characterized and structurally strongly related to SelW; however, in contrast to SelW, SelV expression is detected only in testes, and thus it

may be involved in male reproduction (*Mariotti et al., 2012*). The function of this selenoprotein is not known.

3. The Rxr member Selenoprotein T (SelT or SELENOT)

SelT is a novel thioredoxin-like enzyme, whose gene was originally identified using a bioinformatics algorithm (*SECISearch*), that allows the recognition of the SECIS element at the 3'-untranslated regions (UTRs) in nucleic acid sequences of selenoproteins (*Kryukov et al., 1999*). The algorithm was based on three steps: 1) search of primary consensus sequence; 2) analysis of mRNA secondary structure; and 3) calculation of the free energy, estimated for known SECIS elements, in order to predict the secondary structure (*Kryukov et al., 1999*). According to the program, authors showed that the cDNA sequence of SelT (**Fig. 12**) corresponds to 1002 nucleotides and contains an ORF of 163 amino acid residues; the Sec residue, Sec17, encoded by TGA, was located in the N-terminal portion of the protein and the SECIS element was located 509 nucleotides downstream of the TGA codon for Sec.

```

TGCAGTCTGTCTGAGGGCGGCCGAAGTGGCTGGCTCATTAAAGATGAGGCTTCTGCTGCTTCTCCTAGTGGCGGCGTCTGCGATGGTCCG 90
GAGCGAGGCCTCGGCCAATCTGGGCGGCGTGCCAGCAAGAGATTAAGATGAGTACGCCACGGGCGCTGCTCAAGTTCCAGATTGT 180
                                     m q y a t g p l l k f q i c 14

GTTTCCTGAAGGTTATAGGCGGGTGTGTTGAGGAGTACATGCGGGTTATTAGCCAGCGGTACCCAGACATCCGCATTGAAGGAGAGAATTAC 270
v s u g y r r v f e e y m r v i s q r y p d i r i e g e n y 44

CTCCCTCAACCAATATATAGACACATAGCATCTTTCCTGTCAAGTCTTCAAAGTATGATTAATAGGCTTAATAATGTTGGCAAGGATCCT 360
l p q p i y r h i a s f l s v f k l v l i g l i i v g k d p 74

TTTGCTTTCTTTGGCATGCAAGCTCCTAGCATCTGGCAGTGGGGCCAAAGAAAATAAGGTTTATGCATGTATGATGGTTTTCTTCTTGAGC 450
f a f f g m q a p s i w q w g q e n k v y a c m m v f f l s 104

AACATGATTGAGAACCAGTGTATGTCAACAGGTGCATTGAGATAACTTTAAATGATGTACCTGTGTGGTCTAAGCTGGAATCTGGTCAC 540
n m i e n q c m s t g a f e i t l n d v p v w s k l e s g h 134

CTTCCATCCATGCAACAACCTTGTTCAAATCTTGACAATGAAATGAAGCTCAATGTGCATATGGATTCAATCCCACACCATCGATCATAG 630
l p s m q q l v q i l d n e m k l n v h m d s i p h h r s 163
                                     ←————— SECIS —————→
CACCACCTATCAGCACTGAAAACCTCTTTTGCATTAAGGGATCATTGCAAGAGCAGCGTGACTGACATTATGAAGGCCTGTACTGAAGACA 720
                                     →—————
GCAAGCTGTAGTACAGACCAGATGCTTTCTTGGCAGGCTCGTTGTACCTCTTGAAAAACCTCAATGCAAGATAGTGTTCAGTGTGCGC 810
ATATTTTGGAAATCTGCACATTCATGGAGTGCAATAAATACTGTATAGCTTTCCCCACCTCCCACAAAATCACCCAGTTAATGTGTGTGT 900
GTGTGTTTTTTTTAAGGTAACATTACTACTTGTAACTTTTTTTCTTTAGTCATATTTGGAAAAAGTAGAAAATTTGGAGTTACATTTGGA 990
TTTTTTTTTCCAA 1002

```

Fig. 12. Human SelT cDNA and protein sequences (*Kryukov et al., 1999*).

It has been shown that the SelT region containing Sec has a high degree of homology across species (*Kryukov et al., 1999*), and one of the conserved residues, Cys-14, separated from

Sec by two different amino acid residues (*Kryukov et al., 1999*). This putative Sec-containing redox center of human SelT, C-V-S-U, is similar to that found in thioredoxins and glutaredoxins (*Siedler et al., 1993*) such as the selenoproteins Sep15, SelM, and SelW and other redox active proteins. This, suggests the suitability of SelT for the catalysis of redox reactions in a mechanism typical of thiol/disulfide oxidoreductases (*Korotkov et al., 2001; Ferguson et al., 2006*). Intracellular localization studies in mouse (*Dikiy et al., 2007*) and in rat cell lines (*Grumolato et al., 2008*), as well as the use of antibodies against the protein GRP78 (specific ER marker), demonstrated that SelT is predominantly localized in the ER. It is also located in the Golgi apparatus with possible occurrence in cytosol. Contrarily, a localization in the nucleus, peroxisomes, and mitochondria was excluded (*Dikiy et al., 2007*). By using oligonucleotides derived from a related expressed sequence tag (ESTs), initially available in Genbank, the full-length cDNA encoding for rat SelT was isolated from PC12 cells (*Grumolato et al., 2008*). It was found that rat SelT mRNA contains a translation start site localized 96 bp upstream of the start codon originally described in the human sequence. This new initiation site is conserved in rat, mouse, and human sequences and generates an open reading frame encoding a rat protein of 195 amino acids (*Grumolato et al., 2008*) (**Fig. 13A**).

A

```

ggtttttgggctgcaagtctctcggtctctgaaggccggccgggagccggctgtctcaattaag  M R 2
L L L L L L V A A S A V V R S R 61
CTC TTG CTG CTT CTG CTG GTG GCG GCG TCG GCG GTG GTC CGC AGC GAG 109
A S A N L G G V P S K R L K M Q 34
GCC TCT GCC AAC CTG GGC GGC GTG CCC AGC AAG AGA TTA AAG ATG CAG 157
Y A T G P L L K F Q I C V S U G 60
TAC GCC ACG GGG CCG CTG CTC AAG TTT CAG ATT TGT GTA TCC TGA GGG 205
Y R R R V F E E Y M R V I S Q R Y 66
TAC AGG CCG GTG TTT GAG GAG TAC ATG CCG GTT ATT AGC CAG CCG TAT 263
P D I R I E G E N Y L P Q P I Y 82
CCA GAC ATC CGC ATT GAG GGG GAG AAT TAT CTC CCT CAA CCA ATT TAT 301
R H I A S F L S V F K L V L I G 68
AGA CAC ATA GCA TCT TTC CTG TCA GTC TTC AAA CTA GTA TTA ATA GGC 349
L I I V G K K D P F A F F G M Q A 114
TTA ATA ATT GTT GGC AAA GAT CCT TTT GCT TTT TTC GGC ATG CAA GCT 397
P S I W Q W G Q E N K V Y A C M 130
CCT AGC ATC TGG CAG TGG GGC CAA GAA AAT AAG GTT TAT GCA TGT ATG 445
M V F F L S N M I E N Q C M S T 148
ATG GTC TTC TTC TTG AGC AAC ATG ATT GAG AAC CAG TGT ATG TCA ACA 483
G A F E I T L N D V P V W S K L 162
GGT GCA TTT GAG ATA ACT TTA AAT GAT GTA CCG GTA TGG TCT AAG CTG 541
E S G H L P S M Q Q L V Q I L D 178
GAA TCT GGA CAT CTT CCA TCC ATG CAA CAA CTT GTT CAA ATT CTT GAC 589
N E M K A L N V H M D S I P H H R 194
AAT GAA ATG AAA CTC AAT GTG CAT ATG GAT TCA ATC CCA CAT CAT CGA 637
S 195
TCA TAG ccctacctatcagcaactgaaaactcttttacctt aagggtttttgcaagagcagc 696
gtgactgacattatgaaggccctgtactgaagacagcaagctgttagt acagaccagatgtttc 761
tggcaggctcgtttgtacctcttggaaaacctcagtgcaagacagttttccatgctggcaagt 824
gctgaaactctgcacacacatgcagtgccagtgatactgtgtgacttccccagagcccactgttaa 887
tagtttcttcttgacatggcattactacttgtmattcttttcttgggtcatgtttaagaaagt a 950
cagaattgagttgcaacttg 970

```

B

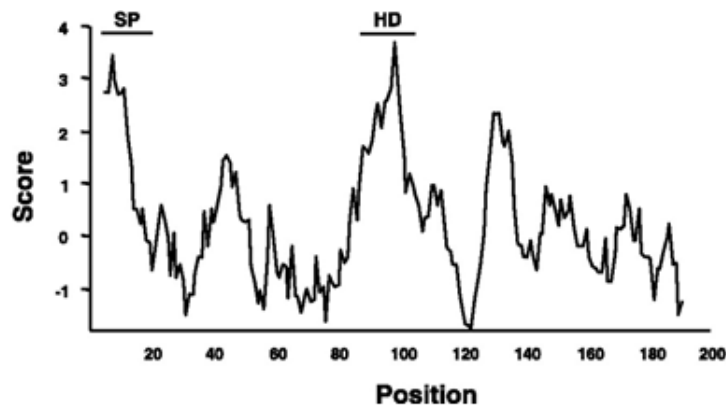


Fig. 13. Rat SelT sequence. **A.** Nucleotide and deduced amino acid sequences of rat SelT. The signal peptide is underlined; the highly hydrophobic amino acid sequence is boxed and the SECIS element present in the 3'-UTR, which allows the recognition of the TGA codon (position 49, bold) as a signal for Sec incorporation, is double-underlined. **B.** Hydrophobicity plot of SelT showing the SP and the HD (Grumolato et al., 2008).

In the sequence analysis of SelT, Grumolato and collaborators (Grumolato et al., 2008) observed a 19-amino acid signal peptide (SP) at positions 1–19 that is important for the protein function, as demonstrated by the loss of activity when deleted (Grumolato et al., 2008). They also found a highly hydrophobic stretch of 16-amino acids at positions 87–102 of the predicted protein, which may represent a transmembrane domain (HD) and which is required for the targeting of SelT to intracellular compartments, including the ER (Grumolato et al., 2008) (**Fig. 13B**).

3.1 Involvement of SelT in the regulation of Ca²⁺ homeostasis and neuroendocrine function

SelT has been also identified as a novel target gene of the neuropeptide pituitary adenylate cyclase-activating polypeptide (PACAP). This was suggested by the exclusive PACAP ability to induce a rapid increase in SelT mRNA levels during PC12 cell differentiation with a cAMP-dependent mechanism (Grumolato et al., 2008). During this process, PACAP promotes cell cycle arrest, cell survival, and PC12 cell secretory activity in a Ca²⁺-dependent manner (Ghzili et al., 2008). It was found that SelT plays an essential role in this mechanism through

the regulation of Ca^{2+} homeostasis. In fact, it was observed that SelT overexpression induces an increase of the intracellular Ca^{2+} concentration in PC12 cells; in particular, using site-directed mutagenesis of the Sec residue of SelT, it was demonstrated that PACAP stimulates the expression of SelT and its targeting to the ER to control Ca^{2+} release through a Sec-mediated redox mechanism. Simultaneously SelT *knockdown* inhibited PACAP-stimulated release of Ca^{2+} from the ER (Grumolato et al., 2008). The authors proposed a mechanism of action by which the protein may regulate intracellular Ca^{2+} and subsequent hormone/neurotransmitter exocytosis from secretory vesicles during PACAP-induced PC12 cell differentiation, as illustrated in Fig. 14.

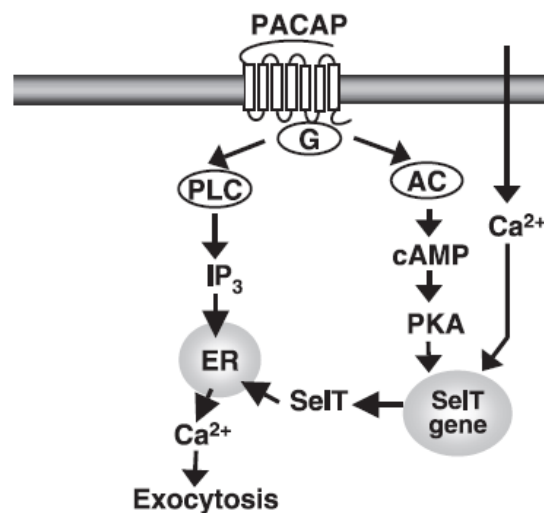


Fig. 14. Proposed model for the mechanism of action of SelT on intracellular Ca^{2+} and hormone secretion during PACAP-induced PC12 cell differentiation (Grumolato et al., 2008).

These data are indicative of a fundamental role of SelT in the regulation of Ca^{2+} homeostasis and neuroendocrine function. However, more recently it has been found that PACAP is unable to stimulate SelT gene expression in adrenomedullary mature cells and that, SelT is highly expressed during adrenal ontogenesis but not in the adult adrenal gland. These results obtained by Tanguy and colleagues (2011) suggest that this protein may exert an important function during cell differentiation and tissue ontogenesis in which PACAP plays a major role (Ghzili et al., 2008). These data have been corroborated by in situ hybridization,

RT-qPCR, western blot and immunohistochemistry analysis, showing a wide expression of SelT and its mRNA during different stages of most rodent embryogenic structures and a progressive decrease during organ development, to vanish in adult phase (*Grumolato et al., 2008; Tanguy et al., 2011*). In addition, different expression patterns were observed in the embryonic central nervous system, thyroid, testis and other organs. A temporal expression pattern of SelT was found in both developing cerebral and cerebellar cortex, in which PACAP exerts potent trophic activities (*Sanchez et al., 2008; Falluel-Morel et al., 2005*). In contrast, it was undetectable in adult nervous cells except rostral migratory-stream astrocytes and Bergmann cells (*Tanguy et al., 2011*). On the other hand, SelT expression was maintained in several adult endocrine tissues such as pituitary, thyroid, or testis (*Tanguy et al., 2011*). According to the authors, the intense SelT expression in fetal thyroid gland and testis, similar to that of DIO and GPx respectively, may be related to the important oxidative burst generated during thyroid hormone biosynthesis and during the normal function of testosterone-producing cells, endocrine cells which are highly sensitive to the continuous stress to which they are exposed (*Tanguy et al., 2011*).

This is in accordance with observations made for several other selenoproteins (i.e. SelN, SelW, SelP and GPx), that are highly expressed in embryos and are involved in protection against oxidative stress (*Chung et al., 2009; Petit et al., 2003; Baek et al., 2005*). In fact, the deletion of the Sec tRNA gene or specific selenoprotein genes, is dramatically associated with early embryonic lethality (*Bösl et al., 1997*). Authors also observed that SelT expression is strongly stimulated in liver cells during the regenerative process that occurs after partial hepatectomy (*Tanguy et al., 2011*), resembling the profile observed after brain hypoxia (*Ikematsu et al., 2007*) and in a mouse model of Parkinson's disease (PD) (*Boukhar et al., 2016*).

3.2 Involvement of SelT in the regulation of pancreatic β -cell function and glucose homeostasis

The specific SelT tissue expression, which is maintained in the adult only in some endocrine structures, prompted Prevost and collaborators in 2013 to investigate the involvement of SelT in the regulation of pancreatic β -cell function and glucose homeostasis by using a

conditional pancreatic β -cell SelT *knockout* mice (SelT-insKO). Considering that selenoproteins are increasingly recognized as important factors in the regulation of glucose homeostasis (Mueller *et al.*, 2009), and that their synthesis alteration is related to diabetes progression (Labunskyy *et al.*, 2011), it has been observed that glucose administration in SelT-insKO mice induces an impairment of glucose tolerance, as shown by a significantly higher ratio of glucose to insulin compared with wild-type. This indicates a deficit in insulin production/secretion in mutant mice (Prevost *et al.*, 2013). In agreement with other evidences, Prevost and collaborators (2013) observed that SelT is strongly and specifically expressed in the adult mouse and human endocrine pancreas, and in particular within the islets of Langerhans, where the protein is mainly expressed in insulin- and in somatostatin-producing cells. In addition, it was also found that SelT is expressed in insulinoma and that SelT-insKO mice showed an alteration of islet morphology, as revealed by their smaller size in comparison to wild-type mice (Prevost *et al.*, 2013). It is known that the pancreatic islet β -cells are characterized by an intrinsic high production of free radicals during insulin synthesis and secretion, and that their ability of oxidant neutralization is lower compared to other cells such as hepatocytes (Lei *et al.*, 2011). This suggests a higher vulnerability of these cells to oxidative stress. In this regard, SelP is suggested to play a major role in glucose homeostasis by acting as a hepatokine able to modulate insulin sensitivity (Misu *et al.*, 2010) and to protect against glucotoxicity in pancreatic β -cells (Steinbrenner *et al.*, 2012). Prevost and colleagues (Prevost *et al.*, 2013) demonstrated for the first time that SelT also contributes to blood glucose regulation especially during pancreatic β -cell stimulation and that this thioredoxin-like protein is essential for pancreatic islet remodeling and function (Prevost *et al.*, 2013).

3.3 Role of SelT in neurodegeneration

It is known that ROS are strongly involved in the pathogenesis of neurodegenerative diseases and various neurodevelopmental disorders, such as Alzheimer's disease (Wang *et al.*, 2014) and PD (Blesa *et al.*, 2015). Considering that SelT is abundantly but transiently expressed in the neural lineage during brain ontogenesis, and that its physiological function in the brain is unknown, Castex and colleagues (2016) and Boukhzar and collaborators (2016) evaluated the patho-physiological impact of SelT in the brain by using a conditional

knockout mouse line (Nes-Cre/SelT^{fl/fl}), in which SelT gene was specifically disrupted in nerve cells, and a mouse model of PD, respectively. In Nes-Cre/SelT^{fl/fl}, the authors observed a significantly reduced volume of different brain structures, including hippocampus, cerebellum, and cerebral cortex at postnatal day 7 (P7) (**Fig. 15**), associated with a loss of immature neuronal cells increased ROS levels and cell death. This phenotype was less evident at the second postnatal week, probably due to a compensatory mechanism in the brain; however, in adulthood this SelT deficiency led to cerebral dysfunction (Castex *et al.*, 2016).

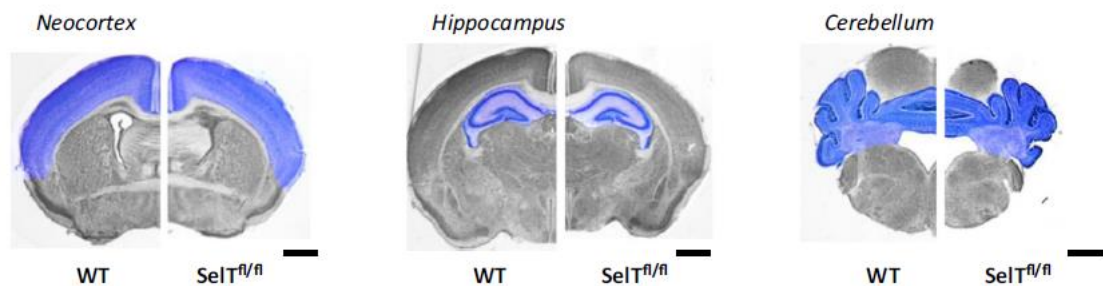


Fig. 15. “Partial black and white” macrophotographs showing P7 brain sections stained for Nissl substance, on which the structures of interest appear in color (Castex *et al.*, 2016).

At the same time, Boukhzar and colleagues (2016) first demonstrated that SelT influences the oxidative state and cell survival in SH-SY5Y cell model of dopaminergic neurons. Subsequently, they observed that specific neurotoxins (1-methyl-4-phenyl-1,2,3,6-tetrahydropyridine, MPTP or rotenone), able to generate PD in mice, provoke SelT expression in the nigrostriatal pathway of wild-type mice and a severe parkinsonian-like motor defect of Nes-Cre/SelT^{fl/fl} mice (Boukhzar *et al.*, 2016). Finally, these authors detected a remarkable increase of SelT in the brain of PD patients, in the caudate putamen tissue, providing insight about the crucial role played by this selenoprotein in the protection of dopaminergic neurons against oxidative stress and cell death (Boukhzar *et al.*, 2016).

4. Oxidative stress in cardiovascular disease (CVD)

CVD and its consequences remain the most common cause of death worldwide, causing more than 4 million deaths each year across Europe, and representing the most significant cause of death in the United States and the most important health problem of the Western world (Townsend *et al.*, 2016; Lloyd-Jones *et al.*, 2009). One of the critical points of free radical-mediated pathogenesis of CVD, is endothelial dysfunction, represented by a disruption of vessel microenvironment, in particular of the vascular endothelium (Zorio *et al.*, 2008). The basis of the endothelium dysfunction derives from a reduction in endothelium-dependent vasorelaxation, caused by a decrease in NO• bioavailability (Zeiher *et al.*, 1991). This lead to a disruption of the intimal surface and promotion of platelet adhesion and aggregation on the endothelial surface, with increasing risk of thrombus formation and acute coronary syndromes (Zeiher *et al.*, 1991). The impaired vasodilatation is associated with increased local ROS production and reduced antioxidant enzyme activity (Heitzer *et al.*, 1996). The decreased NO• bioavailability can derive from diverse factors, such as a reduced eNOS expression, the lack of substrate or cofactors for eNOS activity, and the increase in NO• degradation (Antoniades *et al.*, 2006). In addition to these aspects, the free radical impact is related to the fact that the bioavailability of NOS is influenced by the amount of ROS, that can transform NO• to ONOO⁻ (Zorio *et al.*, 2008). ROS produced by the endothelium and the vascular smooth muscle increase in patients with essential hypertension (Lip *et al.*, 2002). This type of ROS mostly derives from the action of NADPH oxidase, which catalyse the O₂•⁻ production by one electron reduction of O₂ using NADPH as the electron donor (Lassegue *et al.*, 2003).

Furthermore, several data demonstrated an important contribution of ROS in myocardial acute ischaemia and ischemia/reperfusion (IR) injury (Yellon and Hausenloy, 2007; Braunwald *et al.*, 1985). Hypoxia and reoxygenation induce an increase in free radical production in cardiac tissues and represent a major cause of reperfusion damage (Yellon and Hausenloy, 2007; Braunwald *et al.*, 1985). The free radicals produced during this process are responsible for the direct oxidative damage to cellular components and for the indirect injury through the activation of localized inflammation circuits (Griendling and FitzGerald, 2003). They act also as a signalling messenger for the activation of specific pathways responsible of cellular function impairment (Elkind, 2006). Nitrosative stress also

plays a role in cardiovascular disease. During acute ischaemia and heart failure, the increase of iNOS activity leads to increased levels of free radicals and of S-nitrosylated proteins (*Shi et al., 2002*). It has been observed that alteration of NO• formation is crucial for the pathogenesis of the injury that occurs in ischemic and reperfused tissues. In the post-ischemic heart, these alterations result in compromised endothelial function and impaired tissue perfusion (*Cooke and Tsao, 1993*).

It is known that in patients presenting acute myocardial infarction, the infarct size can be limited by early myocardial reperfusion via percutaneous coronary intervention (PCI), in order to preserve the left ventricular systolic function and to improve the clinical outcome (*Murphy and Steenbergen, 2007; Hausenloy and Yellon, 2004*). However, restoring the blood flow after a prolonged ischemic episode may also paradoxically cause irreversible damage to the myocardium in a phenomenon named “lethal reperfusion-induced injury” where ROS and RNS are dramatically involved (*Murphy and Steenbergen, 2007; Hausenloy and Yellon, 2004*). Interventions applied in the onset of reperfusion to salvage the viable tissue, are described as postconditioning treatments (*Bice and Baxter, 2015*). Ischemic postconditioning represents a strategy to limit the lethal myocardial reperfusion injury for patients undergoing primary PCI. It is obtained by stopping the normal myocardial reperfusion through several intermittent episodes of coronary myocardial ischemia induced by low-pressure inflations of the angioplasty balloon in the infarct-related coronary artery (*Hausenloy, 2009*). Administration of pharmacologically active agents in the onset of the reperfusion to induce cardioprotection, is named pharmacological postconditioning which is able to recruit or mimic the established pathways associated with the cardioprotective ischemic postconditioning (*Hausenloy, 2009*).

These observations support the notion that oxidative stress strongly correlates with negative outcomes in CVD, by negatively influencing the endothelial function, oxidizing cellular constituents, impairing the proteins critical for excitation-contraction coupling and by reducing NO• bioactivity (*Zeicher et al., 1991; Goldhaber et al., 2000; Lip et al., 2002*).

Aims of the doctoral project

The protective effect of ischemic postconditioning is of big interest as a therapeutic approach in order to limit the reperfusion injury which contributes to reduce the infarct size in acute myocardial infarction (*Hausenloy, 2009*). Cardiovascular research identified several potential pharmacological targets for the postconditioning cardioprotection (*Bice and Baxter, 2014*). These include ligands for membrane-associated receptors, activators of phosphokinase survival pathways and inhibitors of the mitochondrial permeability transition pore (*Bice and Baxter, 2014*). Although the majority of experimental research is conducted in animal models which do not fully recapitulate the complexity of risk factors and comorbidities of patients, numerous pharmacological agents targeting these mechanisms proved to be promising as postconditioning mimetics with clinical interest (*Bice and Baxter, 2014*). Thus, cardioprotective strategies able to limit the reperfusion injury and further enhance the benefit of reperfusion are of major clinical interest and are needed to improve the efficacy of primary percutaneous coronary intervention (*Bice and Baxter, 2014; Hausenloy, 2009*).

In this context, the research reserves great interest for molecules able to reduce the oxidative stress which represents one of the major problems for the pathogenesis of myocardial ischemia/reperfusion (I/R) injury (*Dhalla et al., 2000*). Antioxidants can act through different mechanisms, by scavenging and by inhibiting the formation of ROS or their precursors, by enhancing endogenous antioxidant generation and by reducing apoptotic cell death (*Maulik et al., 1999*). Accordingly, various studies using a genetically engineered animal model, reported the beneficial cardiac effects of specific endogenous antioxidants (i.e. catalase, superoxide dismutase and glutathione peroxidase) in isolated ischemic-reperfused hearts (*Chen et al., 1998; Woo et al., 1998; Werns et al., 1992*). In this cardiac model, many alterations such as depression in contractile function, arrhythmias, change in gene expression, and loss of adrenergic pathways have been observed (*Temsah et al., 1999; Persad et al., 1998*).

In this context, exogenous antioxidants could be good candidates since they exert a significant protective action against the altered redox balance in cardiac I/R injury (*Kalaycioglu et al., 1999; Khaper et al., 1997*). Among these, some drugs, including thiol-containing compounds, have been reported to exert antioxidant action (*Kalaycioglu et al., 1999; Khaper et al., 1997*).

Several lines of evidence indicate that SelT affects, via its redox activity, the differentiation, the function, and the protection of nervous and endocrine cells in pathophysiological conditions (Prevost *et al.*, 2013; Boukhzar *et al.*, 2016). During the normal function of these organs, SelT controls the oxidative stress to which these tissues are physiologically exposed (Tanguy *et al.*, 2011). Nevertheless, nothing is known about the expression and function of SelT in the heart, a tissue which is normally severely exposed to oxidative stress, particularly as in the case of I/R damage.

Therefore, the present doctoral project aimed to i) evaluate the possible use of rSelT for the development of a specific immunoassay, and ii) investigate the cardiovascular effects of a recombinant form of rat full length SelT (rSelT) and its derived peptide PSELT (SelT₄₃₋₅₂, chemically synthesized in its reduced form, which encompasses the redox Cys-Val-Ser-Sec motif). Particularly:

- the first part of the work, was designed to:
 - optimize the over-expression of a recombinant form of rSelT in *E. coli* cells;
 - calculate the enzymatic activity exerted by the pure protein.
- the second purpose of this doctoral project was to develop specific enzyme-linked immunosorbent assays (ELISAs), by using the recombinant protein and a rabbit polyclonal antiserum against rSelT, as antigen and primary antibody, respectively. In particular, an indirect ELISA (I-ELISA) was firstly designed for antibody titers calculation and then an indirect competitive ELISA (IC-ELISA) was developed for soluble SelT detection.
- the third part of the project aimed to:
 - determine the expression of SelT during rat heart ontogenesis and after *ex-vivo* induced ischemia in adult rat heart;
 - evaluate the cardioprotective effect of rSelT and PSELT against I/R injury in a Langendorff rat heart model, as pharmacological postconditioning agents.

Materials and methods

1. Production of recombinant SelT

1.1 Cloning of rat SelT cDNA

Cloning of rat SelT cDNA was made as previously described (*Boukhzar et al., 2016*). Briefly, rat SelT cDNA, devoid of signal peptide sequence, was amplified by PCR from PC12 cells and the purified DNA was cloned in the pGEM-T vector (Promega). Sequence mutagenesis was carried out by using the QuikChange XL site-directed mutagenesis kit (Agilent Technologies) to convert the Cys-X-X-Sec motive to Cys-X-X-Cys or Ser-X-X-Ser, to allow the production and purification of recombinant SelT (rSelT). The nucleotide sequence of all constructs was verified by DNA sequencing (Beckman Coulter Genomics).

1.2 Preparation of competent *E. coli*

BL21 (DE3) *E. coli* competent cells (Millipore, Billerica) were transformed with pGEM-T/SelT using the heat shock method; 1 µl of a ligation reaction of purified plasmid DNA (10ng/ml) was added directly to the 20 µl competent cells. After a short incubation (5min) in ice, the mixture of competent bacteria and DNA was placed at 42°C for 30 seconds (heat shock) and then placed back in ice for 2min. 100 µl S.O.C. medium was added and the transformed cells were incubated at 37°C for 45 min with agitation (250 rpm). Selection of colonies was performed with 50 µg/mL kanamycin. *E. coli* BL21(DE3) positive cells were inoculated in 5 mL of 25% LB (Luria Bertani) Broth medium (10g/L Tryptone, 10g/L NaCl, 5g/L Yeast extract, pH 7.0) (Sigma-Aldrich) supplemented with 50 µg/mL kanamycin, and cultured overnight at 37 °C with agitation (250 rpm).

1.3 Plasmid DNA purification and enzymatic digestion

The plasmid DNA from small cultures, inoculated with single colonies of *E. coli*, was purified by NucleoSpin® Plasmid kit (Macherey-Nagel) following the manufacturer instructions; 1.5 ml of culture was transferred into an Eppendorf tube. Cells were pelleted by centrifugation at 11000xg for 30 sec, resuspended in 250 µl of buffer A1 and plasmid DNA was liberated from the *E. coli* host cells by SDS/alkaline lysis (buffer A2). Buffer A3 neutralized the

resulting lysate and created appropriate conditions for binding of plasmid DNA to the silica membrane of the NucleoSpin® Column. The mixture was gently mixed and precipitated protein, genomic DNA, and cell debris were then pelleted by a centrifugation step for 10 min at 11000xg to yield an almost clear supernatant, which was loaded onto a NucleoSpin® Column. Salts, metabolites, and soluble macromolecular cellular components, considered as contaminants, were removed by simple washing with ethanolic buffer A4. Pure plasmid DNA was finally eluted under low ionic strength conditions with slightly alkaline buffer AE (5 mM Tris/HCl, pH 8.5) and quantified by NanoDrop™ spectrophotometers at 260nm (Thermo Scientific). 10 µl (containing 0.6-0.7 µg of DNA) were digested for 2.5 hours at 37 °C with 0.3 µl restriction enzymes *NheI* and *XhoI* 10U/µl (Promega) in 1.2 µl of specific enzyme buffer (Tris/HCl 6mM, MgCl₂ 6mM, NaCl 50mM, DTT 1mM) (Promega, Madison, Wisconsin, USA) for a total reaction volume of 20 µl. Finally, the samples were analyzed in 1.5% agarose gel.

1.4 Expression of rSelT in *E. coli*

For the expression of rSelT in *E. coli*, 3 mL of cell culture was transferred to 0.5 L of LB Broth medium supplemented with 50 µg/mL kanamycin. When the optical density of the cell cultures, measured at 600 nm wavelength, was 0.5-0.7, the protein synthesis was induced by adding 1 mM isopropyl β-D-1-thiogalactopyranoside (IPTG, Sigma-Aldrich) at 37 °C with agitation (250 rpm), and the expression of rSelT at different times of IPTG incubation was tested (1, 1.5 and 2.5 hours). An aliquot of the sample was taken immediately before and after the IPTG induction (not-induced control), and the cell pellet was resuspended in 50 µl 1x SDS-PAGE sample buffer for SDS-PAGE analysis. The cell suspension, after 2.5 hours of IPTG incubation, was centrifuged at 4000xg for 20 min at 4°C. The bacterial pellet (about 2.5 g wet weight) was resuspended in 25 mL bacterial lysis buffer (NPI-10, 50 mM NaH₂PO₄, 300 mM NaCl, 10 mM imidazole, pH 8.0) plus 0.2 mL of protease inhibitor cocktail and 0.5 mM PMSF (phenylmethylsulfonyl fluoride). Cells were incubated with lysozyme to 1mg/ml for 30 min in ice and disrupted by mild sonication (Microson Ultrasonic Cell Disruptor, Misonix) at 4°C (6x 10s with 10s pauses at 300W). For determination of protein solubility, the soluble and the insoluble cell fractions were separated by centrifugation at 10000xg for 30 min at 4°C. The supernatant of this centrifugation represents the crude extract A, soluble

protein, while the resuspended pellet with 5 ml NPI-10 represents the crude extract B, insoluble protein.

1.5 Purification of 6His-rSelT protein under denaturing conditions and protein refolding

To investigate the best working condition for dissolving the insoluble fraction (extract B), two methods were performed:

- 1)** The insoluble fraction was dissolved with NPI-10a (50 mM NaH₂PO₄, 300 mM NaCl, 10 mM imidazole, 0.25% v/v Tween-20, 1mM EGTA, pH 8.0) or NPI-10b (50 mM NaH₂PO₄, 300 mM NaCl, 10 mM imidazole, 0.5% v/v Tween-20, 1mM EGTA, pH 8.0) buffers (10 ml for g wet weight), centrifuged at 10000 x g for 30 min at 4°C, and the pellet was solubilized a second time in the same buffers.
- 2)** The insoluble fraction was dissolved with NPI-10 (10 ml per g wet weight), centrifuged at 10000 x g for 30 min at 4°C, and the pellet was solubilized in 2 ml DNPI-10 (50 mM NaH₂PO₄, 300 mM NaCl, 10 mM imidazole, 8M urea, pH 8.0). After a mild sonication at 4°C (6x 10s with 10s pauses at 300W), bacterial cells were stirred in ice for 60 min and centrifuged at 10000 x g for 30 min at 20°C.

The supernatant (cleared lysate) was gently transferred in a new Eppendorf tube and applied onto a His-select Ni-chelating affinity column (1 cm diameter x 6 cm height) pre-loaded, by gravity-flow, with 2.5 ml column volume (CV) of Ni-NTA resin (Qiagen) and equilibrated with 10 CV DNPI-10. The eluate obtained by the column immediately after loading of the cleared lysate, was named flow-through. Protein renaturation was carried out on the Ni-NTA column itself prior to elution by removal of the denaturant agent, through the solid phase renaturation method of metal chelate affinity chromatography purified rSelT (*Holzinger et al., 1996; Misawa and Kumagai, 1999; Petty, 2001*). Contaminant proteins were washed out of the matrix by 2 steps of 10 CV NPI-20 (50 mM NaH₂PO₄, 300 mM NaCl, 20 mM imidazole, pH 8.0) supplemented with 8M urea (DNPI-20). Before protein elution with 5 CV NPI-250 (50 mM NaH₂PO₄, 300 mM NaCl, 250 mM imidazole, pH 8.0), the urea concentration was gradually decreased and it washed out, by applying a renaturation protocol characterized by 10 CV 1:1 (v/v) NPI-20/DNPI-20, 10 CV

3:1 (v/v) NPI-20/DNPI-20, 10 CV 5:1 (v/v) NPI-20/DNPI-20, 10 CV 7:1 (v/v) NPI-20/DNPI-20 and 30 CV NPI-20. Elution fractions of 0.5 ml were collected. The His-tag protein was eluted by competitive interaction of imidazole for the nickel ions. All steps were carried out at 4°C with a peristaltic pump “P-1” (GE Healthcare) connected to the column (flow rate 0.5 ml/min).

The elution fractions, containing the majority of the eluted His-tag protein, were assembled and quantified by Bradford assay method (Bio-Rad) with bovine serum albumin as reference standard; a yield of about 2 mg purified protein per liter of cell culture was obtained; protein concentration and desalting, in order to remove the remaining urea, imidazole and NaCl, were performed by using Amicon® Ultra-4 Centrifugal Filter Units (Millipore) with a 3.000 device nominal molecular weight limit (NMWL) (Amicon Ultra 3K device), according to the manufacturer instructions (*Cappione et al., 2013*); 4 ml of purified rSelT (assembled elution fractions) in the Amicon® falcon were centrifuged at 4000 x g for 40 min at 4°C, and 50 µl fractures of concentrated protein were obtained by this step. The purified, concentrated and desalted fractions were stored at -80°C.

1.6 Post-refolding analysis: activity assessment of rSelT

Enzymatic activity of rSelT (10 µg) was assessed using the Thioredoxin Reductase (TrxR) Colorimetric Assay Kit, and compared to that of a liver native TrxR, according to the manufacturer protocol (Cayman Chemical Company). This assay is based on the reduction of 5,5'-dithio-bis(2-nitrobenzoic) acid (DTNB) with NADPH to 5-thio-2-nitrobenzoic acid (TNB) which at 405-412 nm produces a yellow colour. The Reaction of DTNB reduction due to TrxR activity is shown below:



Measurement of TrxR or rSelT enzymatic activity by DTNB reduction in the absence and presence of aurothiomalate (ATM), a specific TrxR inhibitor, was performed to allow the correction of non-TrxR-independent DTNB reduction. 20 µl of the TrxR (positive control) or 20 µl of a stock rSelT solution 0.5 mg/ml (10µg), were mixed with 140 µL of working buffer (50 mM KH₂PO₄, 50 mM KCl, 1 mM EDTA, 0.2 mg/ml BSA pH 7.0) to obtain a total reaction volume of 160 µl; the same samples were prepared by adding 20 µl of ATM corresponding

to 20 μM , concentration able to remove all thioredoxin reductase activity (*Gromer et al., 1998*). Reactions were initiated by adding 20 μl of NADH and 20 μl of DTNB to all microplate wells to have a total reaction volume of 200 μl ; then, the O.D. 405 were read every minute for 14 times on an Infinite® 200 PRO plate reader (Tecan). Each sample was assayed in duplicate. Enzymatic activity was assessed as follows: first, the change in absorbance per minute ($\Delta\text{O.D.}_{405/\text{min}}$) was calculated selecting two points of the linear portion of the curve and determining the change in O.D.405 during that time using the equation below:

$$\Delta\text{O.D.}_{405/\text{min}} = [\text{O.D.}_{405} (\text{Time } 2) - \text{O.D.}_{405} (\text{Time } 1)] / [\text{Time } 2 (\text{min.}) - \text{Time } 1 (\text{min.})]$$

The $\Delta\text{O.D.}_{405/\text{min}}$ was corrected for the background, subtracting this rate from all the well, based on the following equation:

$$\text{Corrected } \Delta\text{O.D.}_{405/\text{min}} (\text{sample}) = \Delta\text{O.D.}_{405/\text{min}} - [\Delta\text{O.D.}_{405/\text{min}} (\text{sample} + \text{ATM}) - \Delta\text{O.D.}_{405/\text{min}} (\text{background} + \text{ATM})]$$

Then, the enzymatic activity was expressed as $\mu\text{mol}/\text{min}/\text{ml}$, following this equation:

$$\mu\text{mol}/\text{min}/\text{ml} = [\text{corrected } \Delta\text{O.D.}_{405/\text{min}} (\text{sample}) / 7.92 \text{ mM}^{-1}] \times [\text{total reaction volume} / \text{enzymatic volume}] \times \text{sample dilution factor},$$

where 7.92 mM^{-1} is the DTNB extinction coefficient at 405 nm adjusted for the pathlength of the solution in the well (0.619 cm).

1.7 Purity of rSelT

Polyacrylamide gel electrophoresis of the final purified material showed the presence, in the elution fraction, of a single protein band ($\sim 23 \text{ kDa}$) corresponding to SelT, which contained TrxR-like activity.

2. SeIT Enzyme-Linked Immunosorbent Assay development for SeIT detection

2.1 Production of sera against SeIT

rSeIT fractions were used to produce polyclonal sera by repeated immunization of two New Zealand White rabbits. Prior to a course of immunizations, ~ 0.9 ml of test bleed was taken from each rabbit to provide a source of pre-immune serum. A solution containing 200 µg of pure rSeIT was mixed with the Freund's Complete Adjuvant (FCA) (Sigma) and a first intradermal injection (day 0) was performed; then other 4 subcutaneous injections (at days: 7, 14, 29, 77) of rSeIT mixed with Freund's Incomplete Adjuvant (FIA) (Sigma) were carried out. A total of 3 blood samples at different time after rabbit immunization (at days: 27, 42, 91) were performed. The polyclonal sera against rSeIT was provided by Biological System Society BIOTEM (Apprieu, France).

2.2 Western blot for determination of rabbit sera antibodies

An aliquot of the stock solution of purified rSeIT (0.25mg/ml) was diluted, so that 10 µl giving 50 ng of protein was electrophoresed in 12% SDS polyacrylamide gel and then transferred onto a nitrocellulose membrane (GE Healthcare); the rabbit anti-SeIT was used as primary sera and the peroxidase-conjugated goat anti-rabbit IgG antiserum (Abcam) as secondary antibody. The membranes were blocked with no-fat dried milk, and incubated with 1:800 dilution of sera of the two experimentally immunized rabbits at different times after immunization (27th, 42nd and 91st day, indicated as D27, D42, D91) or pre-immune antiserum, in PBSTM for 1 h at room temperature. The secondary antibody was diluted 1:3000 in PBSTM and membranes were incubated for 1 h at room temperature. Immunodetection was performed using the ECL PLUS enhanced chemiluminescence kit (Amersham) and immunoblots were acquired and digitalized using ChemiDoc™ MP System (Bio-Rad).

2.3 Chequerboard titrations (CBTs)

CBTs were performed by immobilizing rSelT directly onto 96 flat-bottomed polystyrene microtitration plates (Nunc MaxiSorp™, Fisher Scientific) in serial two-fold dilutions in bicarbonate/carbonate coating buffer (3.03 g Na₂CO₃, 6.0 g NaHCO₃ in 1 L distilled water, pH 9.6, CB), from the 5 µg/ml stock solution at 0.0048 µg/ml. This concentration range correlated with 500-0.48 ng of protein per well. Rabbit sera D27 or D42 or D91, were serially two-fold diluted in PBSTM from 1:200 to 1:1.638.400, while secondary antibody (goat anti-rabbit IgG-peroxidase) was held constant at 1:120.000 in PBSTM, according to the manufacturer's protocol. Dilutions of secondary antibody used for its CBT were 4-fold higher and 4-fold lower than recommended by commercial company (1:120.000). During this CBT, rSelT and primary sera were held constant on the basis of their CBTs. In addition to CBTs for antigen, primary and secondary antibodies, the highest positive/negative (P/N) ratio was obtained by using the composition and dilution buffers, temperature and reaction time as described in the work.

2.4 I-ELISA for antibody measurement

Antibody reactivity was determined by endpoint titer ELISA. Ninety-six-well flat-bottomed polystyrene microtitration plates were coated with 100 µl of rSelT (31.25 ng/well), selected on the basis of CBT, diluted in CB. The plate was then covered and left at 4°C overnight to allow the passive adsorption of antigens onto the polystyrene plate, before washing three times with PBS solution containing 0.1% Tween-20 (PBSTb) and blocking with 200 µl per well of blocking buffer for 2 h at room temperature. The plate was washed with PBSTb three times and 100 µl per well of primary antibody (antisera) dilution range (1:200-1:1.638.400) or commercial anti SelT (N-term) (Acris) dilution range (1:250-1:16.000), in PBSTM, was added and incubated at room temperature for 2 h. A negative and a positive control were included on each plate. The plate was then washed with PBSTb six times before adding 100 µl per well of secondary antibody (goat anti-rabbit IgG-peroxidase) diluted in antibody solution 1:120.000, according to the manufacturer's protocol. The plate was incubated at room temperature for 1.5 h before washing three times. A blue colour reaction developed after adding (15 min, at room temperature) 100 µl per well of

substrate/chromogen 3,3',5,5'-tetramethylbenzidine (TMB, Abcam); O.D. was read at 450 nm absorbance after stopping with 100 µl per well specific stop solution (Abcam), using Infinite® 200 PRO plate reader (Tecan). Endpoint titer was reported as the reciprocal of the highest serum dilution that had an absorbance ≥ 0.1 O.D. unit above the cutoff value (absorbance of the pre-immune samples) (Huang *et al.*, 2006). For serum antibodies, the lowest dilution tested (1:200) was divided by 2 and used as the titer for the negative samples (i.e., preimmune samples were assigned a titer of 100) (Huang *et al.*, 2006).

2.5 IC-ELISA for antigen detection

Ninety-six-well flat-bottomed polystyrene microtitration plates were used as solid-phase adsorbents. The rSelt was diluted to the appropriate concentration in CB. A total reaction volume of 100 µl was added in all microtitration wells. After an overnight incubation at 4°C, antigen-coated plate was washed three times with PBSTb and saturated for 2 hours at room temperature with blocking buffer. After three wash with PBSTb, the appropriate dilution (1:1600) of primary sera (100 µl) was mixed with a solution of rSelt in dilution range (40-0.0048 µg/ml) for the inhibition/competitive standard curve construction or with the sample with unknown antigen; this mixture was first incubated for 1.5 h at 23°C in a test tube and further incubated for 2 h in the microtiter wells (100 µl mixture/well, reflecting 4000-0.48 ng/well of rSelt) to start the competition of binding to the primary antiserum between the rSelt-coated plate and the soluble rSelt present in the mixture. After washing six times with PBSTb, 100 µl per well of secondary antibody (goat anti-rabbit IgG-peroxidase) (Abcam) diluted 1:120.000 PBSTM was added and the microtiter plate was further incubated for 1.5 h at room temperature. The following steps were the same to that performed for I-ELISA. Each sample was assayed in triplicate. Data for each sample were expressed in percent of competition, calculated by the following formula:

% competition (sample/standard)

$$= 1 - [\text{O.D.}_{450} (\text{sample/standard} + \text{serum anti-Selt}) / \text{O.D.}_{450} (\text{serum anti-Selt alone})] * 100$$

2.5.1 Construction of a standard-inhibition curve

In order to generate a standard-inhibition curve for the IC-ELISA, fifteen 1:2 serial dilution (40-0.0048 µg/ml) of standard rSelT in PBSTM were prepared. Antigen concentrations on the x axis, which is in log scale, and absorbance on the y axis, which is in linear scale, were plotted. The concentration of antigen in the sample test was interpolated from the standard-inhibition curve to obtain the antigen concentration.

3. *Ex vivo* cardiac studies

3.1 Animals

Male Wistar rats (Harlan Laboratories), weighing 250-300 g, were housed (three per cage) in a ventilated cage rack system under standard conditions. The animals had access to food and water *ad libitum*. Embryos (7th embryonic day-E7) were surgically removed from time-mated pregnant rats. In addition, newborn (14th post-natal day-P14) and adult rats (3-month old) were used for the cardiac embryogenic study. These experiments were conducted in accordance with the European Committee Council Directives and approved by the Normandy Ethics Committee on Animal Experiments. The other investigation conforms to Italian law (DL. 26/14) and to the Guide for the Care and Use of Laboratory Animals, according to National Institutes of Health publication 85-23 (revised 1996). The project was approved by the Italian Ministry of Health, Rome, and by the Ethics Review Board of the University of Calabria.

3.2 Peptides and drugs

The SelT-derived peptide 43-52 (PSELT) corresponding to the sequence FQICVSUGYR in its reduced form, and an inactive peptide without Sec used as a control, were chemically synthesized with the method of solid phase on a Fmoc resin as previously described (*Chatenet et al., 2006*), using an Applied Biosystems model 433A peptide synthesizer (AB Sciex). MDL-12,330A (MDL), a specific inhibitor of adenylate cyclase, wortmannin (WT), a potent phosphatidylinositol 3-kinase (PI3K) inhibitor, PD-98059 (PD), a specific inhibitor of

Erk-1/2 and 5-hydroxydecanoate (5HD), a mitoKATP channel blocker, were purchased from Sigma Aldrich. All drug-containing solutions were freshly prepared just before the experiments.

3.3 Isolated heart perfusion

Rats were heparinized (2.500 U i.m.) and anesthetized with ethyl carbamate (2 g/kg rat, i.p.) 10 min later. Hearts were rapidly excised and transferred in ice-cold buffered Krebs-Henseleit solution (KHs) and weighed. The performance of the rat heart was evaluated according to the Langendorff technique. The aorta was immediately cannulated with a glass cannula and connected with the Langendorff apparatus to start the retrograde perfusion (*Cerra et al., 2006*) at a constant flow-rate of 12 mL/min with oxygenated KHs, containing 4.7 mM KCl, 113 mM NaCl, 25 mM NaHCO₃, 1.8 mM CaCl₂, 1.2 mM MgSO₄, 1.2 mM KH₂PO₄, 1.1 mM mannitol, 11 mM glucose, 5 mM Na-pyruvate (Sigma Aldrich) (pH 7.4; 37 °C; 95% O₂ and 5% CO₂). The perfusion pressure was set to 100 mmHg and kept constant throughout the experiments. The hearts were kept in a temperature-controlled chamber (37 °C). To avoid fluid accumulation the apex of the left ventricle (LV) was pierced. A water-filled latex balloon, connected to a pressure transducer (BLPR; WRI, Inc.), was inserted into the left ventricle through the mitral valve, to allow isovolumic contractions and to continuously record cardiac mechanical parameters. Another pressure transducer was located above the aorta to measure coronary pressure (CP). The developed left ventricular pressure (dLVP, an index of contractile activity) and the left ventricular end-diastolic pressure (LVEDP, an index of contracture) were measured to evaluate inotropism (*Pasqua et al., 2013*). The endurance of the preparations was stable up to 190 min. The performance variables were measured every 10 min. Parameters were recorded by using the PowerLab data acquisition system (AD Instruments) as previously reported (*Pasqua et al., 2013*).

3.4 Experimental protocols

3.4.1 PSELT-stimulated preparations

Concentration–response curves were obtained by perfusing the cardiac preparations with KHs enriched with increasing concentrations of PSELT (1 pmol/L–100 nmol/L), each concentration lasting 10 min (data not shown).

3.4.2 Ischemia/Reperfusion (I/R) studies

Each heart was stabilized for 40 min during which the baseline parameters were recorded. After stabilization, hearts were randomly assigned to one of the groups described below and then subjected to 30 min of global, no-flow ischemia followed by 120 min of reperfusion (I/R). The concentration of PSELT (5 nM), corresponding to the EC₅₀ dose, was chosen on the basis of the dose-response curves.

3.4.2.1 Experimental groups

1. In the first group (**Sham group**), hearts were stabilized and perfused for 190 min with KHs alone.
2. In the second group (**I/R group**), hearts were stabilized with KHs alone and subjected to I/R protocol.
3. In the third group (**PSELT 5 nM group**), PSELT at the EC₅₀ dose (**5 nM**) was infused for 20 min at the beginning of 120 min of reperfusion.
4. In the fourth group (**PSELT 100 nM group**), PSELT at a high dose (**100 nM**) was infused for 20 min at the beginning of 120 min of reperfusion.
5. In the fifth group (**Inert PSELT group**), inert PSELT, at the same concentration of PSELT EC₅₀ (**5 nM**) was infused for 20 min at the beginning of 120 min of reperfusion.
6. In the sixth group (**rSelT group**), rSelT, at the same concentration of PSELT EC₅₀ (**5 nM**) was infused for 20 min at the beginning of 120 min of reperfusion.
7. In the groups 7-10 (**PSELT + inhibitors groups**) hearts were perfused with PSELT **5 nM** plus one of the following inhibitors: MDL (100 nM), WT (100 nM), PD (10 nM) or 5HD (10 μM);

perfusion with each inhibitor was started 5 min before ischemia (inhibitor alone) and during the early 20 min of reperfusion in the presence of PSELT 5 nM.

In all experiments, the inhibitor concentration was selected on the basis of previous reports (*Penna et al., 2012*). Previous our published data showed that in the hearts perfused with inhibitors alone, the dLVP recovery, the LVEDP and the infarct size were similar to I/R group (*Penna et al., 2012*).

3.5 Assessment of myocardial injury

To measure the infarct area, hearts were rapidly removed from the perfusion apparatus at the end of reperfusion. The left ventricles were dissected transversely into 2-3 mm slices. After 20 min of incubation at 37°C in 0.1% nitro blue tetrazolium in phosphate buffer (59.8 mM NaH₂PO₄, 484.9 mM Na₂HPO₄, pH: 7.4), unstained necrotic tissues were carefully separated from stained viable tissues by an independent observer who was not aware of the nature of the intervention. The weights of the necrotic and non-necrotic tissues were then determined, and the necrotic mass was expressed as a percentage of total left ventricular mass (% IS/LV), including septum (*Pasqua et al., 2015*).

3.6 SDS-PAGE and Western blot

Apex of cardiac ventricles were homogenized in ice-cold RIPA lysis buffer (Sigma-Aldrich) containing a mixture of protease inhibitors (1 mM aprotinin, 20 mM phenylmethylsulfonyl fluoride, and 200 mM sodium orthovanadate). Then, homogenates were centrifuged at 15000 x g for 20 min at 4 °C for debris removal. Protein concentration was determined using a Bradford reagent according to the manufacturer's procedure (Sigma-Aldrich). Equal amounts of proteins (30 µg) were separated on 12% SDS-PAGE gels [(for SeIT, β-tubulin, Bax, Bcl-2, Active Caspase 3, cytochrome c, (Cyt c), and cytochrome oxidase subunit IV, (COX-4)] or on 10% SDS-PAGE gels (for p-Akt, Akt, p-Erk-1/2, Erk1/2, p-GSK3α/β, GSK3α/β, p-p38MAPK, and p38MAPK), or on 8% SDS-PAGE gels [(for xanthine oxidase, (XO) and aldehyde oxidase-1, (AOX-1)], subjected to electrophoresis and transferred to polyvinyl difluoride membranes. The membranes were blocked with no-fat dried milk, and incubated

overnight at 4 °C with different antibodies including polyclonal rabbit antibodies against SelT (Acris antibodies), p-Akt, Akt, GSK3 α/β , Erk-1/2, monoclonal rabbit against GAPDH, monoclonal mouse antibodies against p-Erk1/2, AOX-1, Bax, Bcl-2, Cyt c, COX-IV, polyclonal goat antibody against XO and β -tubulin (Santa Cruz Biotechnology), Active Caspase 3, p-GSK3 α/β (Sigma Aldrich), p-p38MAPK, p38MAPK (Cell Signaling Technology), diluted 1:1000 in phosphate-buffered saline and 0.5% Tween 20 containing 5% non-fat dry milk (PBSTM). Antibodies against Akt, Erk-1/2, p38MAPK, GSK3 α/β , β -tubulin, GAPDH and COX-IV were used as loading controls. Anti-rabbit and anti-mouse peroxidase-linked secondary antibodies (Santa Cruz Biotechnology) were diluted 1:2000 in PBSTM. Immunodetection was performed using the ECL PLUS enhanced chemiluminescence kit (Amersham). Autoradiographs were obtained by membrane exposure to X-ray films (Hyperfilm ECL, Amersham). Immunoblots were digitalized; densitometric analyses of the bands were performed evaluating the areas and the pixel intensity represented by 256 Gray values (0=white; 256=black) and the background was subtracted. The analyses were carried out using NIH IMAGE 1.6 (National Institutes of Health, Bethesda, Maryland). For the evaluation of rSelT over-expression, 5 μ l of the material derived from each step of protein production, was used for Coomassie blue staining (Bio Rad) and western blot. The procedure was the same of that exposed in this section.

3.7 ELISA for ROS detection

Detection of reactive oxygen species (ROS) in heart samples was performed by ELISA using a commercial kit (Sunred Biological Technology) as follows: left ventricles (n=3 for each group) from Sham, I/R or with PSELT (5 nM) groups were homogenized using Ultra-Turrax[®] in phosphate buffered saline, PBS (137 mM NaCl, 2.7 mM KCl, 10 mM Na₂HPO₄, 1.8 mM KH₂PO₄; pH 7.4) plus a mixture of protease inhibitors and centrifuged at 15000 x g for 20 min (4°C). The supernatants were then assayed with the ELISA kit. According to the provider guidelines, this is an indirect ROS determination assay that recognizes free radicals conjugated with proteins. In particular, the products generated by the oxidants reaction with several amino acids of proteins are used as a general index of ROS detection. Despite this assay selectively recognizes products of protein modifications induced by ROS, such as

carbonylation, which is chemically stable and frequently used as marker for protein oxidation (Stadtman and Berlett, 1991), the ELISA assay for ROS remain semiquantitative.

3.8 Mitochondrial isolation

In order to compare the Cyt c content in mitochondrial and cytosolic fractions, mitochondria were isolated from the ventricles as previously described (Mali *et al.*, 2016). At the end of perfusion, ventricle samples from Sham, I/R and PSELT 5 nM groups were harvested and homogenized in mitochondrial isolation buffer [(IBc): 0.1 M Tris-MOPS, 0.1 M EGTA-Tris and 1 M sucrose, pH 7.4]. Homogenates were centrifuged at 2000 x g for 10 min at 4 °C and the supernatants were collected and centrifuged again at 5000 x g for 10 min at 4 °C. The sedimented mitochondrial pellets were washed twice and resuspended in 50 µL of IBc buffer. The 5000 x g supernatant represented the cytosolic fraction. All manipulations were carried out at 4 °C. To confirm the presence of mitochondria in the pellets, the monoclonal mouse antibody against cytochrome oxidase subunit IV (COX-IV) was used as mitochondrial loading control. COX-IV is an enzyme localized into the inner mitochondrial membrane (Jin *et al.*, 2005), which is not released into the cytosol during I/R injury, largely used as a mitochondrial loading control in evaluating cardioprotection (Jin *et al.*, 2005; Ong *et al.*, 2014).

3.9 Immunofluorescence

For immunohistochemistry, rats were anesthetized with sodium pentobarbital (120 mg/kg; Ceva Santé Animale) and heparinized and perfused through an intracardiac cannula with 0.9% NaCl in 0.1 M phosphate buffer (pH 7.4), followed by 4% paraformaldehyde (PFA) in PBS. Hearts were excised and post-fixed in the same fixative at 4°C, which was changed to PBS azide after 24 h. Tissues were sectioned into 50-µm or 10-µm slices with a vibratome. Sections were incubated with 1% donkey serum diluted in 1% bovine serum albumin and 0.3% Triton X-100 in PBS for 2 h at room temperature, and then exposed overnight at 4 °C to primary antibodies against SelT (Grumolato *et al.*, 2008) diluted 1:200, anti-nitrotyrosine (NT) (Merck Millipore) used as a marker of nitrosative stress diluted 1:200 and calsequestrin-2, used as a marker of cardiac sarcoplasmic reticulum staining (Santa Cruz

Biotechnology) diluted 1:200. Immunostaining was visualized using Alexa Fluor 488 or 594-conjugated secondary antibodies diluted 1:200 (Invitrogen). Counterstaining with 1 µg/mL 4,6-diamino-2-phenylindole (DAPI) (Sigma-Aldrich) in PBS for 1 min was performed prior to mounting the slides with PBS/glycerol 50/50. Samples were analyzed with a Leica SP2 confocal laser scanning microscope (DMRAX-UV) equipped with the Acousto-Optical Beam Splitter system (Leica Microsystems, France). Microscopic observations were made on The Cell imaging platform PRIMACEN (www.primacen-crihan.fr).

4. Statistics

All data were expressed as mean ± SEM. One-way ANOVA, non-parametric Newman-Keuls multiple comparison test (for post-ANOVA comparisons) and t-test were used for the analyses. Differences at * $p < 0.05$, ** $p < 0.01$, *** $p < 0.001$ were considered statistically significant. Two-way ANOVA, followed by non-parametric Bonferroni's multiple comparison test (for post-ANOVA comparisons), was used for the time course of hemodynamic analysis. Statistical analyses were carried out using Graphpad Prism5.

Results

1. Production of recombinant SelT

1.1 Enzymatic digestion of plasmid DNA

To evaluate the correct insertion of cDNA encoding for SelT into the recombinant plasmid, the plasmid DNA derived from small cultures, inoculated with single colonies of *E. coli*, was purified, quantified and digested with *NheI* and *XhoI* restriction enzymes. The agarose gel electrophoresis showed the presence of the cDNA insert, encoding for SelT, represented by a distinct DNA band with an apparent size of about 300 bp, as result of the restriction enzymes action (**Fig. 16, line 2**). On the contrary, the same reaction carried out without restriction enzymes showed the absence of this insert, confirming the achievement of plasmid recombination (**Fig. 16, line 3**).

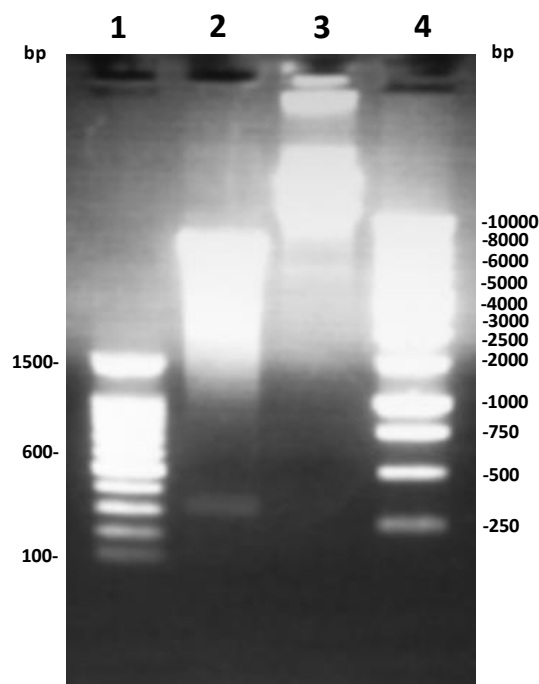


Fig. 16. Analysis of digested plasmids by electrophoresis in 1.5% agarose gel. DNA was extracted as described in Material & Methods section, digested for 2.5 hr with *NheI* and *XhoI* restriction enzymes, and the DNA equivalent of 0.18-0.21 μg was loaded onto a 1.5% agarose gel, electrophoresed at 100 V 25 min, and stained with ethidium bromide. **Lane 1.** Sizer-100bp DNA Ladder (Promega), **Lane 2.** DNA digested with *NheI* and *XhoI*, **Lane 3.** No-digested DNA, **Lane 4.** Sizer-1kb DNA Ladder (Promega).

1.2 Expression of rSelT in *E. coli*

For the assessment of the optimal condition for rSelT expression in *E. coli*, incubations of BL21 (DE3) *E. coli* containing pGEM-T/SelT plus isopropyl β -D-1-thiogalactopyranoside (IPTG) 1 mM at different times (1h, 1.5h, 2.5 h) were made. As shown in **Fig. 17A**, no protein synthesis by *E. coli* was observed in absence of IPTG (**Fig. 17A, line 2**); on the contrary, the 6His-rSelT construct was expressed with increasing efficiency after increasing time of IPTG induction (**Fig. 17A, lines 3-5**). This result was confirmed by western blot, using anti-SelT as primary antibody (**Fig. 17B, lines 2-3**).

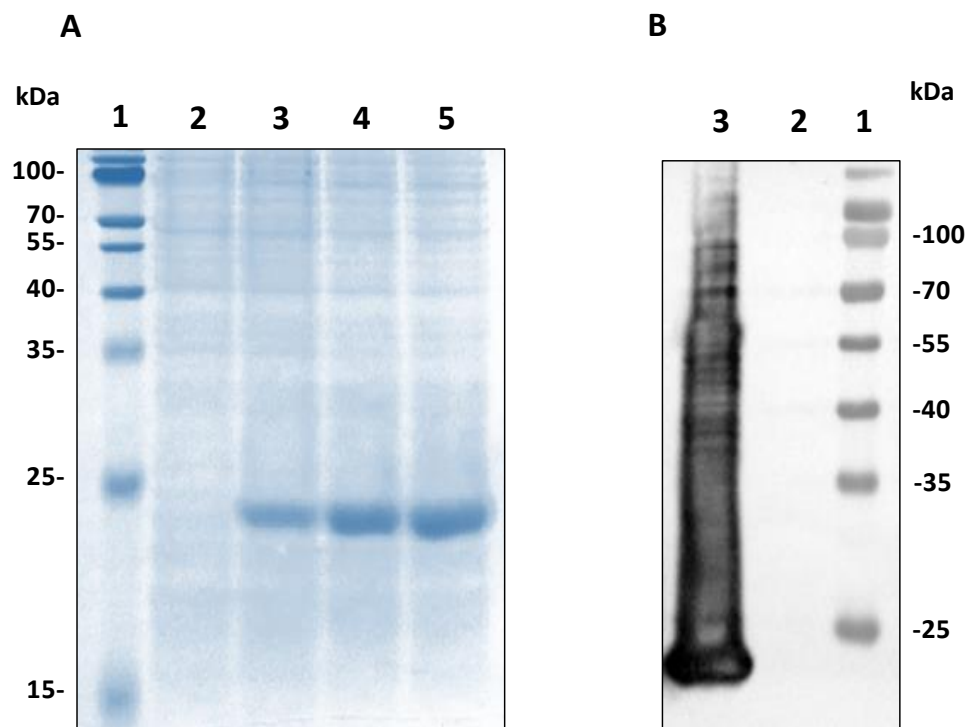


Fig. 17. Analysis of rSelT by SDS-PAGE at different times of IPTG induction. rSelT was analysed using a 12% reducing SDS-PAGE gel followed by Coomassie brilliant blue staining. **A. Lane 1.** Prestained protein size standard, **Lane 2.** Total lysate of BL21(DE3) *E. coli* containing pGEM-T/SelT before IPTG induction, **Lane 3.** Total lysate of BL21(DE3) *E. coli* containing pGEM-T/SelT after 1 h of 1mM IPTG induction, **Lane 4.** Total lysate of BL21(DE3) *E. coli* containing pGEM-T/SelT with 1 mM IPTG induction for 2 h, **Lane 5.** Total lysate of BL21(DE3) *E. coli* containing pGEM-T/SelT with 1mM IPTG induction for 2.5 h. Analysis of rSelT by Western blot before and after 2.5 h of IPTG induction, using anti-SelT (Acris Antibodies) **B. Lane 1.** Protein size standard,

Lane 2. Total lysate of BL21(DE3) *E. coli* containing pGEM-T/rSelT before IPTG induction, **Lane 3.** Total lysate of BL21(DE3) *E. coli* containing pGEM-T/rSelT with 1mM IPTG induction for 2.5 h.

1.3 Determination of 6His-rSelT solubility

Before purifying the over-expressed protein, the 6His-rSelT solubility was determined by SDS-PAGE and Coomassie brilliant blue staining. **Fig. 18** shows that, after bacterial lysis, the protein was collected in its insoluble fraction (pellet) (**Fig. 18, line 3**), but not in the soluble fraction (supernatant) of cell lysate (**Fig. 18, line 2**).

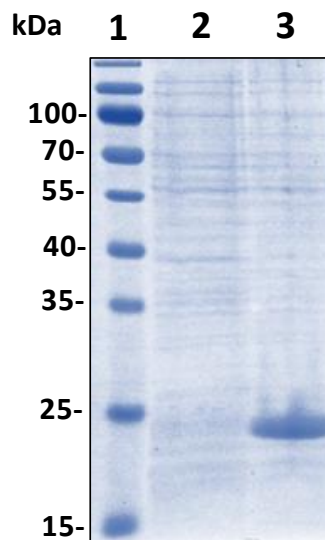


Fig. 18. Determination of rSelT solubility by 12% reducing SDS-PAGE gel followed by Coomassie brilliant blue staining. **Lane 1.** Prestained protein size standard, **Lane 2.** Supernatant after lysis of bacteria cells with lysis buffer (crude extract A), **Lane 3.** Pellet after lysis of bacteria cells with lysis buffer (crude extract B).

1.3.1 Solubilization of 6His-rSelT by the bacterial insoluble fraction

For solubilizing the insoluble matter, where rSelT was expressed, the non ionic detergent Tween-20 at two concentrations (0.25 % and 0.50 %), for two lysis cycles, was firstly used. **Fig. 19** shows that this treatment, at both concentrations, was not suitable for solubilizing rSelT. In particular, **Fig. 19A, lines 2-4**, refers to the Tween-20 0.25% treatment, **Fig. 19A,**

line 5 indicates the soluble fraction without detergent treatment, while the **Fig. 19A, lines 6-8**, refers to the Tween-20 0.50% treatment. In contrast, the chaotropic agent, urea (8 M), was effective in solubilizing the expressed protein with its consequent recovery in the soluble fraction, as shown in **Fig. 19A, lines 9-10**. The Coomassie brilliant blue staining analysis was confirmed by western blot using anti-SelT as primary antibody (**Fig. 19B**).

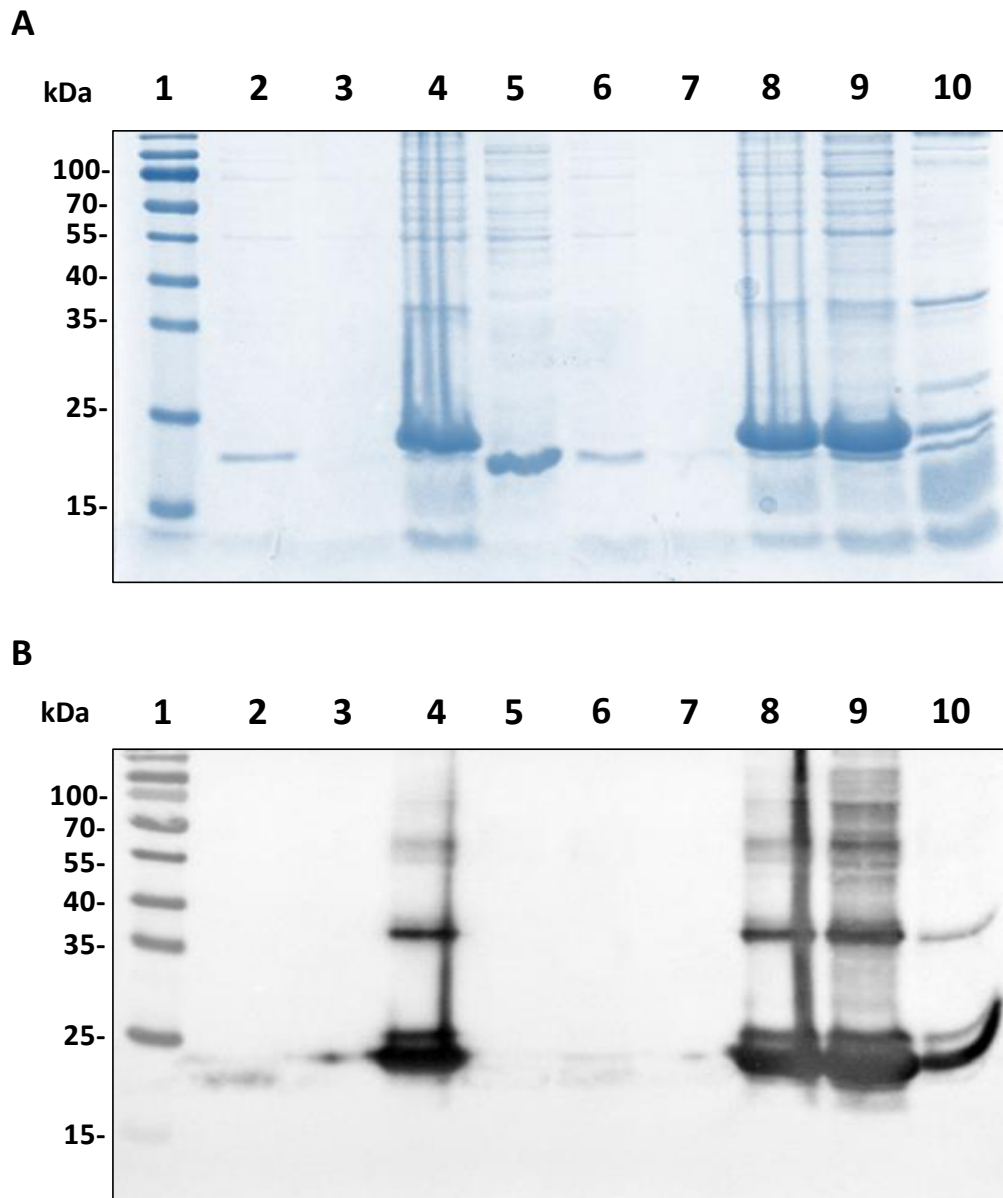


Fig. 19. A. Determination of *rSelT* solubility and solubilization of insoluble fraction results by 12% reducing SDS-PAGE gel followed by Coomassie brilliant blue staining and **B.** Western blot using anti-SelT (Acris Antibodies). **Lane 1.** Prestained protein size standard, **Lane 2.** Supernatant after 1st lysis of bacteria cells with

NPI-10 a, **Lane 3**. Supernatant after 2st lysis of bacteria cells with NPI-10 a, **Lane 4**. Pellet after lysis of bacteria cells with NPI-10 a, **Lane 5**. Supernatant after lysis of bacteria cells with NPI-10 (crude extract A), **Lane 6**. Supernatant after 1st lysis of bacteria cells with NPI-10 b **Lane 7**. Supernatant after 2st lysis of bacteria cells with NPI-10 b, **Lane 8**. Pellet after lysis of bacteria cells with NPI-10 b, **Lane 9**. Supernatant after lysis of bacteria cells with DNPI-10 and urea 8M treatment, **Lane 10**. Pellet after lysis of bacteria cells with DNPI-10 and urea 8M treatment.

1.4 Purification of the expressed 6His-rSelT under denaturing conditions and protein refolding

A His-select Ni²⁺-chelating affinity column was used for rSelT purification; after loading the solubilized protein on the column, most of contaminating proteins were eluted with the washing buffer (**Fig. 20, line 4**); urea concentration was gradually decreased and it was removed by applying a renaturation protocol, allowing the protein refolding on the Ni-NTA column (**Fig. 20, lines 5-6**); the 6His-rSelT was specifically eluted in the presence of imidazole (250 mM); the corresponding eluted fractions contained the purified protein (**Fig. 20, lines 7-16**).

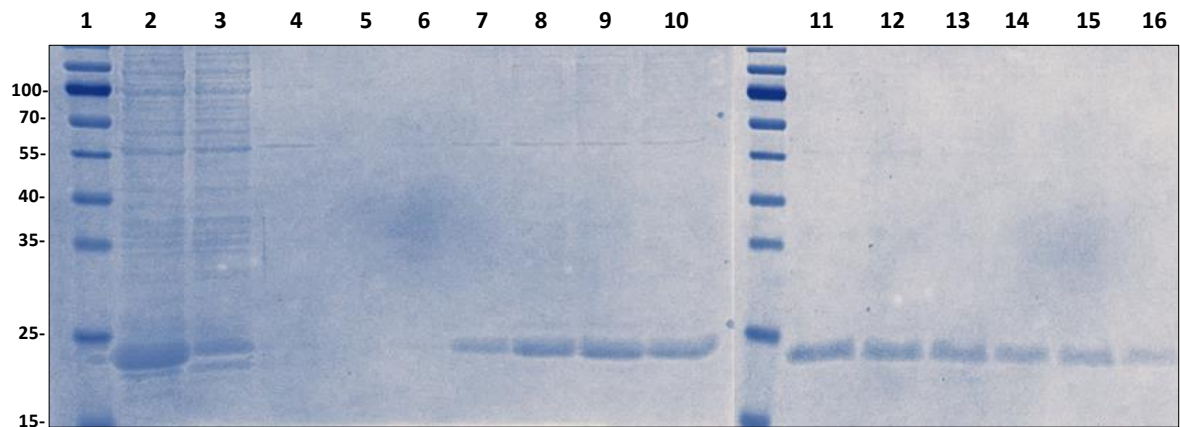


Fig. 20. Purification of 6His-rSelT under denaturing conditions analyzed by 12% reducing SDS-PAGE gel followed by Coomassie brilliant blue staining. **Lane 1**. Prestained protein size standard, **Lane 2**. Supernatant after lysis of bacteria cells with DNPI-10 (cleared lysate), **Lane 3**. Flow-through, **Lane 4**. Wash with DNPI-20, **Lane 5**. Wash with 7:1 (v/v) NPI-20/DNPI-20, **Lanes 6**. Last 10 CV Wash with NPI-20, **Lanes 7-16**. Elution with NPI-250 0.5 ml fractions.

1.5 Post-refolding analysis: activity assessment of rSelT

Since SelT is a thioredoxin-like protein because of its Sec-containing thioredoxin-like fold, its enzymatic activity was tested by using a specific assay for TrxR. **Fig. 21** shows that a purified and concentrated fraction of rSelT exhibited a TrxR-like activity similar to that of a control rat liver TrxR, dependent on Cys/Sec residues of the thioredoxin-like fold; this is demonstrated by the ATM ability to fully abrogate the enzymatic activity of both rSelT and TrxR.

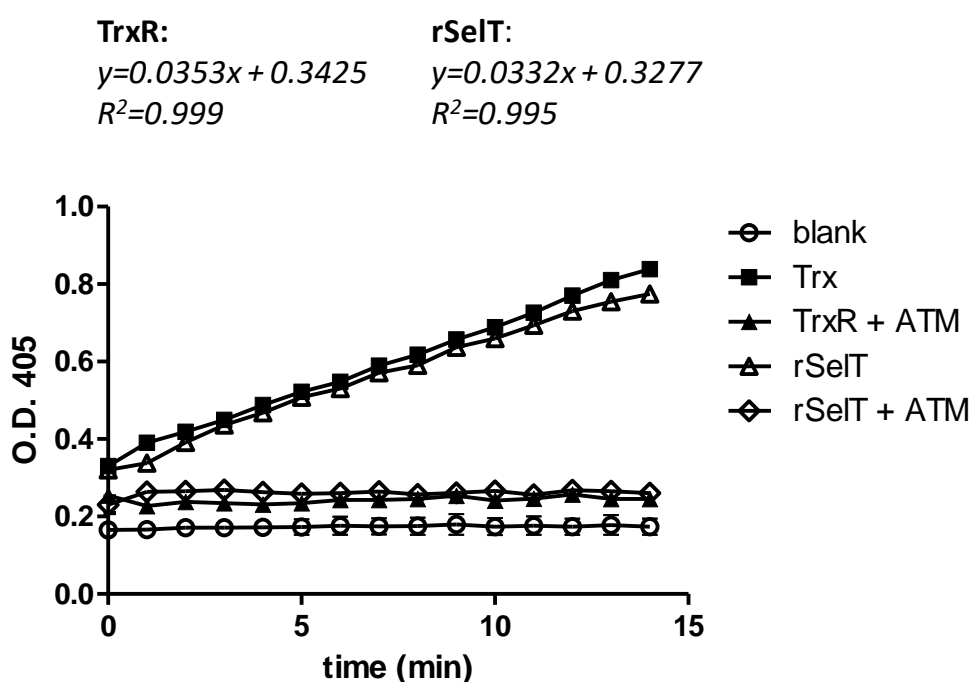


Fig. 21. Activity of rSelT (10 μ g) with a Cys instead of the Sec residue in the redox motif (SelT CVSU/C) tested using a TrxR assay and compared to that of a liver native TrxR (20 μ l of the sample supplied by the manufacturer), in the presence or absence of 20 μ M ATM. The absorbance of the reduced substrate was measured at 405 nm. One representative experiment is shown out of 3 different experiments with similar results.

In this assay, rSelT exhibited an enzymatic activity corresponding to 0.3128 ± 0.18 μ mol/min/ml (31.28 μ mol/min/mg protein) for 10 μ g of protein, giving a final concentration of 2.174 μ M, while TrxR exhibited an enzymatic activity of 0.3799 ± 0.12

$\mu\text{mol}/\text{min}/\text{ml}$ (37.99 $\mu\text{mol}/\text{min}/\text{mg}$ protein) for 20 μl of enzyme as indicated by the manufacturer.

2. Enzyme-Linked Immunosorbent Assay for SelT detection.

rSelT over expressed in *E. coli* was used as the antigen for developing two polyclonal antibody-based indirect Enzyme-Linked Immunosorbent Assays (ELISAs); this allowed to evaluate the antiserum specificity for SelT.

2.1 Assessment of sera ability to react with rSelT and C57Bl/6 mice tissue extracts

The identity of the expressed protein was evaluated by western blot, using the experimentally obtained rabbit sera against a pure fraction of rSelT. **Fig. 22A,B**, which refers to rabbits n.1 and n.2, respectively, shows that the antiserum, but not the preimmune control serum, reacted with rSelT, detecting a ~ 23 kDa band (**Fig. 22 A,B, blots 1-4**).

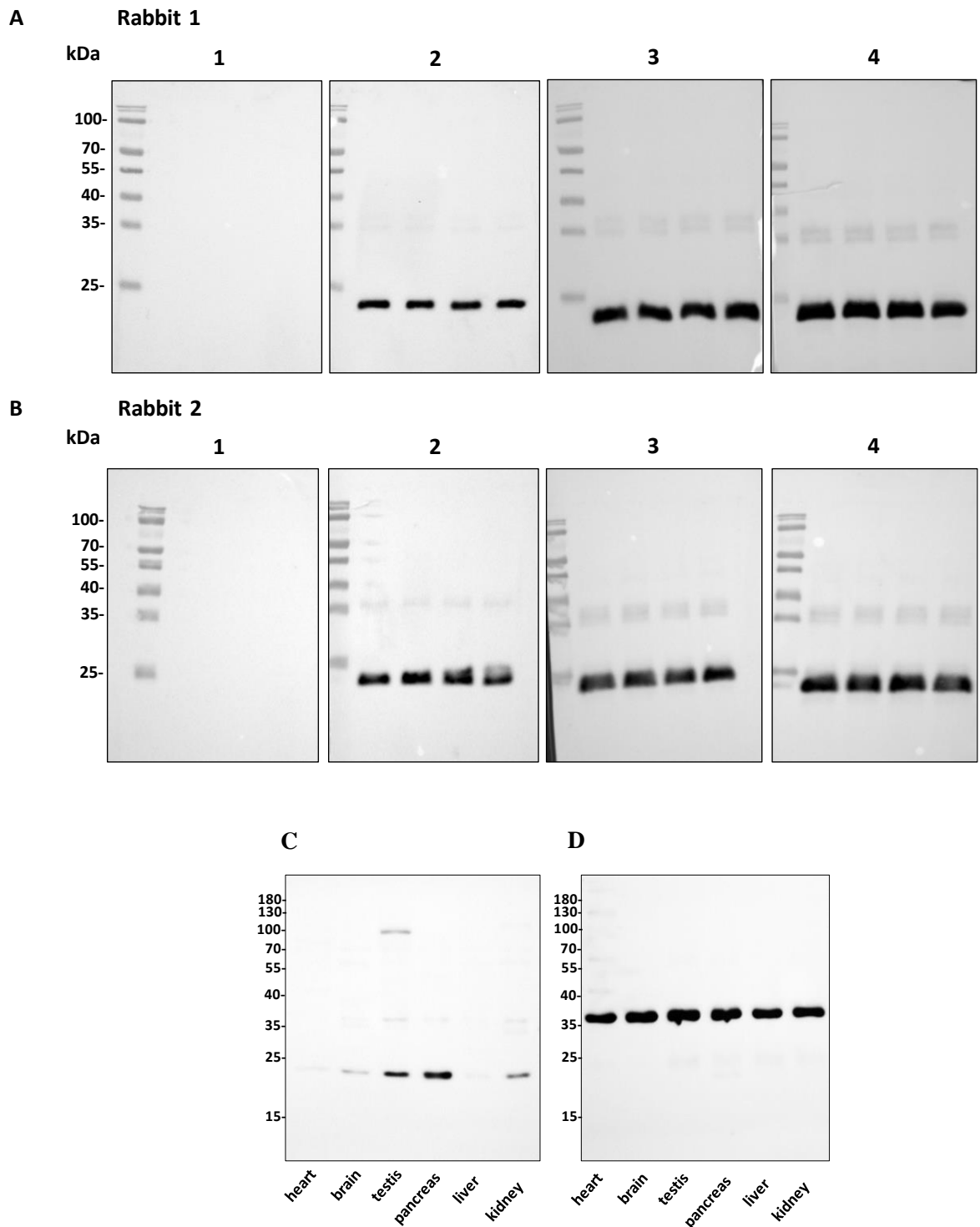


Fig. 22. Western blot analysis with the obtained antisera (1:800 dilution) from **A.** rabbit 1 and **B.** rabbit 2 as primary antibody, against rSelt. Representative results are shown. **Blot 1 of Fig. A,B.** Negative control non-immune serum of rabbit num.1 and num.2, respectively. **Blot 2 of Fig. A,B.** 27-day post-immunization serum of rabbit num.1 and num.2, respectively. **Blot 3 of Fig. A,B.** 42-day post-immunization serum of rabbit num.1 and num.2, respectively. **Blot 4 of Fig. A,B.** 91-day post-immunization serum of rabbit num.1 and num.2, respectively. For each blot, the same fraction of rSelt was repeated 4 times. **C.** Western blot analysis with

serum anti-SelT D42 (1:800 dilution) from rabbit 1 as primary antibody, using different C57Bl/6 mice tissue extracts D. and with anti-GAPDH as loading control. Representative results are shown.

In particular, sera D42 and D91 showed a stronger signal compared to antiserum D27 for in both rabbits. To evaluate sera ability to react also with the protein expressed by specific tissues, adult C57Bl/6 mice protein extracts (heart, brain, testis, pancreas, liver and kidney) were used (**Fig. 22C,D**). Western blot analysis revealed a low signal at an apparent molecular weight of 23 kDa corresponding to SelT, in adult mice heart, brain, liver and kidney; on the contrary, a more intense signal was found in testis and pancreas extracts (**Fig. 22C**). **Fig. 22D** shows the blot probed with anti-*GAPDH* used as loading control.

2.2 Determination of sera and rSelT working conditions by CBT

To determine and quantify the reactivity of SelT-specific antibodies in the rabbit sera, an I-ELISA was developed using the recombinant protein as immobilized antigen in the microtiter plate. Prior to this step, optimal sera dilutions and rSelT concentrations were determined by CBT. The use of different composition and dilution buffers, temperature and reaction times, and the secondary antibody dilution, allowed to select the highest positive/negative (P/N) ratio which was then used for immunoassay development. In **Fig. 23**, CBTs of rSelT and of primary antiserum are indicated.

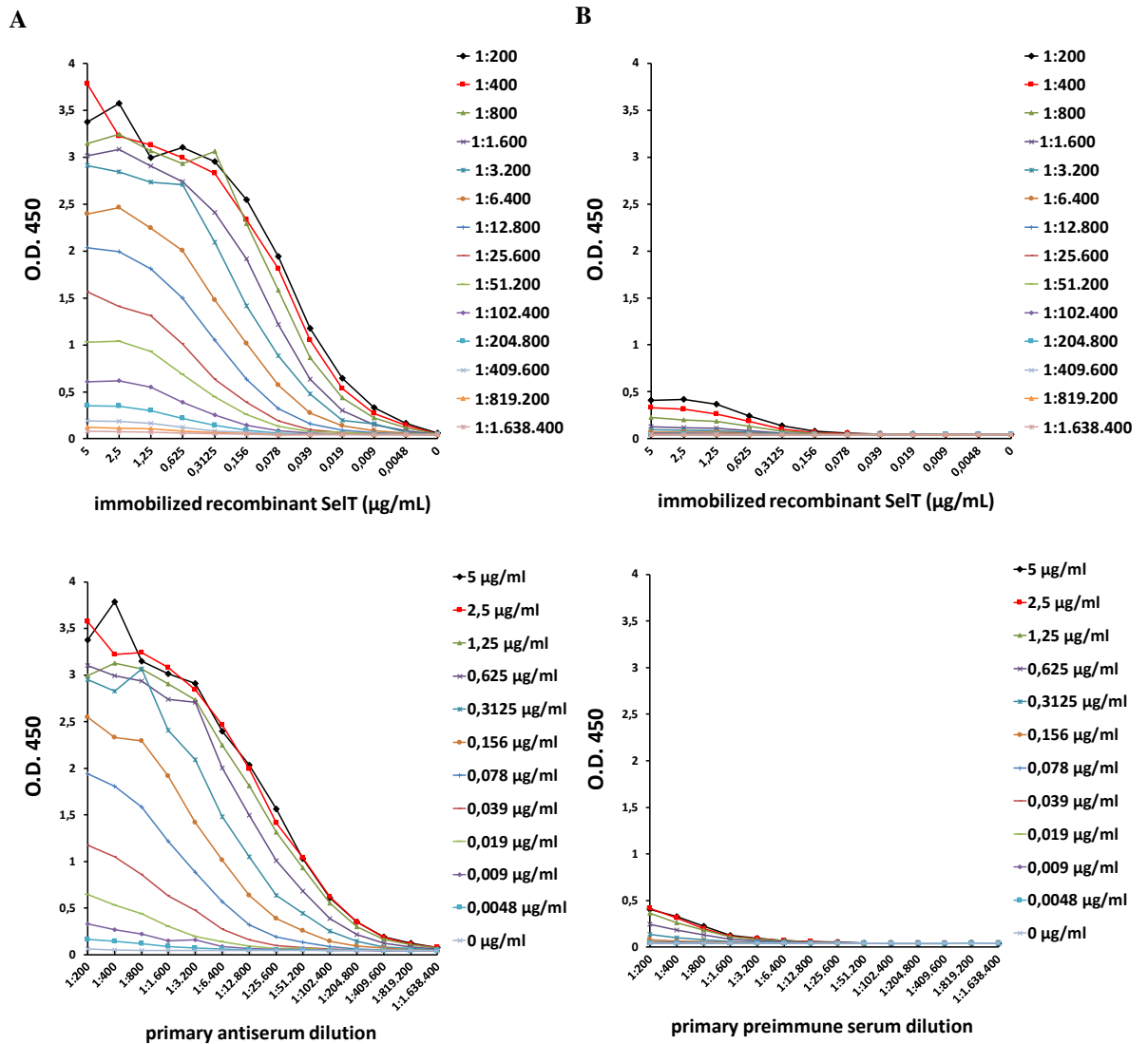
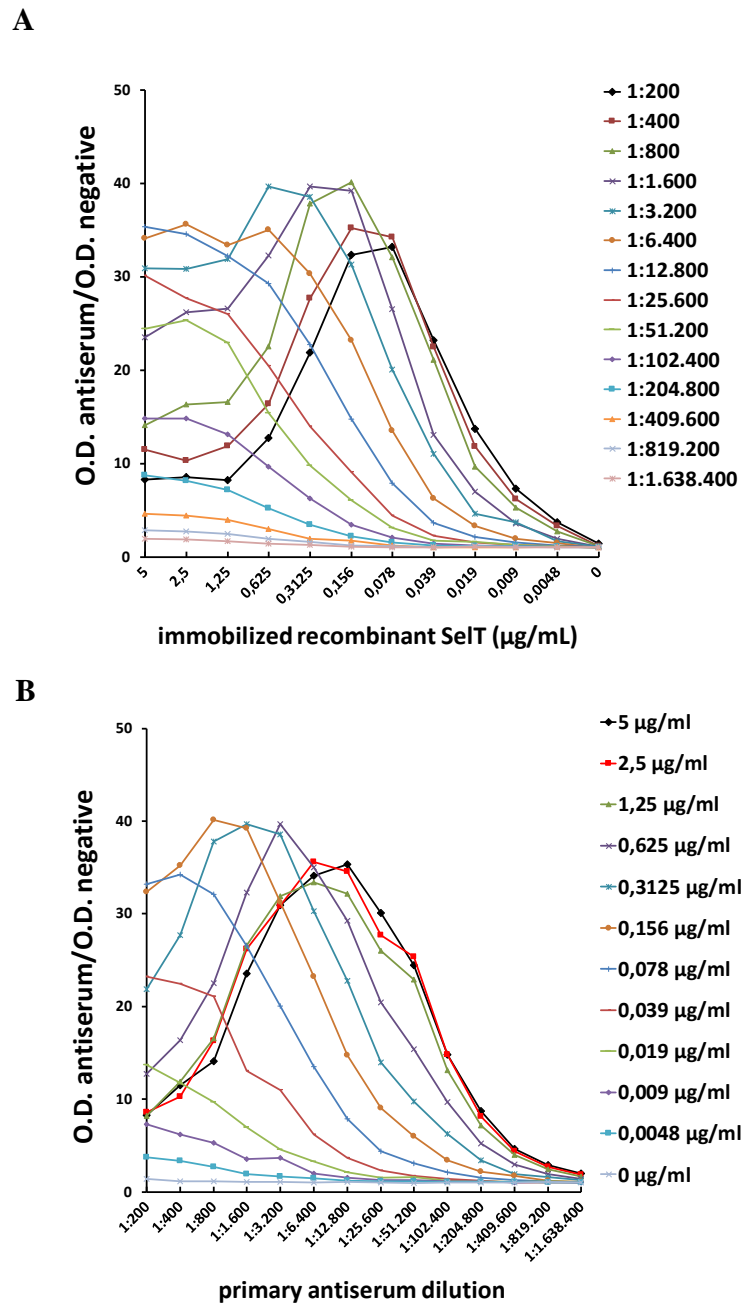


Fig. 23. A. CBT obtained varying two-fold dilution (1:200-1:1.638.400) of primary serum anti-SeIT and two-fold diluted concentration of rSeIT (5-0.0048 $\mu\text{g/ml}$) coated to the plate. B. CBT obtained varying two-fold dilution (1:200-1:1.638.400) of preimmune serum and two-fold diluted concentration of rSeIT (5-0.0048 $\mu\text{g/ml}$) coated to the plate. By convention, the graphs show the CBT for serum anti-SeIT D42 of rabbit n.1. Sera at different days post-infection showed a similar trend.

The graphs show that SeIT antiserum highly reacted with the rSeIT-coated to the plate in a dose dependent manner, as detected by a decreasing O.D. signal observed with increased dilutions of the primary antibody (Fig. 23A,B). The antiserum O.D. values were considerably greater than the preimmune serum O.D. values, for all the antiserum dilution range and for all the rSeIT concentration range. A relatively high background reaction was detected in the

preimmune serum at the 1:200 dilution and at 5 µg/ml concentration of rSelT, but it decreased at higher dilutions (**Fig. 23A,B**).

To obtain a clearer picture of the best conditions for setting up the assays, the binding ratios for the positive and negative titrations were calculated (**Fig. 24**). Binding ratio is represented by the O.D. value at a given dilution for the positive serum divided by that of the negative serum.



Maximum differences between reactions with antiserum and preimmune serum were detected at the 1:800-1:1.600 dilution range of antiserum and at 0.156-0.3125 µg/ml concentration range of rSelT (15.6-31.25 ng/well), where the binding ratios were almost 40, conditions corresponding to the highest specificity and the signal-to-noise ratio, as well as at the optimal percentage of binding between rSelT and antiserum (**Fig. 24A,B**).

Therefore, the dilution of the antiserum and the concentration of rSelT used for ELISAs were 1:800 and 15.6 ng/well, respectively. Notably, positive and negative controls were included to each ELISA plate in order to reduce the variation between the data obtained from different ELISA plates and in different times (*Miura et al., 2008*).

2.3 Measurement of SelT-specific antibodies by endpoint titer ELISA

2.3.1 Determination of the *cutoff* between negative and positive results for SelT-antibody

The negative sera from the two rabbits were used to define the O.D. *cutoff* value for antibody titers of positive anti-SelT sera D27, D42 and D91. All dilutions (1:200-1:1.638.400) of the two anti-SelT IgG-negative sera were tested with the rSelT (15.6 ng/well)-coated plates by I-ELISA. The mean O.D. \pm 1 standard deviation for the negative serum of rabbit n.1 and n.2 at 1:200 dilution was 0.0947 ± 0.0247 , and 0.0939 ± 0.0237 , respectively. This mean O.D. represented the *cutoff* value to discern a negative serum from a positive serum for SelT at 1:200 dilution (*Hackett et al., 2010*).

2.3.2 Determination of the antibody titers by I-ELISA

SelT-specific serum antibody titers were determined by I-ELISA. The reaction was considered positive if the absorbance at 450 nm was 0.1 O.D. unit above that the *cutoff* O.D. value, therefore the highest dilution at which the O.D. was ≥ 0.1947 and ≥ 0.1939 for antiserum D27, D42 and D91 of rabbit n.1 and n.2, respectively, was considered the antibody titer (endpoint) (**Fig. 25A-D**).

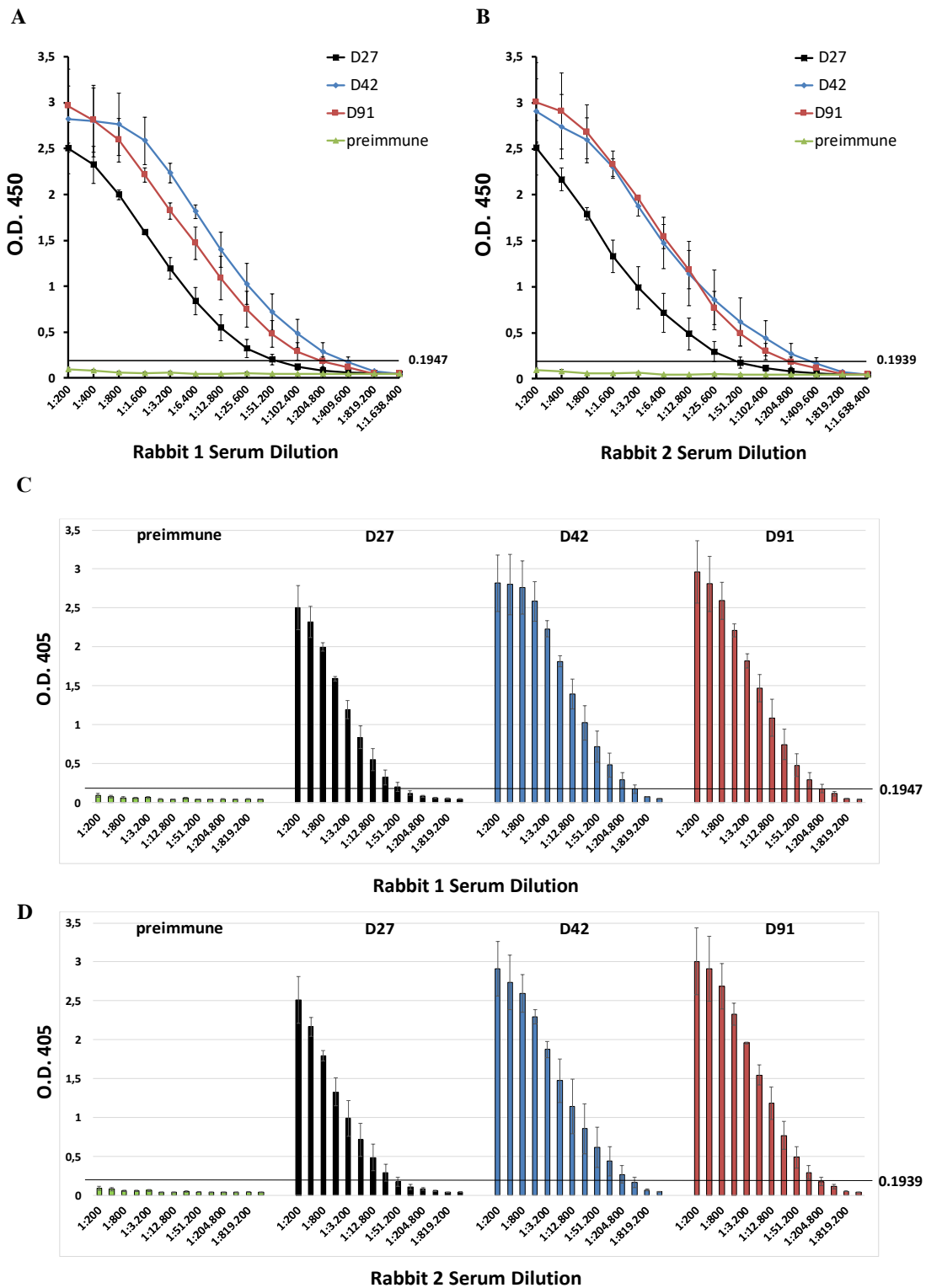


Fig. 25. *A,B.* Kinetics of serum antibodies response (antibody titers) for rabbit n.1 and rabbit n.2 and *C,D.* single O.D. values in relation to the cutoff O.D. 0.1947 and O.D. 0.1939 for rabbit n.1 and rabbit n.2, respectively, measured by I-ELISA, at different intervals post-immunization (D27, D42, D91). Each bar represents the mean O.D. \pm standard error of lectures in duplicate derived by two different experiments.

Sera of both rabbits immunized with rSelT were positive as early as 27 days and continued over the whole period of 91-day post-immunization (**Fig. 25A,B**), while the control pre-immune serum did not elicit any anti-SelT response throughout the whole immunization course (**Fig. 25A,B**). As also shown in the **table 1**, at day 27, rabbits had apparent titer range in serum of 51.200-102.400 and 25.600-51.200 for rabbit n.1 and n.2 respectively, while the titer range increased up to 204.800-409.600 for rabbit n.1 and n.2 after day 42 from immunization.

Rabbit n.1

days post-immunization	ELISA titer range
<i>preimmune</i>	<100
27	51.200-102.400
42	204.800-409.600
91	102.400-204.800

Rabbit n.2

days post-immunization	ELISA titer range
<i>preimmune</i>	<100
27	25.600-51.200
42	204.800-409.600
91	102.400-204.800

Tab. 1. SelT-specific serum titer ELISA ranges at different times after immunization (D27, D42, D91) for rabbit n.1 and n.2 were determined by I-ELISA.

It is also noteworthy that, at day 91 after rSelT administration, the apparent titer range in sera was 102.400-204.800 for rabbit n1 and n.2. Overall, in both rabbits, the profile of serum anti-SelT titer was similar between D42 and D91, showing a higher profile compared to serum anti-SelT D27 titer (**Fig. 25C,D and table 1**). By convention, titers are expressed as reciprocal values of sera dilutions; for serum antibodies, the lowest dilution tested (1:200)

was divided by 2 and used as the titer for the negative samples (i.e., preimmune samples were assigned a titer of 100) (Huang *et al.*, 2006).

2.4 CBT for commercial SeIT-antiserum

In order to compare the specificity between the serum polyclonal antibodies obtained from the rabbits experimentally immunized with rSeIT and a commercial antiserum, a CBT, using the commercial anti SeIT (N-term) primary antibody, was also performed. This antibody recognizes human SeIT (N-term) and also reacts with mouse and rat SeIT. The company dilution recommendation of this 0.5 mg/ml antibody, for ELISA application, is 1:1000; consequently, 2-fold-higher and 4-fold-lower dilutions, respect with those recommended, were carried out. The CBT from 1:250 (in 2-fold steps) to 1:16.000 were considered. The CBT of commercial antiserum is shown in **Fig. 26**.

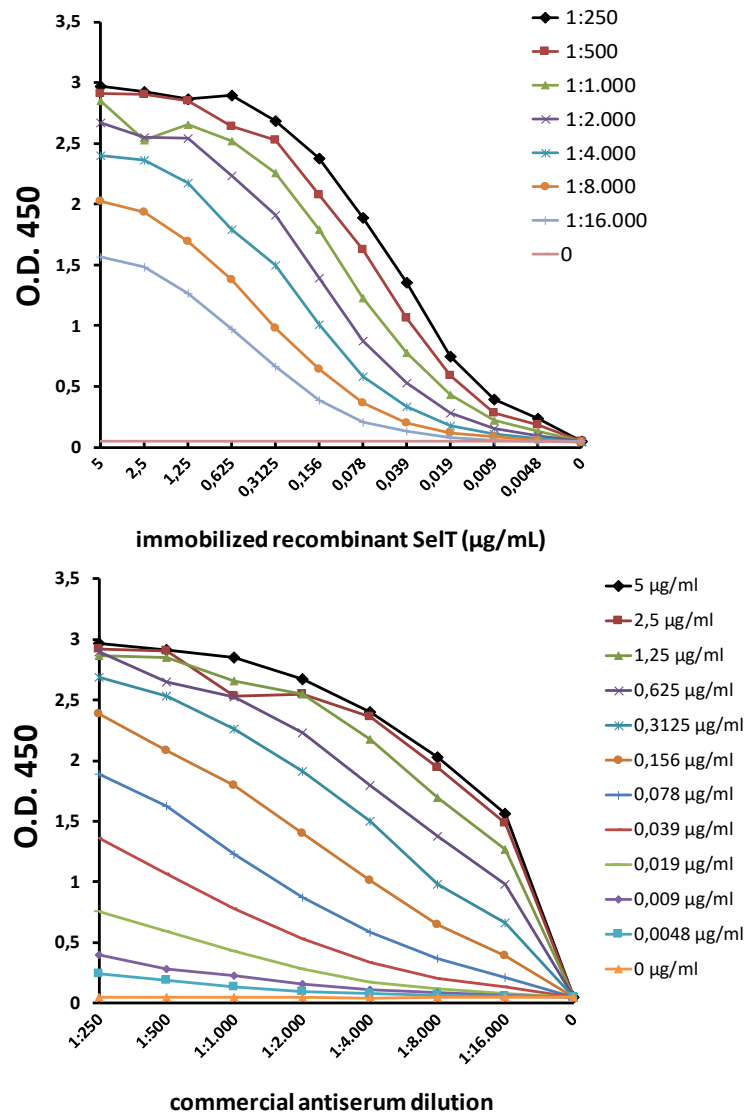


Fig. 26. CBT obtained varying two-fold dilution (1:250-1:16.000) of anti-SeIT (N-term) primary commercial antibody and two-fold diluted concentration of rSeIT (5-0.0048 µg/ml) coated to the plate.

CBT showed that commercial SeIT antiserum highly reacted with rSeIT coated to the plate in a dose-dependent manner (**Fig. 26**). The O.D. value range, obtained as result of the CBT using the experimental sera, was very similar to that obtained with this commercial antibody, as well as the O.D. values obtained with the optimal working dilution of experimental sera (1:800-1:1600) in respect to the O.D. values obtained with the recommended dilution of commercial antiserum (1:1000).

2.5 SeIT detection by IC-ELISA

2.5.1 Standard antigen-inhibition curve

The specificity of SeIT-generated antibodies was also investigated by an IC-ELISA, which was developed using the optimal concentration of rSeIT as antigen coated-plate and the optimal dilution of antiserum as primary antibody, determined by CBT. The aim was to measure the levels of antigen (SeIT) by using the principle of competitive ELISA, where the unknown antigens in the serum were allowed to compete with the antiserum bound with the standard antigen-coated plate at known concentration. For the standard antigen-inhibition curve generation, serial dilutions of standard rSeIT solution (40-0.0048 $\mu\text{g/ml}$) were used (Fig. 27A-C).

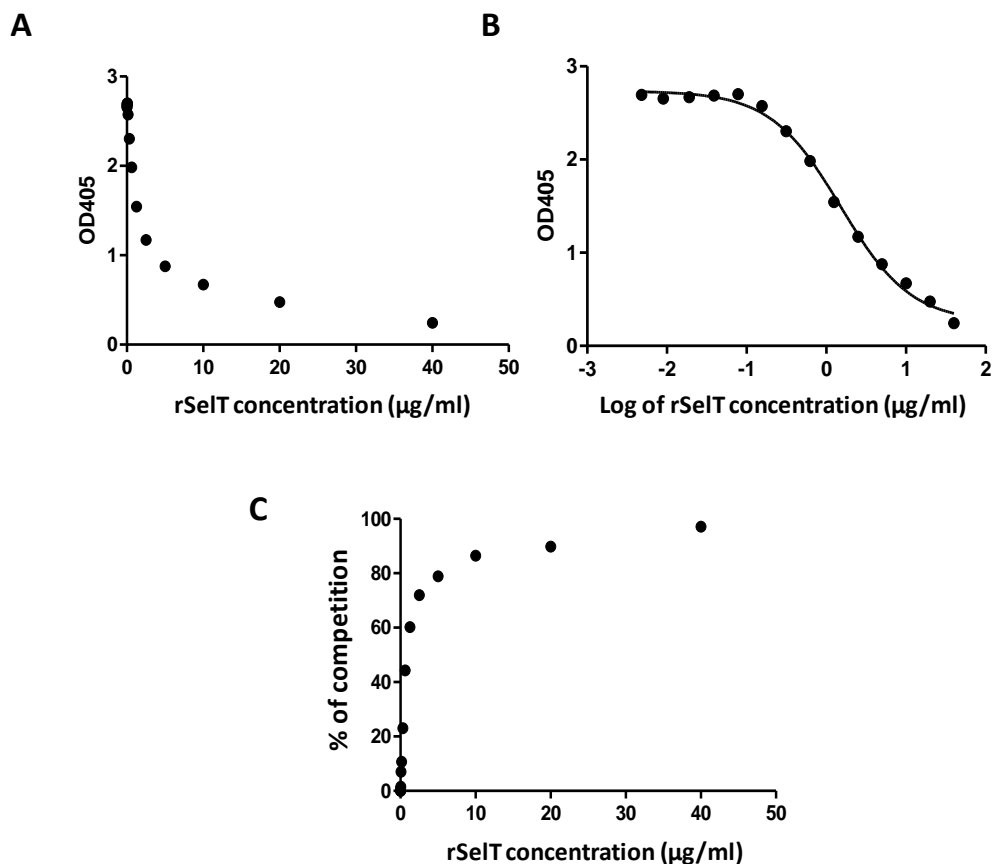


Fig. 27. A. Standard antigen-inhibition curve for rSeIT (0.0048-40 $\mu\text{g/ml}$) with the x-axis at linear scale B. Standard antigen-inhibition curve for rSeIT (0.0048-40 $\mu\text{g/ml}$) with the x-axis at log scale by IC-ELISA, C.

Standard antigen-inhibition curve for rSeIT (0.0048-40 µg/ml) expressed as non-linear regression of the percentage of competition. The three graphs were obtained using the GraphPad four-parameter sigmoidal (logistic) model.

The graphs showed that in this IC-ELISA, increasing concentrations of standard soluble rSeIT clearly led to the inhibition of the binding between the SeIT-specific antiserum and rSeIT coated-plate, in a dose-dependent manner, and that this is associated with an absorbance decrease (**Fig. 27A,B**). **Fig. 27C** shows that increasing concentrations of standard soluble rSeIT are linearly associated with an increase of the percentage of competition.

2.5.2 SeIT detection in C57Bl/6 mice tissue extracts

To assess whether the antiserum was able to recognize SeIT in biological tissues, the IC-ELISA was also applied for tissue extracts of C57Bl/6 mice. In particular, brain, heart, testis, pancreas, liver, kidney and plasma were used; in order to ensure that the unknown antigen concentrations were within the range of the standard curve, three 2-fold dilutions of each tissue and plasma samples with unknown antigen, corresponding to 0.5, 1.0 and 2.0 mg of total proteins, were tested by IC-ELISA. Tissue and plasma SeIT were quantified by interpolation onto the inhibition curve generated as previously indicated, by GraphPad four-parameter sigmoidal (logistic) model; the concentration was expressed as ng/mg tissue or as ng/mg protein (for plasma sample) (**Fig. 28**).

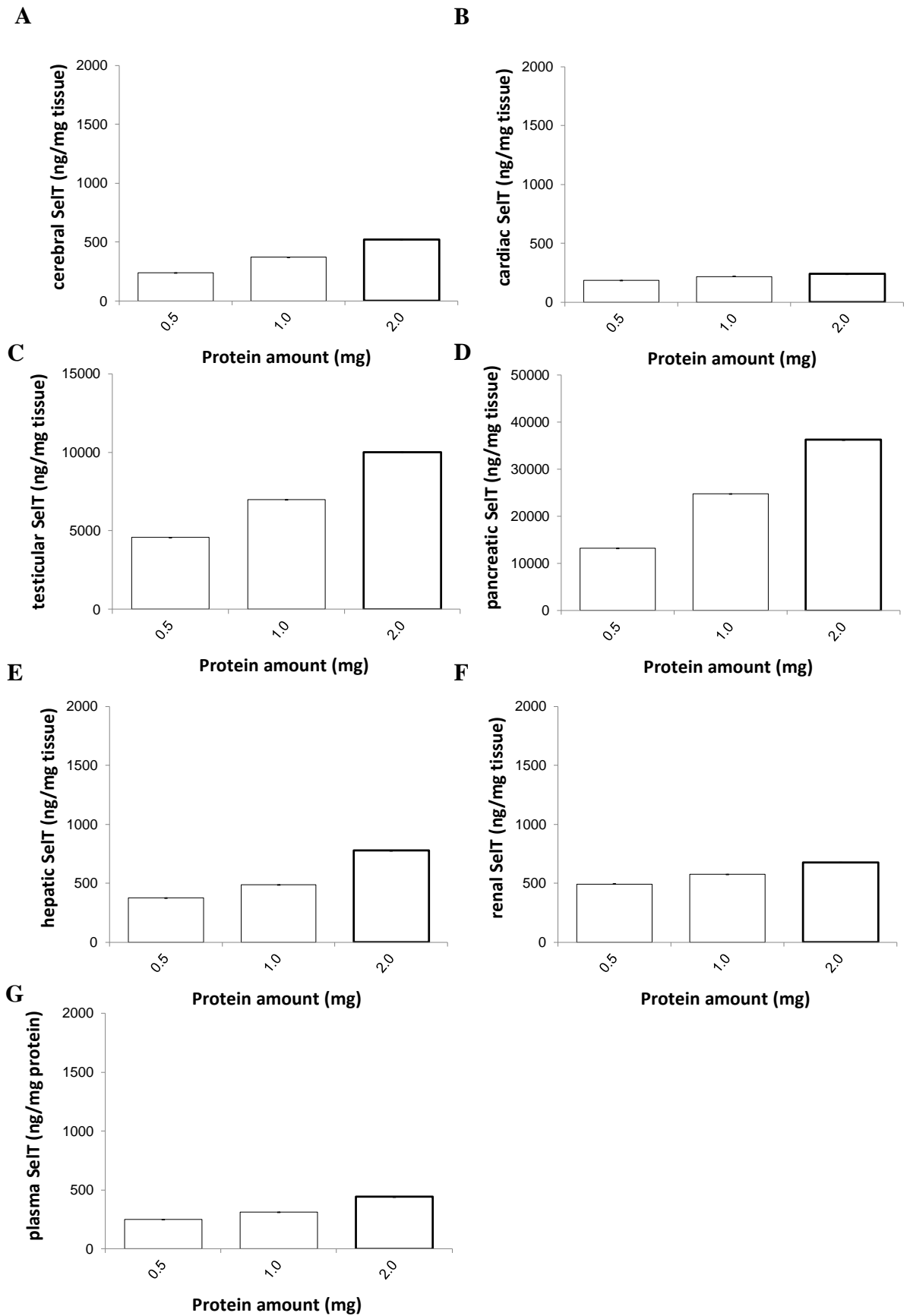


Fig. 28. IC-ELISA for SeIT detection in C57Bl/6 mice **A.** brain, **B.** heart, **C.** testis, **D.** pancreas, **E.** liver, **F.** kidney and **G.** plasma.

The antiserum was able to recognize SeIT in mice tissues; high SeIT levels were detected in pancreas and testis in a concentration dependent manner, while a low amount of SeIT was found in brain, heart, liver, kidney and plasma. The **Fig. 29A** shows the tissue detection profile of SeIT on the same axis scale.

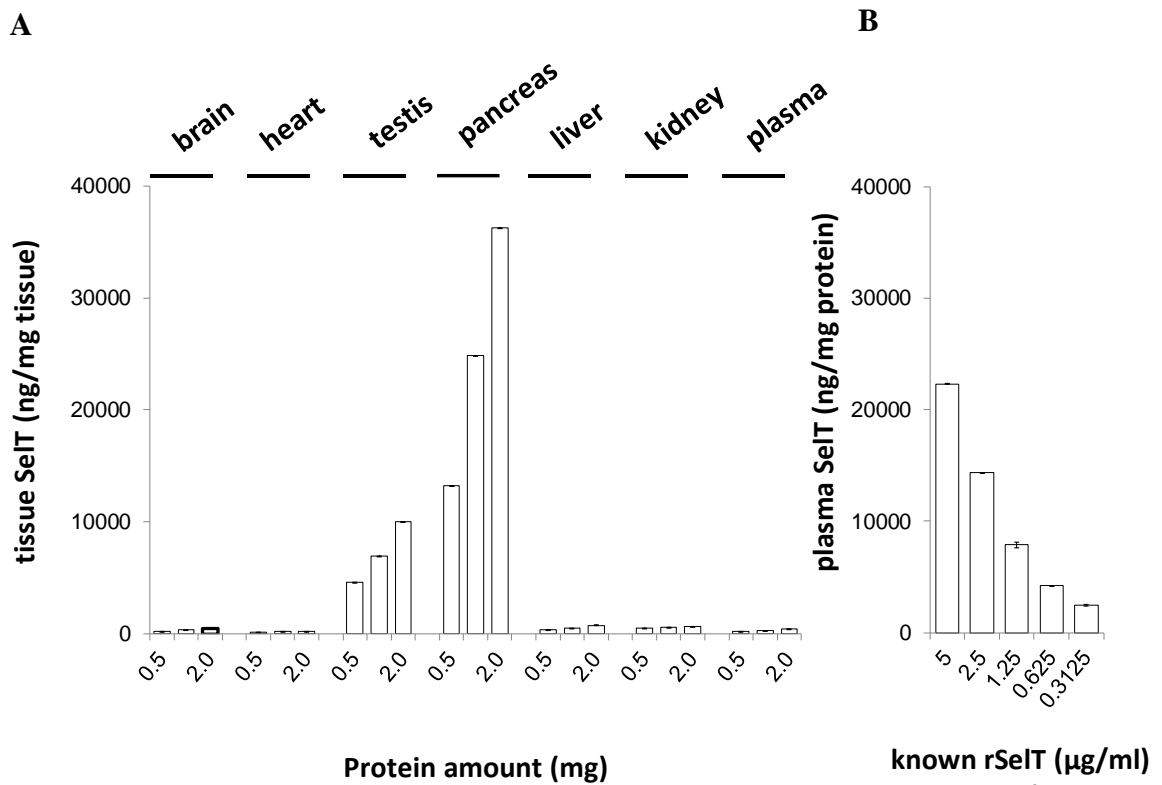


Fig. 29. A. IC-ELISA for SeIT detection in C57Bl/6 mice brain, heart, testis, pancreas, liver, kidney, plasma on the same axis scale. **B.** IC-ELISA for SeIT detection in C57Bl/6 plasma pre-incubated with known rSeIT concentration range (5-0.3125 µg/ml).

To establish whether plasma proteins may generate interferences in the binding of soluble SeIT, eventually present in plasma, and the antiserum, different SeIT increasing concentration (5-0.3125 µg/ml) were pre-incubated with plasma samples (**Fig. 29B**). A high signal was found with 5 µg/ml of rSeIT, which linearly decreased when more diluted solution was pre-incubated with plasma.

3. *Ex vivo* cardiac studies

3.1 SelT expression during heart ontogenesis

We analyzed, by immunofluorescence and western blot, the cardiac expression of SelT at different stages of heart development and in the adult. For this, we used embryonic (E7), newborn (P14), and adult (3-month old) rat cardiac tissues.

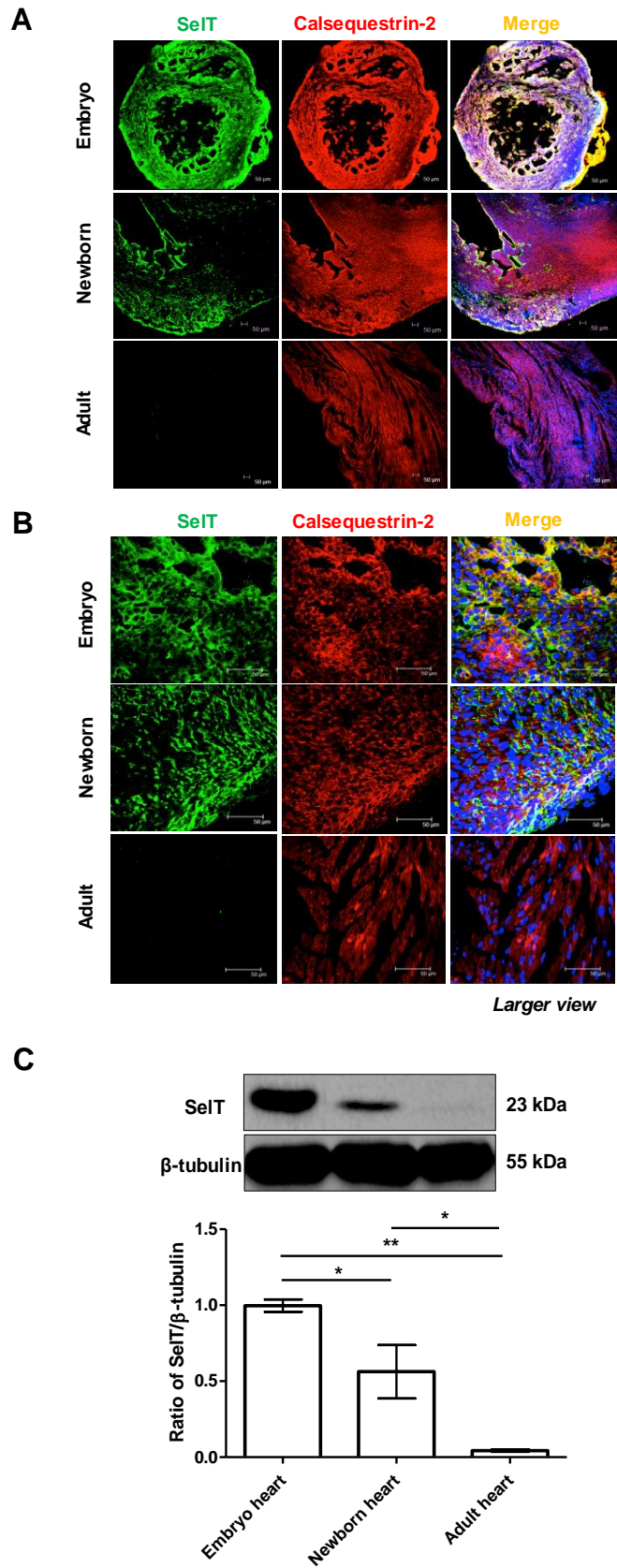


Fig. 30. SeIT expression during heart ontogenesis. A. SeIT and calsequestrin-2 immunoreactivity in the embryo, newborn and adult rat hearts. Anti- calsequestrin-2 was used as a marker of cardiac sarcoplasmic

reticulum. Nuclei were stained in blue by DAPI. **B.** Larger views of the images shown in (A). **C.** Western blot analysis of embryo, newborn and adult rat heart tissues ($n=3$ hearts/group) with SelT antibody. Histograms represent the ratio of densitometric analysis of protein/loading control: $p<0.05$ (*), $p<0.01$ (**), by One-Way ANOVA/Newman-Keuls Multiple Comparison Test.

A strong SelT immunoreactivity was observed in the embryonic tissue, which co-localized with calsequestrin-2 (**Fig. 30A,B**), indicating that cardiomyocytes express high levels of SelT during heart development (**Fig. 30A,B**).

In newborn heart, only some areas of the cardiac tissue, mostly in the periphery was labeled for SelT whereas the remaining tissue exhibited only calsequestrin-2 staining (**Fig. 30A,B**), perhaps reflecting still ongoing postnatal differentiation of heart in this region. In the adult, cardiac tissue was devoid of SelT labeling (**Fig. 30A,B**), thus indicating that SelT expression could be linked to cardiac tissue development and remodeling, and is turned off in mature adult tissue. This ontogenetic pattern of SelT expression was confirmed by western blot analysis (**Fig. 30C**).

3.2 SelT expression during cardiac ischemia

To determine whether SelT expression could be induced in adult heart after injury, immunofluorescence histochemical analysis of cardiac tissue and western blot analysis of cardiac extracts were carried out in order to evaluate SelT levels after I/R compared to controls (**Fig. 31**).

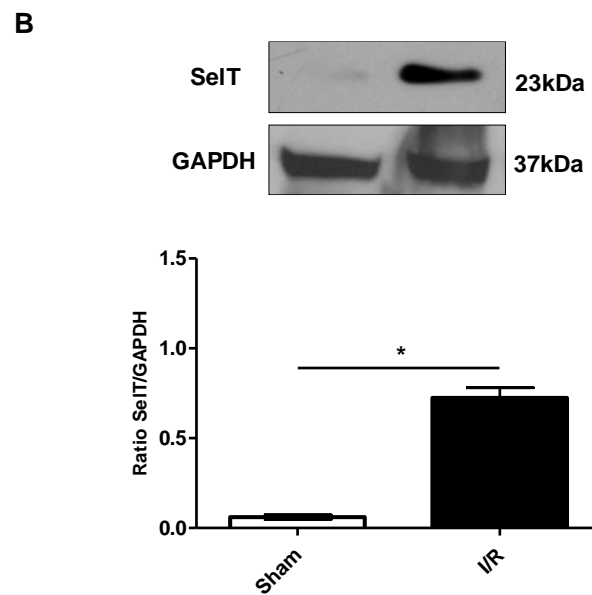
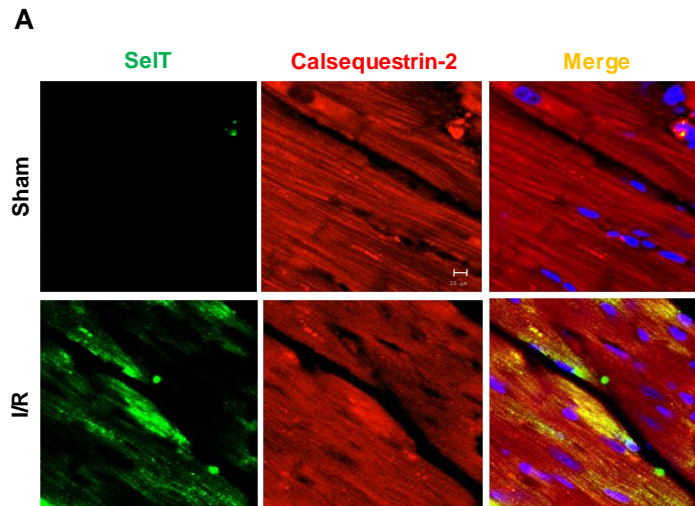


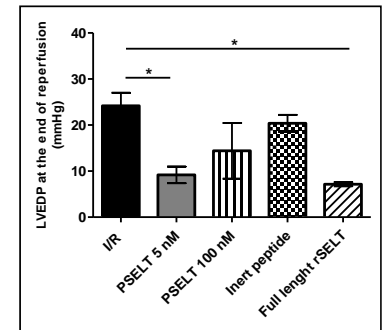
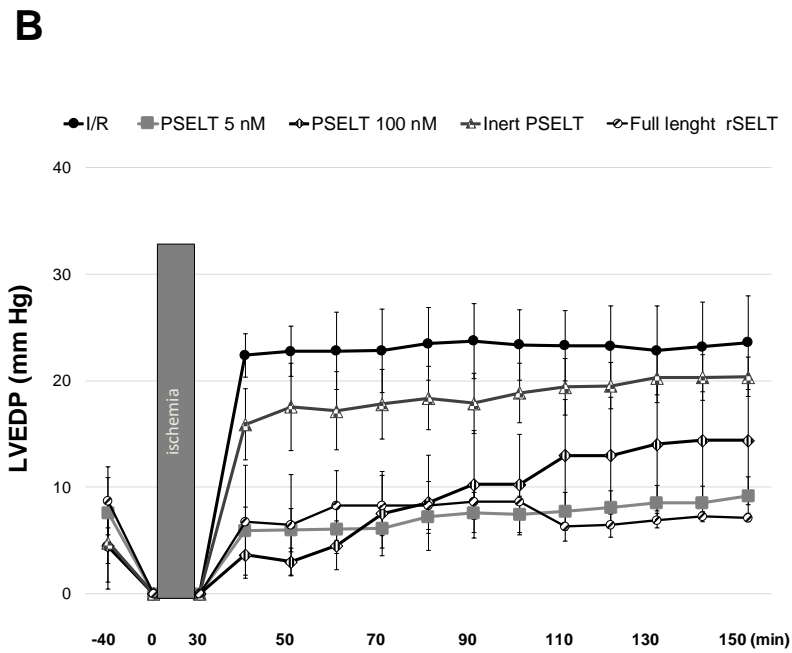
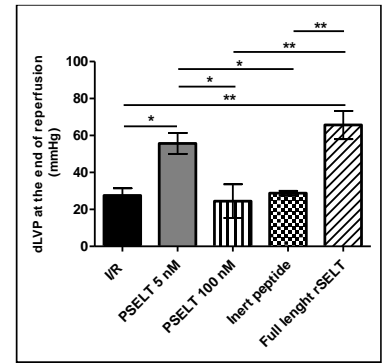
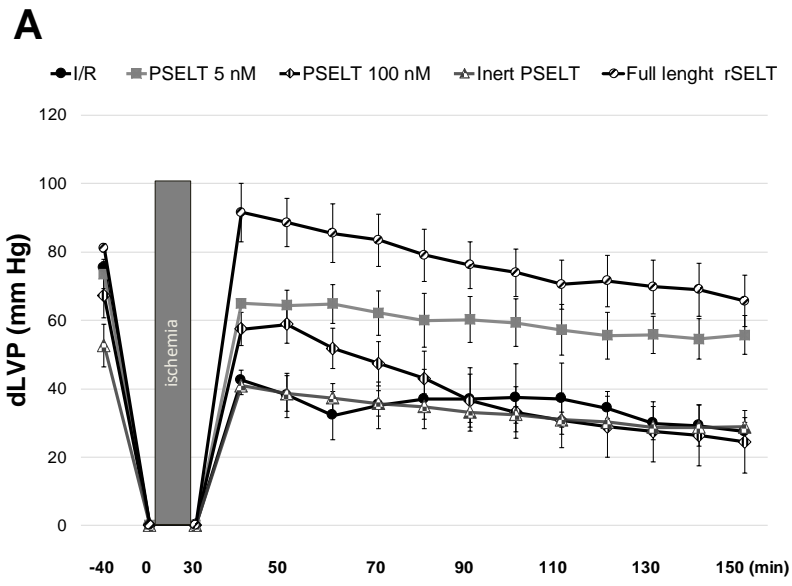
Fig. 31. SelT expression in the rat heart subjected to ischemia. A. Immunoreactivity of SelT and calsequestrin-2 in Sham and I/R-treated rat hearts ($n=3$ hearts/group). Nuclei are stained in blue by DAPI. **B.** Western blot analysis of SelT in hearts ($n=3$ hearts/group) from Sham and I/R groups. Histograms represent the ratio of densitometric analysis of protein/loading control: $p<0.05$ (*) by t-test.

Immunofluorescence analysis revealed that I/R triggers a tremendous increase in SelT immunoreactivity in cardiac tissue (**Fig. 31A**). In contrast, no change was observed for calsequestrin-2 in this condition (**Fig. 31A**). In accordance, western blot analysis showed that SelT is not expressed in control hearts as seen by immunohistochemistry. However, I/R induced a large increase in SelT expression compared to control (**Fig. 31B**).

3.3 Full length rSelT and PSELT effects on post-ischemic cardiac function

At basal conditions, after 40 min of equilibration, the cardiac parameters for all groups were: dLVP=72±2 mmHg; LVEDP=5–8 mmHg; CP=68±7 mmHg; HR=220±11 mmHg. Endurance and stability of the preparations were assessed by measuring the performance variables every 10 min. These parameters were stable up to 190 min.

The possibility that rSelT and PSELT elicit cardioprotection was investigated by comparing the effects induced by the I/R maneuver with those elicited by the full length recombinant protein or by the peptide administered after I/R for post-conditioning (PostC). The effects of PSELT on both systolic and diastolic functions were analyzed at EC₅₀ dose of 5 nM obtained by preliminary dose-response curves (data not shown) and at a higher dose (100 nM). Therefore, rSelT and Inert PSELT were tested at the same concentration (5nM). Systolic function was evaluated by measuring the developed left ventricular pressure (dLVP), an index of inotropic activity. A limited contractility recovery was observed in the I/R group (dLVP at the end of reperfusion: 27±4 mmHg; baseline values: 75±2 mmHg) (**Fig. 32A**).



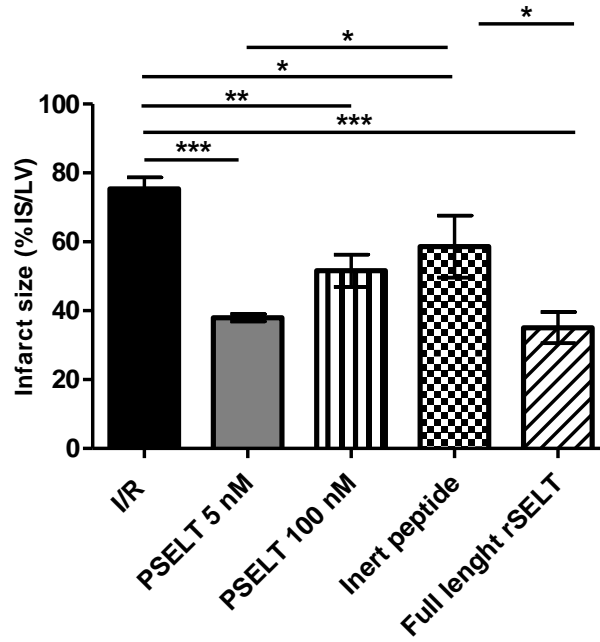
C

Fig. 32. Systolic and diastolic function and infarct size. A. dLVP and B. LVEDP variations. Data are expressed as changes of dLVP and LVEDP values (mmHg) from the stabilization to the end of the 120-min of reperfusion with respect to the baseline values for I/R (n=5) or I/R in the presence of PSELT 5 nM (n=5), PSELT 100 nM (n=5), Inert PSELT (n=4), Full length rSELT (n=5). Grey boxes indicate the ischemic period (Bonferroni Multiple Comparison test, dLVP=50.53% of total variation between groups (p <0.001); LVEDP=38.75 % of total variation between groups (p <0.001). Inset graph shows the dLVP and LVEDP at the end of reperfusion (One-way ANOVA/Newman-Keuls Multiple Comparison Test, *=p <0.05; **=p <0.01). C. Infarct size (n=5 hearts for I/R, PSELT 5 nM, PSELT 100 nM, Full length rSELT, n=4 hearts for Inert PSELT groups). The amount of necrotic tissue measured after 30-min global ischemia and 120-min reperfusion is expressed as percent of the left ventricle mass (LV) (% IS/LV). p<0.05 (*), p<0.01 (**), p<0.001 (***), by One-Way ANOVA/Newman-Keuls Multiple Comparison Test.

Full-length recombinant protein induced a remarkable recovery of dLVP at the beginning of reperfusion (dLVP at the end of reperfusion: 66±8 mmHg; baseline values: 81± 2 mmHg), but its effects were similar to those induced by PSELT at the end of reperfusion. In fact, PSELT (5 nM) induced an important improvement of dLVP recovery during reperfusion (dLVP at the end of reperfusion: 56± 6 mmHg; baseline values: 74±4 mmHg) (**Fig. 32A**). On the contrary, PSELT at a higher dose (100 nM) did not elicit any contractility recovery (dLVP at the end of reperfusion: 25±9 mmHg; baseline values: 67±7 mmHg). The inert peptide

without Sec had no effect, indicating that PSELT exerts a selective action via an intact CXXSec site. It is known that the contracture, evaluated as LVEDP is an index of diastolic function. It has been reported in the rat heart that 4 mmHg or more above the baseline level of LVEDP indicates an important cardiac damage (*Pagliari et al., 2003*). Our results showed that in I/R group, LVEDP markedly increased compared to baseline (4±4 mmHg at baseline; 24±4 mmHg at the end of reperfusion) (**Fig. 32B**). A similar effect was observed in the presence of the inert PSELT (5 ± 4 mmHg at baseline; 20±2 mmHg at the end of reperfusion). In contrast, full length rSelT, as PSELT (5 nM) added during reperfusion abolished contracture, LVEDP being 7±1 mmHg at the end of reperfusion for full length rSelT and 9±2 mmHg at the end of reperfusion for PSELT (**Fig. 32B**), indicating that both the protein and its derived peptide significantly reduce heart damage after I/R. The higher dose (100 nM) of the intact peptide was less efficient (LVEDP = 14±6 mmHg at the end of reperfusion) (100 nM). The IS was also evaluated and was expressed as a percentage of LV mass. The IS was 75±3% after I/R, which was strongly reduced (35±5%) in the presence of full length rSelT, as well as in the presence of PSELT at 5 nM (38±1%) and less at 100 nM (52±5%) (**Fig. 32C**). The inert PSELT yielded an IS of 59±9% (**Fig. 32C**).

3.4 PSELT affects cardioprotective pathways

The mechanism of action underlying the cardioprotective effect of PSELT (5 nM) was studied by using selective inhibitors of intracellular pathways involved in cardioprotection, such as MDL12,330A, a specific inhibitor of adenylate cyclase, wortmannin, a specific inhibitor of PI3K, PD098059, a selective inhibitor of Erk-1/2, and 5-hydroxy-decanoate, a specific inhibitor of mitoKATP-channels. The Infarct Size in the presence of selective inhibitors was compared with I/R and PSELT 5 nM groups showed in **Fig. 32C**. The results indicated that PSELT-dependent reduction of IS was abolished in hearts co-treated with the above inhibitors since the IS was 68±2% in the presence of MDL12,330A; in the presence of wortmannin 83±3%; 73±3% in the presence of PD098059; and 67±10% in the presence of 5-hydroxy-decanoate (**Fig. 33A**).

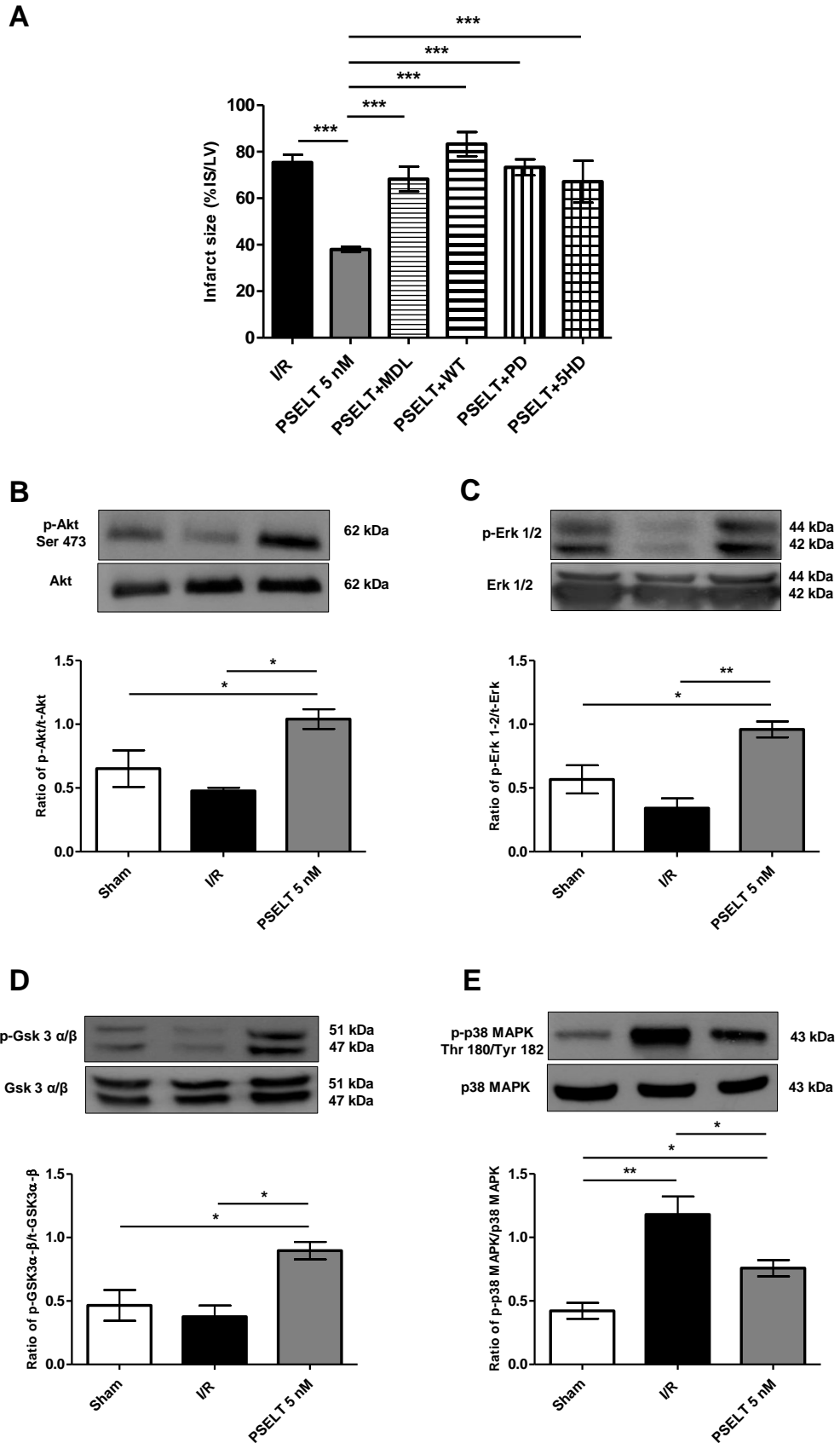


Fig. 33. Mechanism of action of PSELT in cardioprotection. A. Infarct size for I/R, PSELT 5 nM groups (n=5 hearts), and PSELT+inhibitor groups (MDL; WT; PD; 5HD) (n=4) (for comparison, IS values of I/R and PSELT 5

nM groups showed in Fig. 32C have been added). The amount of necrotic tissue measured after 30-min global ischemia and 120-min reperfusion is expressed as percent of the left ventricle mass (LV) (% IS/LV). $p < 0.05$ (*), $p < 0.01$ (**), $p < 0.001$ (***), by One-Way ANOVA/Newman-Keuls Multiple Comparison Test. Western blot analysis of phosphorylated **B.** Akt, **C.** Erk-1/2, **D.** GSK3 α/β , **E.** p38MAPK in heart tissues from Sham, I/R and PSELT 5 nM groups (n=3 hearts/group). Histograms represent the ratio of densitometric analysis of protein/loading control: $p < 0.05$ (*), $p < 0.01$ (**), by One-Way ANOVA/Newman-Keuls Multiple Comparison Test.

A similar trend was observed in the presence of the inhibitors for PSELT-dependent improved recovery of dLVP and contracture (LVEDP) (data not shown).

The involvement of the kinases Akt (*protein kinase B*), Erk-1/2 (*extracellular signal-regulated kinases 1/2*), p38MAPK (*mitogen-activated protein kinase*) and GSK3 α/β (*glycogen synthase kinase 3-beta*) in the PSELT-induced cardioprotection was evaluated by western blot analysis of the phosphorylated and not phosphorylated forms of these enzymes. Representative bands and densitometric analyses for the different kinases are shown in **Fig. 33**. In homogenates from hearts exposed to 5 nM PSELT at the reperfusion, the levels of phosphorylated Akt (**Fig. 33B**), Erk-1/2 (**Fig. 33C**) and GSK3 α/β (**Fig. 33D**) were higher, while those of phosphorylated p-38MAPK (**Fig. 33E**) were lower as compared to I/R.

3.5 PSELT influence on apoptotic indexes

The effect of PSELT (5 nM) administration at the reperfusion on the expression of the pro- and anti-apoptotic proteins, Bax, Bcl-2, active caspase3 and Cyt c are reported in **Fig. 34**.

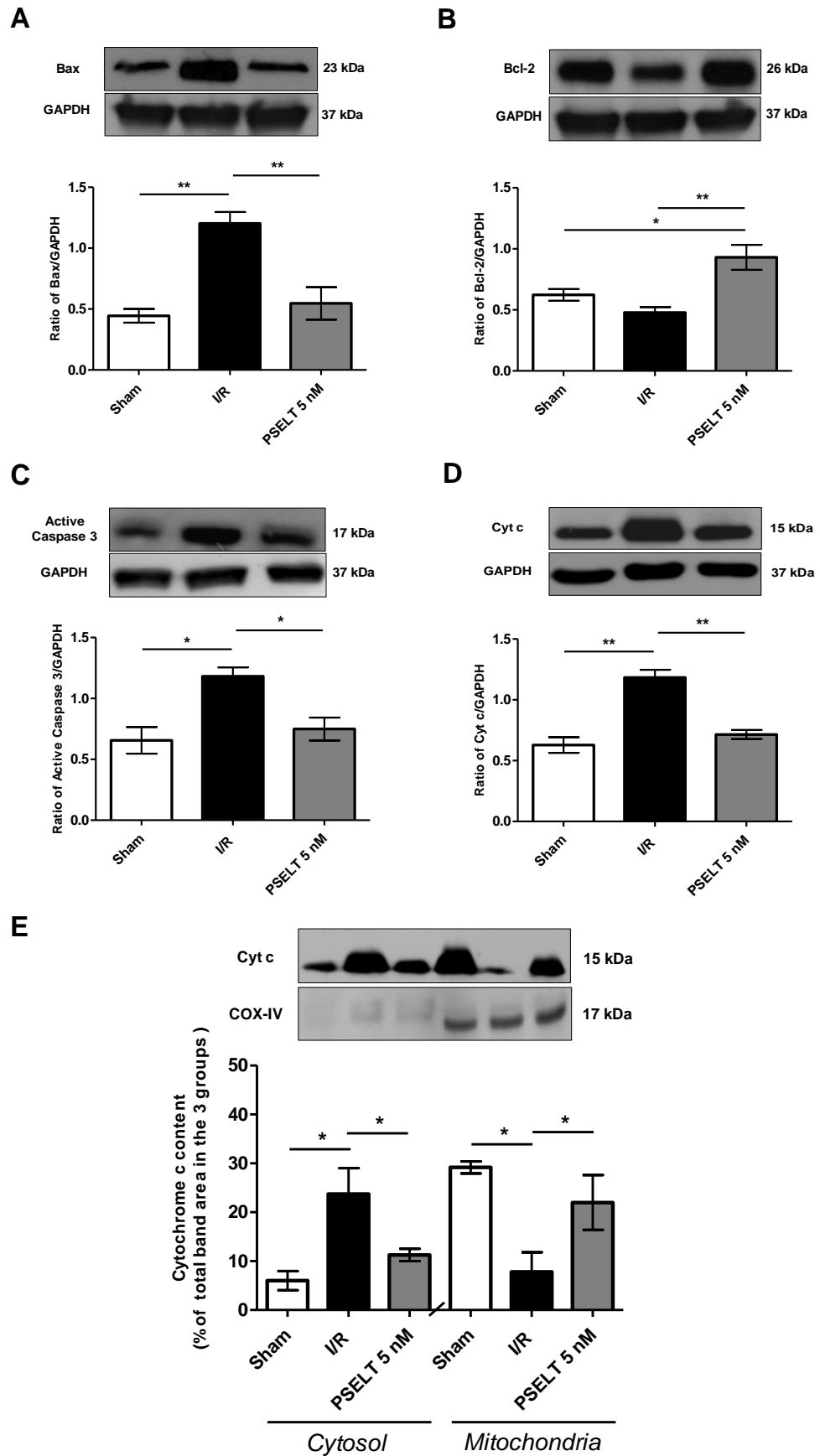


Fig. 34. Effect of PSELT on apoptotic markers. Western blot analysis of **A.** Bax, **B.** Bcl-2, **C.** active caspase 3 and **D.** Cyt c expression in heart tissues of Sham, I/R and PSELT 5 nM groups (n=3 hearts/group). Histograms

represent the ratio of densitometric analysis of protein/loading control: $p < 0.05$ (*), $p < 0.01$ (**), by One-Way ANOVA/Newman-Keuls Multiple Comparison Test. **E.** Western blot analysis of Cyt c expression in heart isolated cytosolic and mitochondrial fractions of Sham, I/R and PSELT 5 nM groups ($n=3$ hearts/group). Anti-COX-IV was used as mitochondrial loading control. Histograms represent the densitometric analysis of the bands: bars represent the area of each band expressed as a percentage of the total area of the same band in the 3 groups for cytosolic and mitochondrial fractions. $p < 0.05$ (*), by One-Way ANOVA/Newman-Keuls Multiple Comparison Test.

The peptide PSELT induced a significant reduction of the expression of the pro-apoptotic factors Bax (**Fig. 34A**), active caspase 3 (**Fig. 34B**) and Cyt c (**Fig. 34C**), and a significant increase of expression of the anti-apoptotic factor Bcl-2 (**Fig., 34D**) compared to I/R.

As shown in **Fig. 34E**, mitochondria exhibited a significant decrease of Cyt c expression in I/R group compared to the Sham group, while a significant recovery was observed in the mitochondria of PSELT group. In accordance, PSELT treatment caused a significant reduction of Cyt c in the cytosol, compared to I/R group.

3.6 PSELT influence on cellular redox balance control

The control of the redox balance by PSELT was evaluated after I/R by analyzing 3-nitrotyrosine by immunohistochemistry, by measuring intracardiac ROS production by ELISA assay and by assessing the expression of specific markers involved in the production of free radicals, such as XO and AOX-1. As shown in **Fig. 35A**, I/R induced a burst of 3-nitrotyrosine, an indicator of nitrosative stress, which was reversed in the presence of 5 nM PSELT.

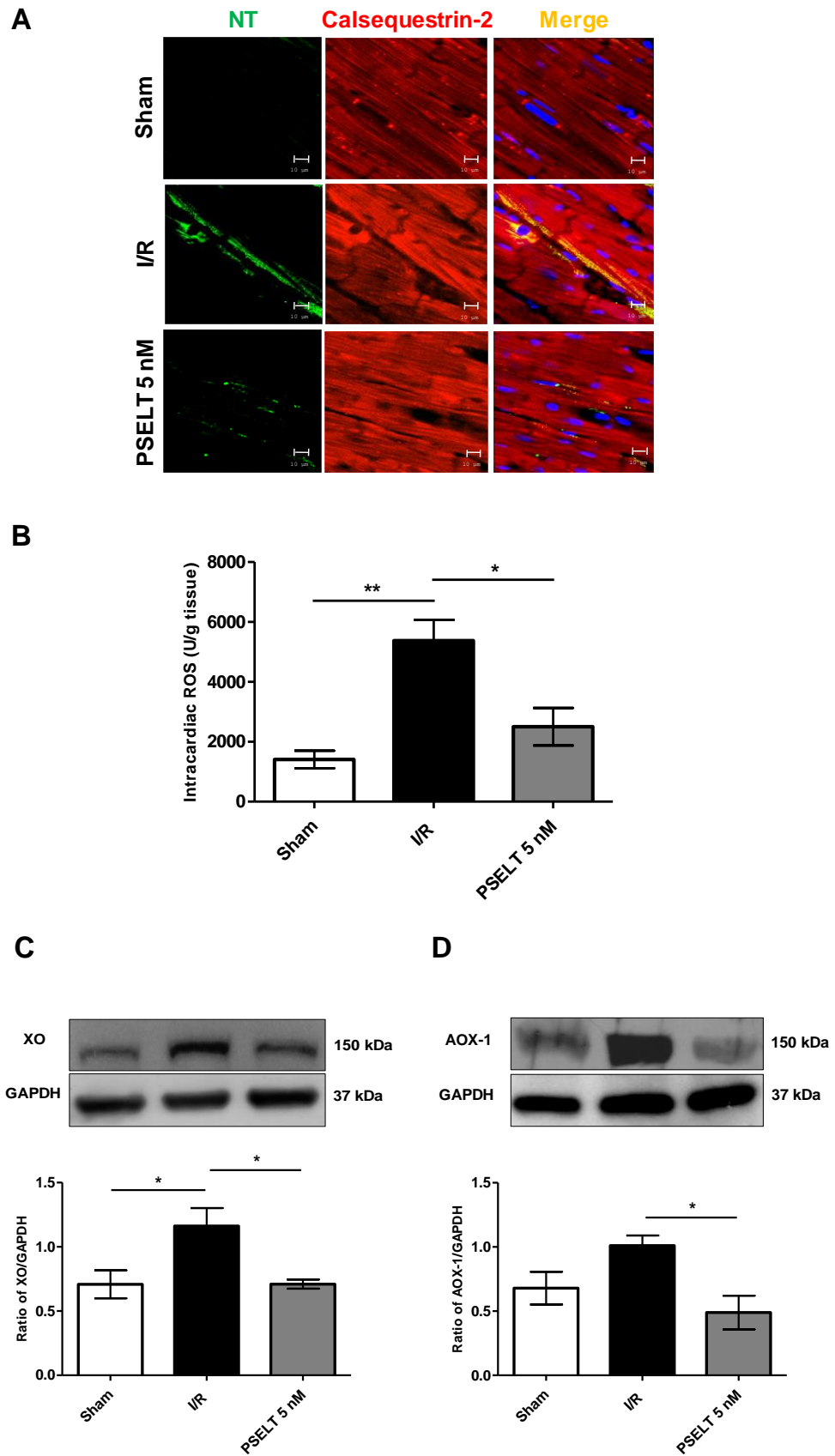


Fig. 35. Effect of PSEL T on redox balance control markers. **A.** Immunoreactivity of nitrotyrosine (NT) in Sham, I/R and PSEL T 5 nM groups (n=3 hearts/group). **B.** Intracardiac levels of reactive oxygen species (ROS) production (n=3 hearts/group) in Sham, I/R and PSEL T 5 nM groups. Western blot analysis of **C.** XO, and **D.**

AOX-1 in heart tissues from Sham, I/R and PSELT 5 nM groups (n=3 hearts/group). Histograms represent the ratio of densitometric analysis of protein/loading control: $p < 0.05$ (*), by One-Way ANOVA/Newman-Keuls Multiple Comparison Test.

Similarly, I/R provoked an increase in intracardiac ROS production, which was significantly reduced in the presence of 5 nM PSELT (**Fig. 35B**). In addition, XO and AOX-1 expression was significantly increased under I/R as compared to Sham, while post-conditioning with 5 nM PSELT abolished the expression of these oxidative stress markers (**Fig. 35C,D**).

Discussion

1. Production of recombinant SelT

A first purpose of the study was to characterize the heterologous expression of SelT. This was obtained by optimizing the protocols of overexpression and purification of a recombinant form of the protein in which Sec is replaced by a Cys in the redox motif. This allowed the protein to be produced in *E. coli*. Among heterologous protein production systems, *E. coli* remains one of the most suitable and genetically well-characterized. In this system, cells undergo a rapid growth at high density on relatively low expensive substrates (Baneyx, 1999).

We observed that the overexpressed cell lysate contained an intense protein band with an apparent molecular weight of 23 kDa, similar to that of SelT. This band increased by increasing the time of IPTG induction, while it was not present in cell lysates obtained in the absence of IPTG induction. The obtained SelT was insoluble, the large part of the protein being present in the insoluble fraction of the post-sonication pellet. These observations suggested that the highly hydrophobic properties of the protein, due to the 87-102 hydrophobic domain involved in the integration of SelT in ER membranes (Grumolato et al., 2008), may have oriented its overexpression as bacterial inclusion bodies (IB). In bacteria, IB formation results from an unbalanced equilibrium between protein aggregation and solubilization (Rosano and Ceccarelli, 2014). High levels of protein expression results in IB formation, molecular instability, and aggregation, attributed to the interaction among the hydrophobic stretches (Rosano and Ceccarelli, 2014). To overcome this limitation, several strategies may be used to obtain a soluble recombinant protein by controlling the factors leading to IB formation. In fact, IB may be completely solubilized by using high concentrations of denaturants and chaotropes like urea (Rudolph and Lilie, 1996, Misawa and Kumagai, 1999). In our experiments, treatment with urea 8M led to protein recovery in the soluble fraction. However, after IB solubilization, the excess of denaturant has to be removed to refold the protein (Misawa and Kumagai, 1999). For this purpose, we performed the solid-phase refolding process, in which the purification and the subsequent protein refolding is simultaneously carried out on column. The protein was purified through its 6His-tag that can be recovered by immobilized metal ion affinity chromatography in the presence of Ni²⁺-loaded nitrilotriacetic acid-agarose resins (Bornhorst and Falke, 2000). The

solid-phase refolding process presents several potential advantages: i) it avoids interactions between proteins since it minimizes aggregation, ii) it maintains relatively higher protein concentration during refolding, and iii) it can decrease the overall refolding process time (*Sinha and Light, 1975; Stempfer et al., 1996*). In our study, after the soluble fraction containing the protein was loaded into the column, thus allowing rSelT adsorption to the resin, urea was gradually removed. This was obtained by a urea-wash buffer that used a decreasing denaturant gradient (renaturation protocol), before protein elution. Its activity was assessed in order to verify the presence of the folded or aggregated protein (*Cabrita and Bottomley, 2004*). To test the putative activity of rSelT after the re-folding, we used a test for TrxR, since it represents one of the most important type of selenoprotein activity (*Dikiy et al., 2007*). We found that the recombinant protein exhibited an important TrxR-like activity which was similar to that of rat liver TrxR, used as control. This confirmed that the activity of rSelT was dependent on the Cys/Sec residues of the thioredoxin-like redox fold, as previously demonstrated (*Boukhzar et al., 2016*). These results suggested that SelT could exert an oxidoreductase activity since it catalyzes the reduction of an oxidized substrate in the presence of NADPH, like a TrxR-like enzyme. They also showed that the refolded protein was active. Most importantly, the study allowed to obtain, for the first time by using this approach, a purified and active rSelT.

2. Development of Enzyme-Linked Immunosorbent Assay for SelT detection

Currently, a selective ELISA assay for SelT quantification is not available. As a consequence, the detection of plasma and tissue SelT under both physiological and physiopathological conditions was not possible yet. However, this may represent a valuable tool for its characterization in term of biological significance and clinical application. For this purpose, we used the refolded protein to produce, in rabbit, polyclonal sera against rat SelT by repeated immunizations. Development of polyclonal antibodies derived from animals immunized with purified proteins or peptides is particularly important for immunoassay development (*Cooper and Paterson, 2009*). We observed that SelT-immunized rabbit antiserum strongly reacts with the homologous immunogen. A high reactivity was also observed in extracts from mouse tissues (heart, brain, testis, pancreas liver and kidney), analyzed by Western blotting. This indicates the effectiveness of the immunization protocol.

To optimize the working conditions for sera application in immunoassay, a pre-immune serum was used to calculate the highest specificity with the lowest background. This allowed to obtain the optimal percentage of antiserum bound rSelT.

To monitor the progress of the immune response, serum samples were collected at different times after immunization and were analyzed by using the developed I-ELISA test for SelT. We observed that rSelT was able to generate, throughout the immunization period, a selective immunogenic response in rabbits, confirming the generation of a hyper-immune antiserum. The absence of signal in pre-immune serum indicated a very specific immunoreactivity. These data indicated that the developed I-ELISA was able to differentiate SelT-negative from SelT-positive sera. Taking advantage from this high antiserum immunoreactivity, we also designed an IC-ELISA assay for SelT detection. Based on the results obtained in mouse tissues, such as heart, brain, testis, pancreas, liver and kidney, the detection range of the IC-ELISA test was set from 4.88 ng/ml to 40.000 ng/ml. The accuracy of the assay was corroborated by the expression profile of the protein in the same organs which was in agreement with the results previously reported by *Tanguy et al., 2011 and Prevost et al., 2013*. These results indicate that the developed ELISA may represent a first attempt to design a standardized ELISA kit for SelT detection on both plasma and tissues. However, further studies are in progress to obtain a conclusive validation of the assay in terms of sensitivity, specificity and accuracy.

3. Ex vivo cardiac studies

3.1 Cardiac expression of SelT during ontogenesis and under ischemic conditions

Selenoproteins are increasingly recognized as essential for the development and function of nervous, endocrine and metabolic tissues (*Petit et al., 2017; Papp et al., 2007; Tanguy et al., 2011*). Alteration of their synthesis is associated with major disorders, including muscular dystrophy, diabetes and thyroid disease (*Fairweather-Tait et al., 2011*). A first interesting finding of our study is that SelT is very abundant in calsequestrin-positive cardiomyocytes during embryonic ontogenesis of rat heart, while its expression was reduced in newborn and was undetectable in the adult heart. It has been shown that

proliferative growth of the myocytes for cardiac development is observed during the entire embryonic and fetal period until birth and that myocytes are in principle only able to increase their volume after birth (*Van den Hoff et al., 1997*), suggesting that SelT is required during early hyperplastic growth of cardiomyocytes. The ontogenetic expression pattern of SelT in heart is similar to that observed in the brain and other organs, such as kidney, liver, lung, skeletal muscle and adrenal gland. In fact, SelT expression is drastically reduced after cell differentiation in most tissues, as observed in chromaffin cells and Purkinje cells (*Tanguy et al., 2011; Boukhzar et al., 2016; Hamieh et al., 2017*). In contrast, its expression is maintained in several adult endocrine tissues, such as pituitary, thyroid or testis and is highly induced in metabolically active proliferating cells and in cells that are endowed with some plasticity and regenerative capacity (*Tanguy et al., 2011; Prevost et al., 2013*). Together, these observations suggest that SelT expression is associated with cell plasticity, a process which requires increased metabolism and energy but which generates free radicals. Our recent studies performed in neuronal cells showed that SelT is required for oxidative stress tolerance and that its biosynthesis is coupled to mitochondrial function during differentiation (*Castex et al., 2016*). Therefore, SelT expression during cardiac tissue ontogenesis is likely involved in cardiomyocyte protection and differentiation. However, in the maturing and adult heart, SelT expression becomes dispensable unless it is submitted to a noxious condition like I/R which triggers its re-expression in cardiomyocytes. This finding is reminiscent of the elevated expression of several selenoproteins in the nervous system (i.e. SelN, SelW, SelT and SelP and GPx) under stressful conditions, which is associated with protection against oxidative stress (*Petit et al., 2003; Baek et al., 2005; Lee et al., 2008; Chung et al., 2009*).

3.2 Cardioprotective effect of rSelT and PSELT

It has been reported that enzymes belonging to the selenoprotein family, e.g. GPx and TrxR in conjunction with Trx play a cardioprotective role after an ischemic injury (*Rose and Hoffmann, 2015*). For instance, GPx1 inhibits I/R-induced apoptosis of cardiac myocytes in mice (*Maulik et al., 1999*), and its deletion causes heart and vascular dysfunction (*Forgione et al., 2002*). The TrxR/Trx system exerts a protective effect against I/R injury by reducing infarct size and improving ventricular function recovery (*Yoshioka and Lee, 2014*).

Furthermore, Nakamura (*Nakamura et al., 1998*) showed that, in patients subjected to bypass surgery, Trx inactivation was deleterious in I/R injury. To date, there are no indications about the role exerted by endogenous or exogenous SelT in cardioprotection. In the present study, we found that pharmacological post-conditioning with the full length rSelT and PSELT, which encompasses SelT active site, protects the Langendorff perfused rat hearts exposed to I/R injury. We found that, compared to the IS detected in hearts exposed to I/R (~75%), hearts post-conditioned with PSELT showed a remarkably reduced IS (~40%), which was similar to that detected in hearts perfused with full length rSelT (~35%). IS reduction correlates with systolic function recovery and with the absence of contracture development. These effects raise the question of the site of action of PSELT. Although no definitive answer can be provided at this point for cardiomyocytes, we have recently shown using neuroblastoma cells that a fluorescent PSELT crosses the plasma membrane and may thus act intracellularly (*manuscript in preparation*). Whether PSELT acts at the level of the sarcoplasmic reticulum where SelT is localized remains to be determined. Cardioprotection was more evident in ischemic hearts exposed to PSELT at the EC50 concentration (5 nM) than in hearts exposed to the highest concentration of the peptide (100 nM). This is shown by the better post-ischemic recovery of dLVP observed in hearts exposed to 5 nM of SelT. In both cases, PSELT reduced contracture. The striking protection elicited by the peptide is indicated by the significant IS reduction, observed with both PSELT concentrations tested (5 and 100 nM). This specific concentration-dependent behaviour resembles that described for major exogenous antioxidant agents known to induce protection at lower doses, but not at higher doses (*Bouayed and Bohn, 2010*). In fact, in vitro and in vivo evidence indicates that high concentrations of antioxidants may be harmful, due to pro-oxidative effects and/or their reactivity with the physiological ROS concentrations required for optimal cellular functioning. This results in a redox disequilibrium in favour of oxidation (*Bouayed and Bohn, 2010*). Of note, PSELT cardioprotection is abolished when a control peptide where the Sec residue was replaced by a Ser, was administered in post-ischemic condition, highlighting the essential role of Sec for the cardioprotective effect.

3.3 PSELT triggers various intracellular signaling mechanisms to provide cardioprotection

It is known that post-conditioning protection involves components of the RISK cascade, such as PI3K-Akt and Erk-1/2, and requires mitoKATP-channel opening (*Hausenloy et al., 2011*). We here evaluated whether these intracellular mediators are involved in PSELT protective effects on the ischemic-reperfused heart. We found that PSELT protection was abolished by exposing the hearts to specific inhibitors of adenylate cyclase, PI3K, Erk-1/2 and mitoKATP-channels, suggesting the involvement of these pathways. Consistent with these results, we observed an increased phosphorylation of Akt, Erk-1/2, and GSK3 α - β after reperfusion with PSELT. Our data suggest that PSELT-induced protection takes place if the pathways involving adenylate cyclase, PI3K and Erk-1/2, as well as mitoKATP-channels are simultaneously activated during early reperfusion. Accordingly, mitochondria appear as the terminal effector of PSELT-induced pharmacological post-conditioning protection. In addition, a decrease in p-38MAPK phosphorylation was observed. This kinase is known for its role in myocyte apoptosis (*Maldonado et al., 2005*). In cardiomyocytes, activation of p-38MAPK results in a rapid onset of lethal cardiomyopathy associated to cardiomyocyte hypertrophy (*Streicher et al., 2010*). Conversely, p-38MAPK inhibition may reduce cardiac hypertrophy, inhibit apoptosis and prevent the progression of heart failure (*Streicher et al., 2010*), suggesting that PSELT could exert similar effects as seen in the present study for its anti-apoptotic action which is involved in the cardioprotective effect. It is known that changes in anti- and pro-apoptotic protein ratios result in inhibition or promotion of cell death (*Gustafsson and Gottlieb, 2007*). For instance, the Bcl-2 family, which includes anti- and pro-apoptotic mediators of proteins is a key regulator of apoptosis. Bcl-2 prevents Cyt c release and caspase activation, while Bax promotes these processes (*Gustafsson and Gottlieb, 2007*). Activated caspase-3 is one of the main apoptosis mediators that acts by cleaving other caspases and the anti-apoptotic Bcl-2 (*Cullen and Martin, 2009*). In agreement with the pharmacological post-conditioning protection induced by PSELT, we observed indeed that exposure of the ischemic heart to the peptide during the early reperfusion increased Bcl-2 on the one hand and decreased Bax, activated caspase-3 and cytosolic release of Cyt c on the other hand.

3.4 PSELT inhibits oxidative and nitrosative stress

In the ischemic heart, a notable increase in mitochondrial superoxide radical anion and hydrogen peroxide production leads to cell damage during reperfusion (Valdez *et al.*, 2011). The contribution of ROS to cardiomyocyte cell death and apoptosis, typical of I/R injury, is well established (Valdez *et al.*, 2011). To maintain a redox balance, cells engage several reducing enzymes including members of the selenoprotein family, such as GPx or TrxR, which play instrumental roles in cell survival and homeostasis (Bellinger *et al.*, 2009). These enzymes exert antioxidant activities that impact diverse cellular functions including redox equilibrium, protein folding and Ca²⁺ homeostasis (Bellinger *et al.*, 2009). On the basis of these observations, we investigated the influence of PSELT on the myocardial redox balance by analyzing the intracardiac oxidative and nitrosative stress (Penna *et al.*, 2011) and by evaluating enzymes and factors involved in free radical production such as XO (Yee and Pritsos, 1997) and AOX-1 (Kundu *et al.*, 2012). Interestingly, compared to I/R condition, hearts perfused with PSELT after ischemia showed a significant reduction of all the oxidative/nitrosative markers used. It is known that XO is important in ischemic conditions. In fact, ATP depletion and the subsequent loss of membrane Ca²⁺ gradient increases Ca²⁺ levels and activates Ca²⁺-dependent proteases which cause selective proteolysis of the dehydrogenase into XO. This in turn acts on both hypoxanthine and xanthine at the expense of molecular oxygen to produce superoxide ion (Yee and Pritsos, 1997). Accordingly, in the ischemic heart, as well as in myocardial infarction, XO may importantly contribute to free radical-mediated damage (Yee and Pritsos, 1997). AOX-1 is a member of the molybdo-flavoenzyme family of proteins, which catalyzes the oxidation of a variety of aldehydes, leading to the production of hydrogen peroxide. Under certain conditions, AOX1 can catalyze the formation of the superoxide free radical, and this suggests its involvement in the I/R heart damage (Kundu *et al.*, 2012). It is of interest that exposure of the reperfused heart to PSELT is accompanied by a decrease of XO and AOX-1. These results agree with those reported by Boukhzar *et al.* which showed that SelT silencing affects oxidative/nitrosative stress and survival of dopaminergic neurons (Boukhzar *et al.*, 2016). In fact, thanks to its thioredoxin-like motif, SelT was effective in catalyzing the reduction of oxidized substrates (Boukhzar *et al.*, 2016). Our findings on the effect of PSELT on components of the redox state in the ischemic heart suggests that SelT is a novel essential

effector of the intracardiac antioxidant system able to counteract free radical damage responsible for cell death during I/R.

Conclusions

In this PhD thesis, we optimized the overexpression of a recombinant form of full length SelT in *E. coli*, and we developed a selective ELISA assay for protein detection and quantification. These results provide important pieces of information for the development of standardized tests to be routinely used in biological samples. In addition, the study described for the first time SelT expression during heart development and after I/R, and also showed the cardioprotective potential of both rSelT and PSELT. We also showed that PSELT was able to counteract the damages induced by myocardial reperfusion, by decreasing IS, and improving the post-ischemic cardiac function through the modulation of various signalling effectors of apoptosis and oxidative stress. This protective action required the activation of prosurvival kinases, and mitoKATP channels. Our observations suggest for the first time that the beneficial effects of PSELT can be attributed to the active redox site CysValSerSec of SelT and this is crucial for the functional characterization of the protein in relation to cardiac function and protection. They also provide the rationale for studies aimed to investigate whether and to which extent SelT and its related peptides may represent a new class of drugs to be tested for reducing cardiac I/R injury. This could allow to develop new adjunctive therapies to be associated with reperfusion manoeuvres to reduce morbidity and mortality (*Schwartz Longacre et al., 2011*).

References

- Agamy O, Ben Zeev B, Lev D, Marcus B, Fine D, Su D, Narkis G, Ofir R, Hoffmann C, Leshinsky-Silver E, Flusser H, Sivan S, Soll D, Lerman-Sagie T, Birk OS. (2010) Mutations disrupting selenocysteine formation cause progressive cerebello-cerebral atrophy. *Am J Hum Genet.* 87: 538–544
- Antoniadou C, Shirodaria C, Warrick N, Cai S, de Bono J, Lee J, Leeson P, Neubauer S, Ratnatunga C, Pillai R, Refsum H, Channon KM. (2006) 5-methyltetrahydrofolate rapidly improves endothelial function and decreases superoxide production in human vessels: effects on vascular tetrahydrobiopterin availability and endothelial nitric oxide synthase coupling. *Circulation.* 114: 1193-1201
- Arnér ES, Nakamura H, Sasada T, Yodoi J, Holmgren A, and Spyrou G. (2001). Analysis of the inhibition of mammalian thioredoxin, thioredoxin reductase, and glutaredoxin by cis-diamminedichloroplatinum (II) and its major metabolite, the glutathione-platinum complex. *Free Radic Biol Med.* 31: 1170–1178
- Arner ES. (2010) Selenoproteins: what unique properties can arise with selenocysteine in place of cysteine? *Exp Cell Res.* 316: 1296–1303
- Atkins JF, Gesteland RF. (2000) The twenty-first amino acid. *Nature.* 407: 463- 465
- Baek IJ, Yon JM, Lee BJ, Yun YW, Yu WJ, Hong JT, Ahn B, Kim YB, Kim DJ, Kang JK, NamSY. (2005) Expression pattern of cytosolic glutathione peroxidase (cGPx) mRNA during mouse embryogenesis. *Anat Embryol (Berl).* 209: 315–321
- Baneyx F (1999) Recombinant protein expression in *Escherichia coli*. *Curr Opin Biotechnol.* 10: 411-421
- Ballihaut G, Mounicou S, Lobinski R. (2007) Multitechnique mass-spectrometric approach for the detection of bovine glutathione peroxidase selenoprotein: focus on the selenopeptide. *Anal Bioanal Chem.* 388: 585–591
- Beckman KB, and Ames BN. (1999) Endogenous oxidative damage of mtDNA. *Mutation Research.* 424: 51- 58
- Beilstein MA, Vendeland SC, Barofsky E, Jensen ON, Whanger PD. (1996) SelenoproteinW of rat muscle binds glutathione and an unknown small molecular weight moiety. *Inorganic. Biochem.* 61: 117–124
- Bellinger FP, Raman AV, Reeves MA, Berry MJ. (2009) Regulation and function of selenoproteins in human disease. *Biochem J.* 422: 11-22
- Bice JS, Baxter GF. (2015) Postconditioning signalling in the heart: mechanisms and translatability. *Br J Pharmacol.* 172: 1933-1946
- Blesa J, Trigo-Damas I, Quiroga-Varela A, Jackson-Lewis VR. (2015) Oxidative stress and Parkinson's disease. *Front Neuroanat.* 9: 91
- Böck A (2000) Biosynthesis of selenoproteins--an overview. *Biofactors.* 11(1-2):77-8
- Böck A, Forchhammer K, Heider J, Leinfelder W, Sawers G, Veprek B, Zinoni F. (1991) Selenocysteine: the 21st amino acid. *Mol Microbiol.* 5: 515-520
- Böck A, Rother M, Leibundgut M, Ban N (2006) Selenium metabolism in prokaryotes. In: *Selenium: Its Molecular Biology and Role in Human Health*, edited by Hatfield DL, Berry MJ, and Gladyshev VN. New York: Springer, p. 9–28.

- Bornhorst JA, Falke JJ. (2000) Purification of proteins using polyhistidine affinity tags. *Methods Enzymol.* 326: 245-254
- Bösl MR1, Takaku K, Oshima M, Nishimura S, Taketo MM. (1997) Early embryonic lethality caused by targeted disruption of the mouse selenocysteine tRNA gene (Trsp). *Proc Natl Acad Sci U S A.* 94: 5531-5534
- Bouayed J, Bohn T. (2010) Exogenous antioxidants--Double-edged swords in cellular redox state: Health beneficial effects at physiologic doses versus deleterious effects at high doses. *Oxid Med Cell Longev.* 3: 228-237
- Boukhzar L, Hamieh A, Cartier D, Tanguy Y, Alsharif I, Castex M, Arabo A, El Hajji S, Bonnet JJ, Errami M, Falluel-Morel A, Chagraoui A, Lihrmann I, Anouar Y. (2016) Selenoprotein T Exerts an Essential Oxidoreductase Activity That Protects Dopaminergic Neurons in Mouse Models of Parkinson's Disease. *Antioxid Redox Signal.* 24: 557-574
- Braunwald E, Kloner RA. (1985) Myocardial reperfusion: a double-edged sword? *J Clin Invest.* 76: 1713-1719
- Bubenik JL, Driscoll DM. (2007) Altered RNA binding activity underlies abnormal thyroid hormone metabolism linked to a mutation in selenocysteine insertion sequence binding protein 2. *J Biol Chem.* 282: 34653-34662
- Cabrita LD, Bottomley SP. (2004) Protein expression and refolding--a practical guide to getting the most out of inclusion bodies. *Biotechnol Annu Rev.* 10: 31-50
- Castex MT, Arabo A, Bénard M, Roy V, Le Joncour V, Prévost G, Bonnet JJ, Anouar Y, Falluel-Morel A. (2016) Selenoprotein T Deficiency Leads to Neurodevelopmental Abnormalities and Hyperactive Behavior in Mice. *Mol Neurobiol.* 53: 5818-5832
- Cerra MC, De Iuri L, Angelone T, Corti A, Tota B. (2006) Recombinant N-terminal fragments of chromogranin-A modulate cardiac function of the Langendorff-perfused rat heart. *Basic Res Cardiol.* 101: 43-52
- Chatenet D, Dubessy C, Boularan C, Scalbert E, Pfeiffer B, Renard P, Lihrmann I, Pacaud P, Tonon MC, Vaudry H, Leprince J. (2006) Structure-activity relationships of a novel series of urotensin II analogues: identification of a urotensin II antagonist. *J Med Chem.* 49: 7234-7438
- Chen Z, Siu B, Ho YS, Vincent R, Chua CC, Hamdy RC, Chua BH. (1998) Overexpression of MnSOD protects against myocardial ischemia/reperfusion injury in transgenic mice. *J Mol Cell Cardiol.* 30 :2281-9
- Chung YW, Jeong D, Noh OJ, Park YH, Kang SI, Lee MG, Lee TH, Yim MB, Kim IY. (2009) Antioxidative role of selenoprotein W in oxidant-induced mouse embryonic neuronal cell death. *Mol Cells.* 27: 609-613
- Cooke JP and Tsao PS. (1993) Cytoprotective effects of nitric oxide. *Circulation.* 88: 2451-2454
- Cooper HM, Paterson Y. (2009) Production of polyclonal antisera. *Curr Protoc Neurosci.* Jul; Chapter 5: Unit 5.5.
- Cullen SP, Martin SJ. (2009) Caspase activation pathways: some recent progress. *Cell. Death Differ.* 16: 935-938
- D'Autreaux B, Toledano MB. (2007) ROS as signalling molecules: mechanisms that generate specificity in ROS homeostasis. *Nature Rev Mol Cell Biol.* 8: 813-824

- Dawson DA, Masayasu H, Graham DI, and Macrae IM. (1995) The neuroprotective efficacy of ebselen (a glutathione peroxidase mimic) on brain damage induced by transient focal cerebral ischaemia in the rat. *Neurosci Lett.* 185: 65–69
- Dhalla NS, Elmoselhi AB, Hata T, Makino N. (2000) Status of myocardial antioxidants in ischemia-reperfusion injury. *Cardiovasc Res.* 18;47: 446-56
- Dikiy A, Novoselov SV, Fomenko DE, Sengupta A, Carlson BA, Cerny RL, Ginalski K, Grishin NV, Hatfield DL, Gladyshev VN. (2007) SelT, SelW, SelH, and Rdx12: genomics and molecular insights into the functions of selenoproteins of a novel thioredoxin-like family. *Biochemistry.* 46: 6871–6882
- Dumitrescu AM, Liao XH, Abdullah MS, Lado-Abeal J, Majed FA, Moeller LC, Boran G, Schomburg L, Weiss RE, Refetoff S. (2005) Mutations in SECISBP2 result in abnormal thyroid hormone metabolism. *Nature Genet.* 37: 1247–1252
- Elkind MS (2006) Inflammation, atherosclerosis, and stroke. *Neurologist.* 12: 140-148.
- Fagegaltier D, Hubert N, Yamada K, Mizutani T, Carbon P, Krol A. (2000) Characterization of mSelB, a novel mammalian elongation factor for selenoprotein translation. *EMBO J.* 19: 4796–4805
- Fairweather-Tait SJ, Bao Y, Broadley MR, Collings R, Ford D, Hesketh JE, Hurst R. (2011) Selenium in human health and disease. *Antioxid Redox Signal.* 14: 1337-1383
- Fallab S. (1967) Reactions with Molecular Oxygen. *Angew Chem Int Ed Eng.* 6: 496–507
- Falluel-Morel A, Vaudry D, Aubert N, Galas L, Benard M, Basille M, Fontaine M, Fournier A, Vaudry H, Gonzalez BJ. (2005) Pituitary adenylate cyclase-activating polypeptide prevents the effects of ceramides on migration, neurite outgrowth, and cytoskeleton remodeling. *Proc Natl Acad Sci USA.* 102: 2637–2642
- Ferguson AD, Labunskyy VM, Fomenko DE, Arac D, Chelliah Y, Amezcua CA, Rizo J, Gladyshev VN, Deisenhofer J. (2006) NMR structures of the selenoproteins Sep15 and SelM reveal redox activity of a new thioredoxin-like family. *J. Biol. Chem.* 281: 3536–3543
- Flohe L, Gunzler WA, Schock HH. (1973) Glutathione peroxidase: a selenoenzyme. *FEBS Lett.* 32: 132–134
- Forgione MA, Cap A, Liao R, Moldovan NI, Eberhardt RT, Lim CC, Jones J, Goldschmidt-Clermont PJ, Loscalzo J. (2002) Heterozygous cellular glutathione peroxidase deficiency in the mouse: abnormalities in vascular and cardiac function and structure. *Circulation.* 106: 1154-1158
- Ghzili H, Grumolato L, Thouénon E, Tanguy Y, Turquier V, Vaudry H, Anouar Y. (2008) Role of PACAP in the physiology and pathology of the sympathoadrenal system. *Front Neuroendocrinol.* 29: 128–141
- Gladyshev VN, Jeang KT, Stadtman TC. (1996) Selenocysteine, identified as the penultimate C-terminal residue in human T-cell thioredoxin reductase, corresponds to TGA in the human placental gene. *Proc. Natl. Acad. Sci. U. S. A.* 93: 6146–6151
- Goldhaber JI, Qayyum MS. (2000) Oxygen free radicals and excitation-contraction coupling. *Antioxid Redox Signal.* 2: 55-64
- Griendling KK, FitzGerald GA. (2003) Oxidative Stress and Cardiovascular Injury Part I: Basic Mechanisms and In Vivo Monitoring of ROS. *Circulation.* 108: 1912-1916

- Gromer S, Arscott LD, Williams CH Jr, Schirmer RH, Becker K. (1998) Human placenta thioredoxin reductase. Isolation of the selenoenzyme, steady state kinetics, and inhibition by therapeutic gold compounds. *J Biol Chem.* 273: 20096-20101
- Grumolato L, Ghzili H, Montero-Hadjadje M, Gasman S, Lesage J, Tanguy Y, Galas L, Ait-Ali D, Leprince D, Guérineau NC, Elkahloun AG, Fournier A, Vieau D, Vaudry H, Anouar Y. (2008) Selenoprotein T is a PACAP-regulated gene involved in intracellular Ca²⁺ mobilization and neuroendocrine secretion. *FASEB J.* 22: 1756-1768
- Gu QP, Sun Y, Ream LW, Whanger PD. (2000) Selenoprotein W accumulates primarily in primate skeletal muscle, heart, brain and tongue. *Mol Cell Biochem.* 204: 49–56
- Gustafsson AB, Gottlieb RA. (2007) Bcl-2 family members and apoptosis, taken to heart. *Am J Physiol Cell Physiol.* 292: 45-51
- Hamieh A, Cartier D, Abid H, Bucharles C, Calas A, Burel C, Jehan C, Grumolato L, Landry M, Lerouge M, Anouar Y, Lihrmann I. (2017) Selenoprotein T is a novel OST subunit that regulates UPR signaling and hormone secretion. *EMBO Rep.* 18: 1935-1946
- Hatfield DL, Choi IS, Ohama T, Jung JE, Diamond AM. (1994) Selenocysteine tRNA isoacceptors as central components in selenoprotein biosynthesis in eukaryotes. In: *Selenium in Biology and Human Health*. Edited by Burk RF. New York: Springer-Verlag, p. 25–44.
- Hausenloy DJ, Lecour S, Yellon DM. (2011) Reperfusion injury salvage kinase and survivor activating factor enhancement prosurvival signaling pathways in ischemic postconditioning: two sides of the same coin. *Antioxid Redox Signal.* 14: 893-907
- Hausenloy DJ, Yellon DM. (2004) New directions for protecting the heart against ischaemia-reperfusion injury: targeting the Reperfusion Injury Salvage Kinase (RISK)-pathway. *Cardiovasc Res.* 61: 448-60
- Hausenloy DJ. (2009) Signalling pathways in ischaemic postconditioning. *Thromb Haemost.* 101: 626-634.
- Holzinger A, Phillips KS, Weaver TE. (1996) Single-step purification/solubilization of recombinant proteins: application to surfactant protein B. *Biotechniques.* 20(5):804-6
- Hondal RJ, Marino SM, Gladyshev VN. (2013) Selenocysteine in Thiol/Disulfide-Like Exchange Reactions. *Antioxid Redox Signal.* 18: 1675-1689
- Hoshi T and Heinemann S. (2001) Regulation of cell function by methionine oxidation and reduction. *Journal of Physiology.* 531,1, pp1-11
- Howard MT, Carlson BA, Anderson CB, Hatfield DL. (2013) Translational redefinition of UGA codons is regulated by selenium availability. *J Biol Chem.* 288: 19401–19413
- Huang Z, Santi L, LePore K, Kilbourne J, Arntzen CJ, Mason HS. (2006) Rapid, high-level production of hepatitis B core antigen in plant leaf and its immunogenicity in mice. *Vaccine.* 24: 2506-2513
- Hurst R, Armah CN, Dainty JR, Hart DJ, Teucher B, Goldson AJ, Broadley MR, Motley AK, Fairweather-Tait SJ. (2010) Establishing optimal selenium status: results of a randomized, double-blind, placebo-controlled trial. *Am J Clin Nutr.* 91: 923-931
- Ikematsu K, Tsuda R, Tsuruya S, Nakasono I. (2007) Identification of novel genes expressed in hypoxic brain condition by fluorescence differential display. *Forensic Sci Int.* 169: 168–172

- Jin ZQ, Zhou HZ, Cecchini G, Gray MO, Karliner JS. (2005) MnSOD in mouse heart: acute responses to ischemic preconditioning and ischemia-reperfusion injury. *Am J Physiol Heart Circ Physiol.* 288(6):H2986-94
- Johnson CC, Fordyce FM, Rayman MP. (2010) Symposium on Geographical and geological influences on nutrition': factors controlling the distribution of selenium in the environment and their impact on health and nutrition. *Proc Nutr Soc.* 69: 119–132
- Jones DP and Go YM. (2011) Mapping the cysteine proteome: analysis of redox-sensing thiols. *Curr. Opin. Chem. Biol.* 15: 103–112
- Kalaycioglu S, Sinci V, Imren Y, Oz E. (1999) Metoprolol prevents ischemia-reperfusion injury by reducing lipid peroxidation. *Jpn Circ J.* 63: 718-21
- Khaper N, Rigatto C, Seneviratne C, Li T, Singal PK. (1997) Chronic treatment with propranolol induces antioxidant changes and protects against ischemia-reperfusion injury. *J Mol Cell Cardiol.* 29: 3335-44
- Kim HY, Gladyshev VN. (2005) Different catalytic mechanisms in mammalian selenocysteine- and cysteine-containing methionine-R-sulfoxide reductases. *PLoS Biol.* 3: e375
- Korotkov, KV, Kumaraswamy E, Zhou Y, Hatfield DL, and Gladyshev, VN. (2001) Association between the 15-kDa selenoprotein and UDP-glucose: glycoprotein glucosyltransferase in the endoplasmic reticulum of mammalian cells. *J. Biol. Chem.* 276: 15330–15336
- Kryukov GV, Castellano S, Novoselov SV, Lobanov AV, Zehtab O, Guigó R, Gladyshev VN. (2003) Characterization of mammalian selenoproteomes. *Science.* 300: 1439-1943
- Kryukov GV, Kryukov VM, Gladyshev VN. (1999) New mammalian selenocysteine-containing proteins identified with an algorithm that searches for selenocysteine insertion sequence elements. *J Biol Chem.* 274: 33888-33897
- Kuiper GG, Kester MH, Peeters RP, Visser TJ. (2005) Biochemical mechanisms of thyroid hormone deiodination. *Thyroid.* 15: 787–798
- Kundu TK, Velayutham M, Zweier JL. (2012) Aldehyde oxidase functions as a superoxide generating NADH oxidase: an important redox regulated pathway of cellular oxygen radical formation. *Biochemistry.* 51: 2930-2939
- Labunskyy VM, Hatfield DL, Gladyshev VN. (2014) Selenoproteins: molecular pathways and physiological roles. *Physiol Rev.* 4: 739-777
- Lassegue B, Clempus RE. (2003) Vascular NAD(P)H oxidases: specific features, expression and regulation. *Am J Physiol Regul Integr Comp Physiol.* 285: 277–297
- Lee BJ, Worland PJ, Davis JN, Stadtman TC, and Hatfield DL. (1989) Identification of a selenocysteyl-tRNA(Ser) in mammalian cells that recognizes the nonsense codon, UGA. *J Biol Chem.* 264: 9724–9727
- Lee SR, Kim JR, Kwon KS, Yoon HW, Levine RL, Ginsburg A, Rhee SG. (1999) Molecular cloning and characterization of a mitochondrial selenocysteine-containing thioredoxin reductase from rat liver. *J. Biol. Chem.* 274: 4722–4734
- Lee SR, Yon JM, Baek IJ, Kim MR, Park CG, Lee BJ, Yun YW, Nam SY. (2008) Spatiotemporal expression of the selenoprotein P gene in postimplantational mouse embryos. *Int J Dev Biol.* 52: 1005-1011
- Lei XG, Vatamaniuk MZ. (2011) Two tales of antioxidant enzymes on β -cells and diabetes. *Antioxid Redox Signal.* 14 :489–503

- Leibundgut M, Frick C, Thanbichler M, Böck A, and Ban N. (2005) A Selenocysteine tRNA-specific elongation factor SelB is a structural chimaera of elongation and initiation factors. *EMBO J.* 24: 11-22
- Leinfelder W, Stadtman TC, and Bock A. (1989) Occurrence in vivo of selenocysteyl-tRNA(SERUCA) in Escherichia coli: effect of sel mutations. *J Biol Chem.* 264: 9720–9723
- Lillig CH and Holmgren A. (2007) Thioredoxin and related molecules--from biology to health and disease. *Antioxid. Redox Signal.* 9: 25–47
- Lip GY, Edmunds E, Nuttall SL, Landray MJ, Blann AD, Beevers DG. (2002) Oxidative stress in malignant and non-malignant phase hypertension. *J Hum Hypertens.* 16: 333–336
- Lloyd-Jones D, Adams R, Carnethon M, De Simone G, Ferguson TB, Flegal K, Ford E, Furie K, Go A, Greenlund K, Haase N, Hailpern S, Ho M, Howard V, Kissela B, Kittner S, Lackland D, Lisabeth L, Marelli A, McDermott M, Meigs J, Mozaffarian D, Nichol G, O'Donnell C, Roger V, Rosamond W, Sacco R, Sorlie P, Stafford R, Steinberger J, Thom T, Wasserthiel-Smoller S, Wong N, Wylie-Rosett J, Hong Y, American Heart Association Statistics Committee and Stroke Statistics Subcommittee. (2009) Heart disease and stroke statistics--2009 update: a report from the American Heart Association Statistics Committee and Stroke Statistics Subcommittee. *Circulation.* 119: 480-486
- Lobanov AV, Hatfield DL, Gladyshev VN. (2009) Eukaryotic selenoproteins and selenoproteomes. *Biochim Biophys Acta.* 1790: 1424-1428
- Low SC, Berry MJ. (1996) Knowing when not to stop: selenocysteine incorporation in eukaryotes. *Trends Biochem Sci.* 21: 203–208
- Lu J, Holmgren A. (2009) Selenoproteins. *J Biol Chem.* 284: 723-727
- Lubos E, Loscalzo J, Handy DE. (2011) Glutathione peroxidase-1 in health and disease: from molecular mechanisms to therapeutic opportunities. *Antioxidants Redox Signaling.* 15: 1957–1997
- Maldonado C, Cea P, Adasme T, Collao A, Díaz-Araya G, Chiong M, Lavandero S. (2005) IGF-1 protects cardiac myocytes from hyperosmotic stress-induced apoptosis via CREB. *Biochem Biophys Res Commun.* 336: 1112-1118
- Mali VR, Pan G, Deshpande M, Thandavarayan RA, Xu J, Yang XP, Palaniyandi SS (2016) Cardiac Mitochondrial Respiratory Dysfunction and Tissue Damage in Chronic Hyperglycemia Correlate with Reduced Aldehyde Dehydrogenase-2 Activity. *PLoS One.* 11: e0163158
- Mariotti M, Ridge PG, Zhang Y, Lobanov AV, Pringle TH, Guigo R, Hatfield DL, Gladyshev VN. (2012) Composition and evolution of the vertebrate and mammalian selenoproteomes. *PLoS One.* 7: e33066
- Mau BL and Powis G. (1992) Inhibition of cellular thioredoxin reductase by diaziquone and doxorubicin: relationship to the inhibition of cell-proliferation and decreased ribonucleotide reductase-activity. *Biochem Pharmacol.* 43: 1621–1626
- Maulik N, Yoshida T, Das DK. (1999) Regulation of cardiomyocyte apoptosis in ischemic reperfused mouse heart by glutathione peroxidase. *Mol Cell Biochem.* 196: 13-21
- Maulik N, Engelman RM, Rousou JA, Flack JE 3rd, Deaton D, Das DK (1999) Ischemic preconditioning reduces apoptosis by upregulating anti-death gene Bcl-2. *Circulation.* 100: 11369-75

- Mihara H, Kurihara T, Watanabe T, Yoshimura T, Esaki N. (2000) cDNA cloning, purification, and characterization of mouse liver selenocysteine lyase. Candidate for selenium delivery protein in selenoprotein synthesis. *J Biol Chem.* 275: 6195–6200
- Misawa S, Kumagai I. (1999) Refolding of therapeutic proteins produced in *Escherichia coli* as inclusion bodies. *Biopolymers.* 51: 297-307
- Misu H, Takamura T, Takayama H, Hayashi H, Matsuzawa-Nagata N, Kurita S, Ishikura K, Ando H, Takeshita Y, Ota T, Sakurai M, Yamashita T, Mizukoshi E, Yamashita T, Honda M, Miyamoto K, Kubota T, Kubota N, Kadowaki T, Kim HJ, Lee IK, Minokoshi Y, Saito Y, Takahashi K, Yamada Y, Takakura N, Kaneko S. (2010) A liver-derived secretory protein, selenoprotein P, causes insulin resistance. *Cell Metab.* 12: 483-495
- Mueller AS, Mueller K, Wolf NM, Pallauf J. (2009) Selenium and diabetes: an enigma? *Free Radic Res.* 43: 1029-1059
- Murphy E, Steenbergen C. (2008) Mechanisms underlying acute protection from cardiac ischemia-reperfusion injury. *Physiol Rev.* 88: 581-609
- Nakamura H, Vaage J, Valen G, Padilla CA, Björnstedt M, Holmgren A. (1998) Measurements of plasma glutaredoxin and thioredoxin in healthy volunteers and during open-heart surgery. *Free Radic Biol Med.* 24: 1176-1186
- Nathan C, Cunningham-Bussell A. (2013) Beyond oxidative stress: an immunologist's guide to reactive oxygen species. *Nat Rev Immunol.* 13: 349-361
- Nauser T, Dockheer S, Kissner R, Koppenol WH. (2006) Catalysis of electron transfer by selenocysteine. *Biochemistry.* 45: 6038-6043
- Novoselov SV, Kryukov GV, Xu XM, Carlson BA, Hatfield DL, Gladyshev VN. (2007) SelenoproteinHis a nucleolar thioredoxin-like protein with a unique expression pattern. *J Biol Chem.* 282: 11960–11968
- Omi R, Kurokawa S, Mihara H, Hayashi H, Goto M, Miyahara I, Kurihara T, Hirotsu K, Esaki N. (2010) Reaction mechanism and molecular basis for selenium/sulfur discrimination of selenocysteine lyase. *J Biol Chem.* 285: 12133–12139.
- Ong SG, Lee WH, Theodorou L, Kodo K, Lim SY, Shukla DH, Briston T, Kiriakidis S, Ashcroft M, Davidson SM, Maxwell PH, Yellon DM, Hausenloy DJ. (2014) HIF-1 reduces ischaemia-reperfusion injury in the heart by targeting the mitochondrial permeability transition pore. *Cardiovasc Res.* 104(1):24-36
- Osawa S, Jukes TH, Watanabe K, and Muto A. (1992) Recent evidence for evolution of the genetic code. *Microbiol Rev.* 56: 229–264.
- Panee J, Stoytcheva ZR, Liu W, Berry MJ. (2007) Selenoprotein H is a redox-sensing high mobility group family DNA-binding protein that up-regulates genes involved in glutathione synthesis and phase II detoxification. *J Biol Chem.* 282: 23759–23765
- Papp LV, Lu J, Holmgren A, Khanna KK. (2007) From selenium to selenoproteins: synthesis, identity, and their role in human health. *Antioxid Redox Signal.* 9: 775-806
- Papp LV, Lu J, Striebel F, Kennedy D, Holmgren A, Khanna KK. (2006) The redox state of SECIS binding protein 2 controls its localization and selenocysteine incorporation function. *Mol Cell Biol.* 26: 4895–4910
- Pasqua T, Corti A, Gentile S, Pochini L, Bianco M, Metz-Boutigue MH, Cerra MC, Tota B, Angelone T. (2013) Full-length human chromogranin-A cardioactivity: myocardial,

coronary, and stimulus-induced processing evidence in normotensive and hypertensive male rat hearts. *Endocrinology*. 154: 3353-3365

- Pasqua T, Filice E, Mazza R, Quintieri AM, Cerra MC, Iannacone R, Melfi D, Indiveri C, Gattuso A, Angelone T. (2015) Cardiac and hepatic role of r-AtHSP70: basal effects and protection against ischemic and sepsis conditions. *J Cell Mol Med*. 19: 1492-1503
- Penna C, Pasqua T, Perrelli MG, Pagliaro P, Cerra MC, Angelone T. (2012) Postconditioning with glucagon like peptide-2 reduces ischemia/reperfusion injury in isolated rat hearts: role of survival kinases and mitochondrial KATP channels. *Basic Res Cardiol*. 107: 272
- Penna C, Perrelli MG, Tullio F, Moro F, Parisella ML, Merlino A, Pagliaro P. (2011) Post-ischemic early acidosis in cardiac postconditioning modifies the activity of antioxidant enzymes, reduces nitration, and favors protein S-nitrosylation. *Pflugers Arch*. 462: 219-233
- Persad S, Panagia V, Dhalla NS. (1998) Role of H₂O₂ in changing beta-adrenoceptor and adenylyl cyclase in ischemia-reperfused hearts. *Mol Cell Biochem*. 186: 99-106.
- Petit N, Lescure A, Rederstorff M, Krol A, Moghadaszadeh B, Wewer UM, Guicheney P. (2003) Selenoprotein N: an endoplasmic reticulum glycoprotein with an early developmental expression pattern. *Hum Mol Genet*. 12: 1045–1053
- Petty KJ. (2001) Metal-chelate affinity chromatography. *Curr Protoc Mol Biol*. Chapter 10:Unit 10.11B
- Poole LB. (2015) The Basics of Thiols and Cysteines in Redox Biology and Chemistry. *Free Radic Biol Med*. 0: 148–157.
- Prevost G, Arabo A, Jian L, Quelennec E, Cartier D, Hassan S, Falluel-Morel A, Tanguy Y, Gargani S, Lihmann I, Kerr-Conte J, Lefebvre H, Pattou F, Anouar Y. (2013) The PACAP-regulated gene selenoprotein T is abundantly expressed in mouse and human β -cells and its targeted inactivation impairs glucose tolerance. *Endocrinology*. 154: 3796-3806
- Rahman T, Hosen I, Islam MMT, Shekhar HU. (2012) Oxidative stress and human health. *Advances in Bioscience and Biotechnology*. 3: 997-1019
- Rayman MP, Infante HG, Sargent M. (2008) Food-chain selenium and human health: spotlight on speciation. *Br J Nutr*. 100: 238-253
- Rayman MP. (2004) The use of high-selenium yeast to raise selenium status: how does it measure up? *Br J Nutr*. 92: 557–73
- Rayman MP. (2012) Selenium and human health. *Lancet*. 379: 1256-1268
- Roman M, Jitaru P, Barbante C. (2014) Selenium biochemistry and its role for human health. *Metallomics*. 6: 25-54
- Rosano GL, Ceccarelli EA. (2014) Recombinant protein expression in Escherichia coli: advances and challenges. *Front Microbiol*. 5: 172
- Rose AH, Hoffmann PR. (2015) Selenoproteins and cardiovascular stress. *Thromb Haemost*. 113: 494-504
- Rudolph R, Lilie H. (1996) *In vitro* folding of inclusion body proteins. *FASEB J*. 10(1):49-56
- Sanchez A, Chiriva-Internati M, Grammas P. (2008) Transduction of PACAP38 protects primary cortical neurons from neurotoxic injury. *Neurosci Lett*. 448: 52–55
- Sandalova T, Zhong L, Lindqvist Y, Holmgren A, Schneider G. (2001) Three-dimensional structure of a mammalian thioredoxin reductase: implications for mechanism and evolution of a selenocysteine-dependent enzyme. *Proc. Natl. Acad. Sci. U. S. A*. 98: 9533–9538

- Schwartz Longacre L, Kloner RA, Arai AE, Baines CP, Bolli R, Braunwald E, Downey J, Gibbons RJ, Gottlieb RA, Heusch G, Jennings RB, Lefer DJ, Mentzer RM, Murphy E, Ovize M, Ping P, Przyklenk K, Sack MN, Vander Heide RS, Vinten-Johansen J, Yellon DM. (2011) New horizons in cardioprotection: recommendations from the 2010 National Heart, Lung, and Blood Institute Workshop. *Circulation*. 124: 1172-1179
- Shi W, Wang X, Shih DM, Laubach VE, Navab M, Lusis AJ. (2002) Paradoxical reduction of fatty streak formation in mice lacking endothelial nitric oxide synthase. *Circulation*. 105: 2078-2082
- Siedler F, Rudolph-Böhner S, Doi M, Musiol HJ, Moroder L. (1993) Redox potentials of active-site bis(cysteinylyl) fragments of thiol-protein oxidoreductases. *Biochemistry*. 32: 7488-7495
- Sies H and Jones D. (2007) Oxidative stress, in: G. Fink (Ed.), *Encyclopedia of Stress*, vol. 3, Elsevier, Amsterdam, pp. 45–48
- Sies H. (1986) Biochemistry of oxidative stress. *Angew. Chem. Int. Ed. Engl.* 25:1058–1071
- Sinha NK, Light A. (1975) Refolding of reduced, denatured trypsinogen and trypsin immobilized on Agarose beads. *J Biol Chem*. 250: 8624-8629
- Stadtman ER and Berlett BS. (1991) Fenton chemistry. Amino acid oxidation. *J Biol Chem*. 266(26):17201-11
- Steinbrenner H and Sies H. (2009) Protection against reactive oxygen species by selenoproteins. *Biochimica et Biophysica Acta*. 1790: 1478–1485
- Steinbrenner H, Hotze AL, Speckmann B, Pinto A, Sies H, Schott M, Ehlers M, Scherbaum WA, Schinner S. (2012) Localization and regulation of pancreatic selenoprotein P. *J Mol Endocrinol*. 50: 31-42
- Steinmann D, Nauser T, Koppenol WH. (2010) Selenium and sulfur in exchange reactions: a comparative study. *J Org Chem*. 75: 6696-6699
- Stempfer G, Höll-Neugebauer B, Rudolph R. (1996) Improved refolding of an immobilized fusion protein. *Nat Biotechnol*. 14: 329-334
- Stone JR and Yang S (2006) Hydrogen peroxide: a signaling messenger. *Antioxid Redox Signal*. 8: 243–270
- Streicher JM, Ren S, Herschman H, Wang Y. (2010) MAPK-activated protein kinase-2 in cardiac hypertrophy and cyclooxygenase-2 regulation in heart. *Circ Res*. 106: 1434-1443
- Sun QA, Kirnarsky L, Sherman S, Gladyshev VN. (2001) Selenoprotein oxidoreductase with specificity for thioredoxin and glutathione systems. *Proc.Natl. Acad. Sci. U. S. A.* 98: 3673–3678
- Tanguy Y, Falluel-Morel A, Arthaud S, Boukhzar L, Manecka DL, Chagraoui A, Prevost G, Elias S, Dorval-Coiffec I, Lesage J, Vieau D, Lihrmann I, Jégou B, Anouar Y. (2011) The PACAP-regulated gene selenoprotein T is highly induced in nervous, endocrine, and metabolic tissues during ontogenetic and regenerative processes. *Endocrinology*. 152: 4322-4335
- Temsah RM, Netticadan T, Chapman D, Takeda S, Mochizuki S, Dhalla NS. (1999) Alterations in sarcoplasmic reticulum function and gene expression in ischemic-reperfused rat heart. *Am J Physiol*. 277: H584-94.
- Thomson CD. (2004) Assessment of requirements for selenium and adequacy of selenium status: a review. *Eur J Clin Nutr*. 58: 391-402.

- Townsend N, Wilson L, Bhatnagar P, Wickramasinghe K, Rayner M, Nichols M. (2016) Cardiovascular disease in Europe: epidemiological update 2016. *Eur Heart J.* 37: 3232-3245.
- Tujebajeva RM, Copeland PR, Xu XM, Carlson BA, Harney JW, Driscoll DM, Hatfield DL, Berry MJ. (2000) Decoding apparatus for eukaryotic selenocysteine insertion. *EMBO Rep.* 1: 158-63
- Turner DC, Stadtman TC. (1973) Purification of protein components of the clostridial glycinereductase system and characterization of protein A as a selenoprotein. *Arch Biochem Biophys.* 154: 366–381
- Valdez LB, Zaobornyj T, Bombicino S, Iglesias DE, Boveris A, Donato M, D'Annunzio V, Buchholz B, Gelpi RJ. (2011) Complex I syndrome in myocardial stunning and the effect of adenosine. *Free Radic Biol Med.* 51: 1203-1212
- Van den Hoff MJ, Deprez RH, Monteiro M, De Boer PA, Charles R, Moorman AF. (1997) Developmental changes in rat cardiac DNA, RNA and protein tissue base: implications for the interpretation of changes in gene expression. *J Mol Cell Cardiol.* 29: 629-639
- Vinceti M, Wei ET, Malagoli C, Bergomi M, and Vivoli G. (2001) Adverse health effects of selenium in humans. *Rev Environ Health.* 16: 233–251.
- Voet D, Voet JG, Pratt CW. (1999) Fundamentals of biochemistry. New York: John Wiley & Sons. Manque volume et pages
- Wang X, Wang W, Li L, Perry G, Lee HG, Zhu X. (2014) Oxidative stress and mitochondrial dysfunction in Alzheimer's disease. *Biochim Biophys Acta.* 1842: 1240-1247
- Werns SW, Fantone JC, Ventura A, Lucchesi BR (1992) Myocardial glutathione depletion impairs recovery of isolated blood-perfused hearts after global ischaemia *J Mol Cell Cardiol* 24: 1215-20
- Wessjohann LA, Schneider A, Abbas M, Brandt W. (2007) Selenium in chemistry and biochemistry in comparison to sulfur. *Biol Chem.* 388: 997-1006
- Winterbourn CC, Hampton MB. (2008) Thiol chemistry and specificity in redox signaling. *Free Radic Biol Med* 45: 549–561
- Wirth EK, Conrad M, Winterer J, Wozny C, Carlson BA, Roth S, Schmitz D, Bornkamm GW, Coppola V, Tessarollo L, Schomburg L, Kohrle J, Hatfield DL, Schweizer U. (2010) Neuronal selenoprotein expression is required for interneuron development and prevents seizures and neurodegeneration. *FASEB J.* 24: 844–852
- Wittwer AJ, Tsai L, Ching WM, Stadtman TC. (1984) Identification and synthesis of a naturally occurring selenonucleoside in bacterial tRNAs: 5-[(methylamino)methyl]-2-selenouridine. *Biochemistry.* 23: 4650-4655
- Woo YJ, Zhang JC, Vijayarathy C, Zwacka RM, Englehardt JF, Gardner TJ, Sweeney HL. (1998) Recombinant adenovirus-mediated cardiac gene transfer of superoxide dismutase and catalase attenuates postischemic contractile dysfunction. *Circulation.* 98: 11255-60
- Xu XM, Carlson BA, Mix H, Zhang Y, Saira K, Glass RS, Berry MJ, Gladyshev VN, Hatfield DL. (2007) Biosynthesis of selenocysteine on its tRNA in eukaryotes. *PLoS Biol.* 5:e4
- Xu XM, Turanov AA, Carlson BA, Yoo MH, Everley RA, Nandakumar R, Sorokina I, Gygi SP, Gladyshev VN, Hatfield DL. (2010) Targeted insertion of cysteine by decoding UGA codons with mammalian selenocysteine machinery. *Proc Natl Acad Sci USA.* 107: 21430–21434

- Yee SB and Pritsos CA. (1997) Comparison of oxygen radical generation from the reductive activation of doxorubicin, streptonigrin, and menadione by xanthine oxidase and xanthine dehydrogenase. *Arch Biochem Biophys.* 347: 235-241
- Yellon DM and Hausenloy DJ. (2007) Myocardial reperfusion injury. *N Engl J Med.* 357: 1121-1135
- Yoshioka J, Lee RT. (2014) Thioredoxin-interacting protein and myocardial mitochondrial function in ischemia-reperfusion injury. *Trends Cardiovasc Med.* 24: 75-80
- Zeiher AM, Drexler H, Wollschläger H, Just H. (1991) Endothelial dysfunction of the coronary microvasculature is associated with coronary blood flow regulation in patients with early atherosclerosis. *Circulation.* 84:1984-1992.
- Zhao R and Holmgren A. (2002) A novel antioxidant mechanism of ebselen involving ebselen diselenide, a substrate of mammalian thioredoxin and thioredoxin reductase. *J Biol Chem.* 277: 39456–39462
- Zhong L and Holmgren A. (2000) Essential role of selenium in the catalytic activities of mammalian thioredoxin reductase revealed by characterization of recombinant enzymes with selenocysteine mutations. *J. Biol. Chem.* 275:1 8121–18128
- Zorio E, Gilibert-Estellés J, España F, Ramón LA, Cosín R, Estellés A. (2008) Fibrinolysis: the key to new pathogenetic mechanisms. *Curr Med Chem.* 15: 923-929

Abbreviations

5HD: 5-hydroxydecanoate

Akt: Protein kinase B

AOX-1: Aldehyde oxidase-1

ATP: Adenosine triphosphate

Bcl 2: B-cell lymphoma 2

CB: Carbonate coating buffer

CBT: Chequerboard titrations

COX IV: Cytochrome c Oxidase Subunit IV

CP: Coronary pressure

CVD: Cardiovascular disease

Cys: Cysteine

Cyt c: Cytochrome c

DIO2: Deiodinase type 2

DIO3: Deiodinase type 3

dLVP: developed left ventricular pressure

DTNB: 5,5'-dithio-bis(2-nitrobenzoic) acid

eEFSec: Sec-specific translation elongation factor

ELISA: Enzyme-linked immunosorbent assays

eNOS: Endothelial NOS

ER: Endoplasmic reticulum

Erk 1/2: Extracellular signal-regulated kinase

GAPDH: Glyceraldehyde 3-phosphate dehydrogenase

GGSeMCys: Gamma-glutamyl-Se-methylselenocysteine

GPx1: Glutathione peroxidase isoforme 1

GPx3: Glutathione peroxidase isoforme 3

Gsk3 α/β : Glycogen synthase kinase 3 alpha/beta

I/R: Ischemia/Reperfusion

IC-ELISA: Indirect Competitive Enzyme-Linked Immunosorbent Assay

I-ELISA: Indirect ELISA

iNOS: Inducible NOS

IPTG: Isopropyl β -D-1-thiogalactopyranoside

IS: Infarct Size

KHs: Krebs-Henseleit solution

LV: Left ventricular

LVEDP: Left ventricular end-diastolic pressure

mitoKATP: Mitochondria ATP-sensitive potassium channels

NADPH: Nicotinamide adenine dinucleotide phosphate

NO: Nitric oxide

NOS: Nitric oxide synthase

NPI-10: Bacterial lysis buffer

NT: Nitrotyrosine

p38MAPK: p38 Mitogen-Activated Protein Kinases

PACAP: Pituitary adenylate cyclase-activating polypeptide

PCI: Percutaneous coronary intervention

PI3K: Phosphatidylinositol 3-kinase
PMSF: Phenylmethylsulfonyl fluoride
PSELT: SelT-derived peptide
PSTK: Phosphoseryl-tRNA kinase
RISK: Reperfusion Injury Salvage kinase
RNS: Reactive Nitrogen Species
ROS: Reactive Oxygen Species
rSELT: Recombinant full length SelT
SBP2: SECIS binding protein-2
SCL: Selenocysteine lyase
Sec: Selenocysteine
SECIS: Selenocysteine insertion sequence
SecS: Selenocysteine synthase
SelD: Selenoprotein D
SelP: Selenoprotein P
SelT: Selenoprotein T
SelT-insKO: Selenoprotein T *knockout* mice
SelV: Selenoprotein V
SelW: Selenoprotein W
SeMCys: Se-methyl-selenocysteine
SeMet: Selenomethionine
SeO₃²⁻/ SeO₃²⁻ : Selenate/selenite
Ser: Serine
SerRS: Seryl-tRNA synthetase
tRNAs: Transfer RNAs
TrxR/Trx: Thioredoxin reductases/Thioredoxin
WT: Wortmannin
XO: Xanthine Oxidase